

**CAROM, A NOVEL GENE, IS UPREGULATED BY HOMOCYTEINE THROUGH DNA
HYPOMETHYLATION TO INHIBIT ENDOTHELIAL CELL MIGRATION AND
ANGIOGENESIS**

A Dissertation
Submitted to
The Temple University Graduate Board

In Partial Fulfillment
Of the Requirements for the Degree of
DOCTOR OF PHILOSOPHY

By
Xinyu Xiong
May 2014

Dissertation Examining Committee:

Dr. Hong Wang, Advisor, Department of Pharmacology, Temple University
Dr. Xiao-Feng Yang, Co-Advisor, Department of Pharmacology, Temple University
Dr. Barrie Ashby, Department of Pharmacology, Temple University
Dr. Salim Merali, Department of Biochemistry, Temple University
Dr. Weidong Xiao, Department of Microbiology and Immunology, Temple University
Dr. Katalin Susztak, External Examiner, University of Pennsylvania

©

Copyright

2014

by

Xinyu Xiong
All Rights Reserved

ABSTRACT

CAROM, A NOVEL GENE, IS UPREGULATED BY HOMOCYSTEINE THROUGH DNA HYPO METHYLATION TO INHIBIT ENDOTHELIAL CELL MIGRATION AND ANGIOGENESIS

Xinyu Xiong

Doctor of Philosophy

Temple University, 2014

Doctoral Advisory Committee Chair: Hong Wang, MD, PhD, EMBA

Hyperhomocysteinemia (HHcy) is an independent risk factor for cardiovascular disease (CVD). We previously demonstrated that homocysteine (Hcy) suppresses endothelial cell (EC) proliferation, migration, and post-injury EC repair, but the molecular mechanism underlying Hcy-induced EC injury is unclear. In this study, we identified a novel gene, Carom, which mediates Hcy-induced suppression of EC migration and angiogenesis.

We identified FCH and double SH3 domains 2 (FCHSD2), a novel gene, as an Hcy-responsive gene through Differential Display in Hcy (50 μ M)-treated human umbilical vein endothelial cells (HUVEC). FCHSD2 was initially named as Carom, based on the identification of this molecule as an interacting protein of calcium/calmodulin-dependent serine protein kinase (CASK) and membrane associated guanylate kinase, WW and PDZ domain containing 1 (MAGI1). In this thesis, we describe this gene as Carom. Carom belongs to the Fes/CIP4 homology and Bin/amphiphysin/Rvs (F-BAR) protein family, which is a group of multivalent adaptors linking plasma membrane and cytoskeleton, involved in endocytosis and cell migration. However,

Carom's function is poorly characterized. Based on the findings that CASK and MAGI1 inhibit cell migration and growth, and the role of F-BAR proteins in cell migration, we hypothesize that Hcy up-regulates Carom to inhibit EC growth and/or migration, finally leading to CVD.

We confirmed the significant induction of Carom mRNA expression in Hcy-treated HUVECs or human aortic endothelial cells (HAEC) by Northern blot and Real-time PCR. In addition, we found that Carom protein expressions were significantly increased both in Hcy-treated HAECs and lung ECs isolated from HHcy mice by Western blot using our homemade rabbit antibody against Carom. These data indicate that Hcy increases endothelial expression of Carom both *in vitro* and *in vivo*. Furthermore, in order to characterize Carom function in EC, we generated recombinant adenovirus Adv-Carom to transduce Carom for gain-of-function study and Adv-Carom-shRNA to express Carom shRNA for loss-of-function study. We found that neither adenovirus-transduced Carom expression nor adenoviral Carom shRNA had any impact on HUVEC proliferation by using [³H]-thymidine incorporation. Interestingly, we demonstrated that Adv-Carom inhibited HAEC migration, while Hcy-induced HEAC migration inhibition could be rescued by Adv-Carom-shRNA. These data suggest that Carom may inhibit angiogenesis via a cell proliferation-independent mechanism.

Furthermore, we found that Hcy significantly increased the intracellular level of S-adenosyl homocysteine (SAH) but not S-adenosyl methionine (SAM), and decreased the SAM/SAH ratio, an indicator of cellular methylation, in HAECs, by using High-performance liquid chromatography/electrospray tandem mass spectrometry (HPLC-MS) to measure SAH and SAM levels. Meanwhile, Carom protein expression was significantly induced by azacytidine (AZC), a DNA methyltransferase inhibitor, in a dose-dependent manner in HAECs. Based on these data, we speculated that Hcy-induced hypomethylation could associate with Carom up-regulation. Thus

we used bisulfite deep sequencing to profile methylation status of Carom gene in Hcy-treated HUVECs and found that Carom promoter was hypomethylated by Hcy. In addition, eight transcriptional factor binding sites on Carom were hypomethylated by Hcy. These data suggest that Hcy may induce Carom via a DNA hypomethylation-dependent mechanism.

Moreover, we found that adenovirus-transduced Carom expression significantly increased the secretions of two anti-angiogenic chemokines, CXCL10 and CXCL11 in HAECs by using human cytokine array. Similarly, Hcy also significantly increased mRNA expressions of CXCL10 and CXCL11, while Adv-Carom-shRNA blocked down the inductions of CXCL10 and CXCL11 by Hcy. We further demonstrated that adenovirus-transduced Carom expression inhibited angiogenesis by performing tube formation assay of HAECs, whereas Hcy-induced angiogenesis suppression were rescued by Adv-Carom-shRNA as well as the neutralizing antibodies of CXCL10 and CXCL11. These data suggest that Hcy induces Carom to trigger CXCL10 and CXCL11 downstream to inhibit angiogenesis.

In conclusion, Hcy induces Carom expression through DNA hypomethylation to inhibit EC migration and angiogenesis.

ACKNOWLEDGMENTS

I would like to first and foremost thank my mentor, Dr. Hong Wang for opening her laboratory to me and giving me the great opportunity to engage in vascular biology study. I am truly grateful for her guidance, input and support throughout my graduate studies. Her dedication to science, desire for excellence, passion and unbeatable spirit in revealing the unknown always inspire me and provide a solid foundation on which I could build a career.

I would also like to express my sincere thanks to my co-supervisor, Dr. Xiao-Feng Yang. He always paid close attention to my work. He provided me critical suggestions for every breakthrough in my research. I must acknowledge his willingness to help, his creative idea, and his guidance in all aspects of my thesis.

I would like to thank Dr. Barrie Ashby, Dr. Salim Merali and Dr. Weidong Xiao for standing by me as devoted committee members all these years. Their suggestions and feedback to my studies are greatly appreciated. I would especially like to thank Dr. Ashby for always being helpful at every step of my studies, Dr. Merali for his guidance for protein interaction study, Dr. Xiao for his support in virus work. I am also thankful to Dr. Katalin Susztak, my external reader, for her support in reading and providing feedback on my dissertation.

I would like to thank all the current and past members of Dr. Wang and Dr. Yang's laboratory. I would like to thank you all for the friendship, support and help. I would particularly like to thank

our lab manager Xiaohua Jiang for her detailed teaching of laboratory skills and helping me throughout the seven years. I would also like to personally acknowledge Dr. Hang Xi, Dr. Shu Meng, Dr. Xiaojin Sha, Dr. Pu Fang, Dr. Ying Yin, Dr. Ramon Cueto and Dr. Yafeng Li who have given me endless support. Most importantly, they have provided their friendships have made the past years so enjoyable and unforgettable. I would particularly thank Michael Jan, Jietang Mai, Dr. Meghana Pansuria, Anthony Virtue, Dr. Jun Zhou, Dr. Zhongjian Cheng, Xinyuan Li and Lixiao Zhang for the helpful discussions and leisure talks in the busy lab day. I also want to thank Huimin Shan for her help with animal work.

I would like to thank all the faculties and staff in Department of Pharmacology and Cardiovascular Research Center for their warmth and support.

Finally, I would like to thank my parents and the rest of the family for their love and support during all these years. Last, but by no means least, I would like to thank my wife Qun. I am thankful for your understanding and sacrifice during the past seven years. Words are not enough to acknowledge you!

DEDICATION

This dissertation is dedicated to my wife, Qun Yao.

TABLE OF CONTENTS

	PAGE
ABSTRACT.....	iii
ACKNOWLEDGMENTS.....	vi
DEDICATION.....	viii
LIST OF FIGURES.....	xiii
LIST OF TABLES.....	xv
LIST OF ABBREVIATIONS.....	xvi
CHAPTER	
1. INTRODUCTION.....	1
Homocysteine.....	1
Hcy and cardiovascular disease.....	4
Hcy-lowering therapy and CVD.....	5
Biological mechanisms of HHcy pathology.....	6
Biochemical basis of Hcy pathology... ..	8
Hcy metabolism and cellular methylation.....	11
F-BAR protein family.....	19
Structure of F-BAR proteins.....	19
Functions of F-BAR proteins	21
Carom, an F-BAR protein, is up-regulated by EC.....	23
Angiogenesis and EC migration.....	27
Angiogenesis process.....	28
EC migration in angiogenesis.....	29
Angiogenesis and CVD.....	30
Key knowledge gaps.....	31
Hypothesis of Dissertation	32
2. MATERIALS AND METHOD.....	36

Tissue Expression Profiling of Carom Gene in Human and Mouse.....	36
Chemicals and Antibodies.....	37
Animals.....	37
Mice Genotyping.....	38
Cell Culture.....	39
Differential Display.....	39
Generation of Rabbit anti-Carom antibody.....	42
Antigen Analysis.....	42
Production of GST-CaromAG fusion protein as the antigen.....	42
Production and Purification of Rabbit anti-Carom Antibody.....	42
Plasma and Intracellular SAM, SAH, and Hcy Measurement.....	45
Protein Extraction and Western Blot Analysis.....	45
Primary Mouse Lung EC Isolation.....	46
[³ H]Thymidine Incorporation	46
RNA Extraction and Real-Time PCR.....	47
Cytokine Array.....	48
Northern Blot Hybridization.....	48
Construction of Recombinant Adenoviruses and Adenovirus Infection.....	49
Adv-Carom to transduce human Carom in EC	49
Adv-Carom-shRNAs to transduce Carom shRNAs in EC.....	50
Bisulfite Next-Generation Sequencing.....	51
Analysis of Transcription Factor Binding Frequencies.....	51
Scratch Wound Assay.....	51
Tube Formation Assay.....	52
Statistical analysis.....	52
 3. RESULTS.....	 53
Carom is identified as an early induced gene by Hcy in EC.....	53
Carom gene is differentially expressed in Human and Mouse tissues.....	55
Hcy up-regulates both mRNA and protein expression levels of Carom in EC.....	57
Generation of rabbit anti-Carom antibody.....	57

Purification of anti-Carom antibody.....	62
Hcy Up-regulates Carom mRNA Expression in Cultured EC.....	64
Hcy Up-regulates Carom Protein Expression in Cultured EC.....	66
Carom Protein Expression Is Increased in EC from HHcy mice.....	67
Carom inhibits EC migration	71
Construction of recombinant adenovirus expressing Carom.....	71
Construction of recombinant adenovirus expressing Carom shRNA.....	74
Carom does not play a role in EC growth.....	77
Carom mediates Hcy-induced suppression of EC migration.....	79
Hcy upregulated Carom expression through DNA hypomethylation.....	82
Hcy increases intracellular SAH level and decreases SAM/SAH ratio in EC.....	82
AZC, a DNMTs inhibitor, up-regulates Carom expression in EC.....	82
Hcy alone without adenosine does not induce Carom expression.....	83
H ₂ O ₂ Decreases Carom Expression in EC.....	83
Hcy Hypomethylates Carom Promoter in EC.....	86
Carom mediates Hcy-inhibited angiogenesis via CXCL10 and CXCL11.....	92
Adenovirus expressed Carom induces CXCL10, CXCL11 and CCL5 in EC as well as Hcy.....	92
Carom inhibits tube formation.....	95
4. DISCUSSION.....	98
Carom is a novel Hcy-responsive gene in EC.....	99
Carom induction by Hcy is associated with promoter hypomethylation in EC.....	102
Carom mediates Hcy-induced inhibition of EC migration and angiogenesis through..... CXCL10 and CXCL11.....	105

Conclusion and Future Directions.....	109
REFERENCES CITED.....	113

LIST OF FIGURES

	Page
Figure 1.1. Chemical Structures of Homocysteine, Cysteine, and Methionine.....	1
Figure 1.2. Homocysteine metabolism Pathway	3
Figure 1.3. Homocysteine autooxidation	9
Figure 1.4. Methione-homocysteine metabolic cycle and cellular methylation	13
Figure 1.5. Diagram of the domain structures of selected F-BAR proteins.....	20
Figure 1.6. Carom gene and protein	25
Figure 1.7. Hypothesis and specific aims.....	35
Figure 2.1. Differential Display to identify Hcy-induced genes in HUVECs	40
Figure 2.2. Antigen analysis for production of anti-Carom antibody.....	44
Figure 3.1. BLAST result of cDNA clones A2 and A12 obtained from differential display of HUVECs with 12h Hcy treatment.....	54
Figure 3.2. Tissue mRNA Expression Profile of Carom Gene.....	56
Figure 3.3. Generation of Rabbit Anti-Carom Antibody.....	59
Figure 3.4. Purification of anti-Carom antibody.....	63
Figure 3.5. Hcy induces Carom expression in cultured endothelial cells.....	65
Figure 3.6. Carom protein expression in HHcy mice EC.....	69
Figure 3.7. Generation of Recombinant Adenovirus Adv-Carom to Express Carom in EC.....	72
Figure 3.8. Generation of Recombinant Adenoviruses Adv-Carom-shRNAs to Express Carom shRNA in EC.....	75
Figure 3.9. The effects of adenovirus-transduced Carom gene and Carom shRNA genes on DNA synthesis in HUVECs.....	78

Figure 3.10. The effects of adenovirus-transduced Carom gene and Carom shRNA gene on EC migration.....	80
Figure 3.11. DNA methylation inhibitor upregulates Carom expression in EC.....	84
Figure 3.12. Hcy induces Carom promoter hypomethylation.....	88
Figure 3.13. Transduction of Carom gene by Adv-Carom upregulates CXCL10, CXCL11 and CCL5 in HAECs as well as Hcy.....	93
Figure 3.14. The effects of adenovirus-transduced Carom gene and Carom shRNA gene on tube formation.....	96
Figure 4.1. Working model of the mechanisms underlying Hcy-Carom induction and the impact on CVD.....	112

LIST OF TABLES

	Page
Table 2.1. Real-time PCR Primers of Target Human Genes.....	47
Table 2.2. Carom shRNAs targeting sequences.....	50
Table 3.1. Carom cDNA clones are identified with Differential Display.....	53

LIST OF ABBREVIATIONS

Ade	adenosine
Adv-Carom	recombinant adenovirus expressing Carom protein
Adv-Carom-shRNA	recombinant adenovirus expressing Carom shRNA
Adv-Ct	recombinant adenovirus for protein expression control
Adv-Ct-shRNA	recombinant adenovirus expressing control shRNA
AZC	azacitidine
BHMT	betaine: homocysteine methyltransferase
BLAST	Basic Local Alignment Search Tool
BSA	bovine serum albumin
CBS	cystathionine β -synthase
CCL5	chemokine (C-C motif) ligand 5
cDNA	complementary DNA
CGI	CpG island
CSE	cystathionine- γ -lyase
CVD	cardiovascular disease
CXCL10	C-X-C motif chemokine 10
CXCL11	C-X-C motif chemokine 11
5-MTHF	5-methyltetrahydrofolate
5,10-CH ₂ -THF	5,10-methylenetetrahydrofolate
Cys	cysteine
CVD	cardiovascular disease
DNMT1	DNA methyltransferase 1
DTT	dithiothreitol
EC	endothelial cell
ECGS	endothelial cell growth supplement
EHNA	erythro-9-(2-hydroxy-3-nonyl)-adenine
ER	endoplasmic reticulum
eNOS	endothelial nitric oxide synthase
F-BAR	Fes/CIP4 homology and Bin/amphiphysin/Rvs
FBS	fetal bovine serum
FCHSD2	FCH and double SH3 domains 2
GFP	green fluorescent protein
GST	Glutathione S-transferase
HAEC	human aortic endothelial cell

Hcy	homocysteine
HHcy	hyperhomocysteinemia
HDAC	histone deacetylase
HPLC	High Performance Liquid Chromatography
HUVEC	human umbilical vein endothelial cell
KO	knockout
MAT	methionine adenosyltransferase
MCP-1	Monocyte chemotactic protein-1
Met	methionine
MOI	multiplicity of infection
MLEC	mouse lung endothelial cell
mRNA	messenger RNA
MTHFR	methylenetetrahydrofolate reductase
NGS	next-generation sequencing
NO	nitric oxide
PCR	polymerase chain reaction
PMSF	phenylmethanesulfonylfluoride
ROS	reactive oxygen species
SAH	s-adenosylhomocysteine
SAM	s-adenosylmethionine
SH3	Src Homology 3
TESS	Transcriptional Element Search System
VEGF	Vascular Endothelial Growth Factor
VSMC	Vascular Smooth Muscle Cell

CHAPTER 1

INTRODUCTION

Homocysteine (Hcy)

Homocysteine (Hcy) is a sulfhydryl containing nonessential amino acid produced during the metabolism of methionine. Hcy was first isolated in 1932 from urinal bladder stone by Vincent du Vigneaud, a Nobel laureate in chemistry. Hcy is a homologue of the essential amino acid cysteine, differing by an additional methylene bridge (-CH₂-). The chemical structures of homocysteine, methionine, and cysteine are shown in Figure 1.1.

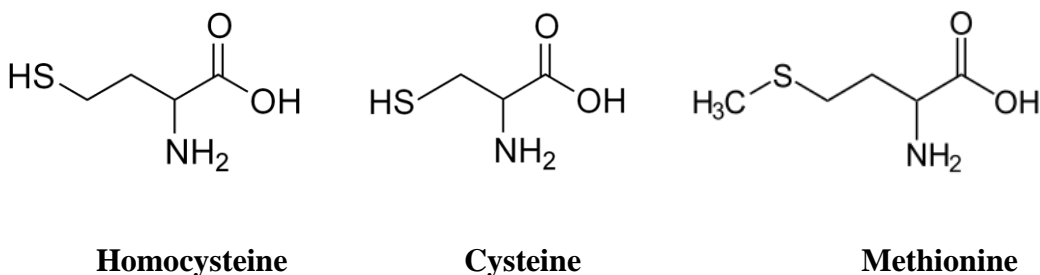


Figure 1.1. Chemical Structures of Homocysteine, Cysteine, and Methionine.

Hcy is an intermediary product of methionine metabolism. As shown in Figure 1.2, methionine is preferentially activated by ATP to form S-adenosylmethionine (SAM). SAM is then converted to S-adenosylhomocysteine (SAH) by donating a methyl group for cellular methylation and finally SAH is converted to Hcy. Conversion of SAH to Hcy is a reversible process. Hcy can utilize adenosine, a normal constituent of all body fluids,

to become SAH, a potent inhibitor of cellular methylation. Hcy can be further eliminated through two pathways: transsulfuration to cysteine and remethylation to methionine.

The key enzyme in the transsulfuration pathway is cystathionine β -synthase (CBS). CBS, with its cofactor pyridoxal-phosphate (active form of vitamins B6), condenses Hcy with serine to form cystathionine. Then cystathionine is transformed into cysteine through cystathionine- γ -lyase (CSE). The remethylation pathway requires a methyl group derived from either 5-methyltetrahydrofolate (5-MTHF) through 5-methyltetrahydrofolate-homocysteine S-methyltransferase (MTR) or betaine through betaine-homocysteine methyltransferase (BHMT) (M. E. Lee & Wang, 1999). MTR requires methylcobalamin (MeCbl), a derivative of cobalamin (vitamin B12), for its normal activity. The remethylation cosubstrate 5-MTHF is converted from 5,10-methylenetetrahydrofolate (5,10-CH₂-THF) through methylenetetrahydrofolate reductase (MTHFR). 5,10-CH₂-THF itself is derived from tetrahydrofolate (THF), a folic acid derivative.

According to the American Heart Association advisory statement, normal levels of plasma Hcy are between 5 and 15 μ M. Elevation of plasma levels of Hcy creates a condition called hyperhomocysteinemia (HHcy). Moderate HHcy refers to plasma Hcy levels between 15 and 30 μ M, intermediate HHcy levels are between 31 and 100 μ M, and severe HHcy levels are higher than 100 μ M. Genetic mutations of the key enzymes involved in transsulfuration pathway, such as CBS, or in remethylation pathway, such as MTR and MTHFR, lead to Hcy accumulation in the plasma. Deficiencies of dietary vitamins B6, B12 and folic acid which are essential in Hcy metabolism also contribute to elevated Hcy level (Maron & Loscalzo, 2009).

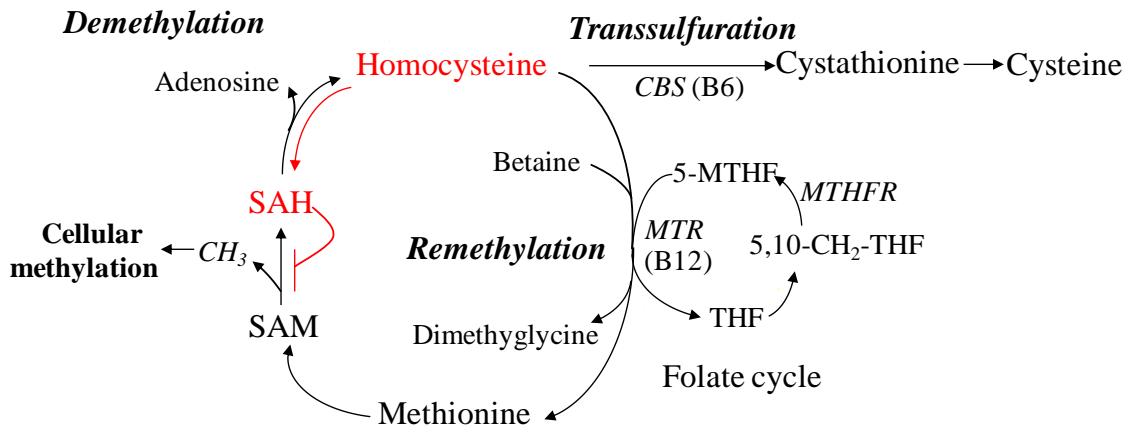


Figure 1.2. Homocysteine metabolism Pathway. Hcy is an intermediate metabolite of methionine, an essential amino acid. SAM is synthesized from methionine and is further converted to SAH after donating a methyl group for cellular methylation. SAH is then hydrolyzed to Hcy. Hcy can be metabolized either through the transsulfuration pathway to cysteine or through the remethylation pathway to methionine. In the remethylation pathway, Hcy could receive a methyl group either through 5-MTHF or betaine. Increased Hcy level contributes to SAH accumulation. SAH is a potent inhibitor of methyltransferase and thus inhibit the biological methyl-transfer reaction. SAM, S-adenosylmethionine; SAH, S-adenosylhomocysteine; CBS, cystathionine- β -synthase; THF, tetrahydrofolate; 5-MTHF, 5-methyltetrahydrofolate; 5,10-CH₂-THF, 5,10-methylenetetrahydrofolate; MTR, 5-methyltetrahydrofolate-homocysteine S-methyltransferase; MTHFR, methylenetetrahydrofolate reductase.

HHcy and cardiovascular disease (CVD)

In 1969, McCully first suggested that elevated Hcy levels are responsible for widespread vascular lesions in a HHcy infant with an inborn error of vitamin B12 metabolism, and that moderate HHcy may be a potential cause for cardiovascular disease (McCully, 1969). However, this hypothesis was overlooked for many years, probably due to the low prevalence of inborn errors of metabolism that were accompanied by HHcy. In 1976, Wilcken and Wilcken observed an abnormal rise in plasma Hcy after oral methionine loading in patients with coronary artery disease (Wilcken & Wilcken, 1976). Since then, HHcy began to be a focus of CVD research and numerous studies provide evidence to associate HHcy with CVD. About 21% of the population in Framingham Heart Study, an epidemiology study begun in 1948 with 5209 ordinary adult subjects from Framingham, MA to study CVD risk factors, had an Hcy concentration $\geq 14.5 \mu\text{M}$. Considered against the risk profile derived from the Physicians' Health Study, a randomized trial with 5-year follow-up of 85,078 US male physicians, this plasma concentration of Hcy would increase the risk of heart attack by 3.4-fold (Selhub et al., 1995; Stampfer et al., 1992). Furthermore, in the meta-analysis, an increase of $5 \mu\text{M}$ in plasma Hcy enhanced the risk of CVD by 1.6- to 1.8-fold (Boushey, Beresford, Omenn, & Motulsky, 1995). Thus, it is predicted that an increase of plasma Hcy from $10 \mu\text{M}$ to $15 \mu\text{M}$ will correspond to an increase in total cholesterol from 189 mg/dL to 275 mg/dL in terms of the increased risk of CVD mortality (Omenn, Beresford, & Motulsky, 1998). It is now recognized that HHcy is a common risk factor for CVD, similar to smoking and hyperlipidemia (Folsom et al., 1998).

Hcy-lowering therapy and CVD

Although there is convincing evidence from epidemiological studies indicating that mild HHcy is associated with an increased risk of vascular events, it is not yet known if treatment to lower Hcy reduces the risk of CVD. Lowering plasma Hcy levels improved endothelial dysfunction and reduced the incidence of major adverse events after percutaneous coronary intervention (Schnyder, Roffi, Flammer, Pin, & Hess, 2002; Title, Cummings, Giddens, Genest, & Nassar, 2000). However, several secondary prevention trials of Hcy-lowering therapy (folic acid, vitamin B12 and/or pyridoxine) have failed to demonstrate a clinical benefit of Hcy-lowering therapy for the secondary prevention of vascular events in subjects with stroke (Toole et al., 2004) or myocardial infarction (Lonn et al., 2006). These may be related to the nature of existing disease, sample size, lack of adequate statistical power, confounding effects of other medication and folate fortification, and limited benefit or potential adverse effects of supplemented vitamins (Spence, 2006). It is likely that Hcy-lowering therapy is more beneficial for the primary prevention of CVD rather than the secondary prevention of vascular events in subjects who already have severe vascular disease and who are receiving other interventions. Indirect evidence for such a benefit was recently obtained from a large population based cohort study, which demonstrated that Hcy-lowering due to folic acid fortification significantly reduced stroke mortality in the general population in Canada and the US (Q. Yang et al., 2006). Therefore, the negative results of recent Hcy-lowering therapy in secondary prevention should not exclude the causative role of HHcy in CVD.

Biological mechanisms of HHcy pathology

Human clinical studies together with studies in cultured cells and animal models have suggested several mechanisms to explain cardiovascular pathological changes associated with HHcy.

1. Hcy can induce endothelial cell (EC) growth inhibition and promote endothelial injury. Vascular disease may be initiated by endothelial injury resulting from insult to the vessel wall. Endothelial injury subsequently leads to platelet aggregation, coagulation, vascular smooth muscle cell (VSMC) proliferation, and atherosclerosis. Hcy has been implicated in endothelial injury as seen with direct toxic effects on baboon endothelium, induced endoplasmic reticulum stress and apoptosis in cultured EC (Harker, Harlan, & Ross, 1983; Roybal et al., 2004; C. Zhang et al., 2001). Though these studies require relatively high concentrations of Hcy, our laboratory has demonstrated that physiologically relevant concentration (50 μ M) of Hcy inhibit EC growth (H. Wang et al., 1997) through a hypomethylation-related mechanism which leads to cyclin A transcriptional inhibition (M. D. Jamaluddin et al., 2007). Endothelial injury and post-injury repair play an important role in the development of atherosclerosis. Our lab showed that severe HHcy promotes post-injury neointima formation by impairing reendothelialization via inhibition of EC proliferation and migration (Tan et al., 2006).

2. Endothelial dysfunction (ED), an early event in the development of arteriosclerosis, can be induced by HHcy. ED is defined as an impairment of endotheliumdependent relaxation of blood vessels. It is the earliest indicator of the development of CVD and precedes the appearance of atherosclerotic plaque and the frank symptoms of peripheral

vascular disease. Impaired endothelial vasomotor function was observed in human and experimental models of HHcy in minipigs, monkey, rats and mice either with high-Met diet or the deletion of the CBS gene (Dayal & Lentz, 2005; Jiang et al., 2005). Our lab has demonstrated that HHcy impairs endothelial function and eNOS activity via protein kinase C (PKC) activation. Study from other labs showed that severe HHcy impairs endothelium-derived hyperpolarizing factor (EDHF)-mediated vascular relaxation in rat renal arteries (De Vriese et al., 2004; Heil et al., 2004). Further, we found that HHcy impairs EDHF relaxation in small mesenteric arteries (SMAs) by inhibiting small-conductance K_{Ca} (SK)/intermediate-conductance K_{Ca} (IK) activities via oxidation- and tyrosine nitration-related mechanisms (Cheng et al., 2011).

3. Stimulation of vascular smooth muscle cell (VSMC) proliferation is the early focus of HHcy-induced vascular biology change because it is one of the hallmarks of atherosclerosis. We are the first to report a significant growth-promoting effect of Hcy on VSMC through cyclin A transactivation (Tsai et al., 1994; Tsai et al., 1996). In addition, Hcy activates the PKC pathway, increases cmyc and c-myb expression (Dalton, Gadson, Wrenn, & Rosenquist, 1997), increases collagen synthesis (Majors, Ehrhart, & Pezacka, 1997) and inhibits lysyl oxidase, a key enzyme in elastin and collagen crosslinking (Liu, Nellaippan, & Kagan, 1997), in VSMC.

4. Thrombosis activation might be responsible for increased incidence of both arterial and venous thrombosis in HHcy patients (Guba, Fonseca, & Fink, 1999). HHcy activates platelets in humans and rats (Durand, Lussier-Cacan, & Blache, 1997; Riba, Nicolaou, Troxler, Homer-Vaniasinkam, & Naseem, 2004), decreases the largest von Willebrand factor (a thrombophilic protein) multimers in women with thrombosis (Perutelli et al.,

2005), and decreases the activity of thrombomodulin, a thrombin cofactor responsible for protein C activation, in monkey aorta (Lentz et al., 1996).

5. HHcy triggers monocytes differentiation, activation, and transmigration in the development of atherosclerosis. Hcy was reported to increase the expression and secretion of monocyte chemoattractant protein-1 (MCP1) and interleukin-8 in human monocytes (Zeng, Dai, Remick, & Wang, 2003) and EC (Poddar, Sivasubramanian, DiBello, Robinson, & Jacobsen, 2001). MCP-1 enhances the binding of monocytes to the endothelium and their recruitment to the subendothelial cell space, a critical step in atherosclerotic lesion development. Our lab demonstrated that HHcy promotes differentiation of inflammatory monocyte subsets of both bone marrow and tissue origins and their accumulation in atherosclerotic lesions via oxidative stress in CBS deficient mice (D. Zhang, Fang, et al., 2012; D. Zhang et al., 2009).

Biochemical basis of Hcy pathology

Although related studies have established that Hcy has profound biological effects, the biochemical basis by which HHcy contributes to CVD remains largely unknown. Three major biochemical mechanisms have been proposed to explain the vascular pathology of Hcy. These include (1) auto-oxidation through the production of reactive oxygen species (ROS); (2) hypomethylation by forming SAH, a potent inhibitor of cellular methylation; (3) protein homocysteinylation by incorporating Hcy into protein.

1. Oxidation has been proposed as an important biochemical mechanism responsible for Hcy pathogenesis. Hcy contains a free sulfhydryl group, which dominates the redox property. As shown in Figure 1.3, Hcy can be auto-oxidized with another Hcy molecule,

to generate disulfide and reactive oxygen species (ROS) (Loscalzo, 1996). Liberated ROS could initiate lipid peroxidation in circulating lipoproteins and in cell membranes; this process could then lead to impaired endothelial function and the formation of atherogenic low-density lipoprotein (LDL). Oxidized LDL may trigger platelet activation, lead to growth factor releasing resulting in smooth muscle cell proliferation and vascular hypertrophy. Moreover, Hcy may also lead to oxidative injury by inhibiting the expression of anti-oxidant enzymes (Dayal et al., 2002; Weiss, Keller, Hoffmann, & Loscalzo, 2002).

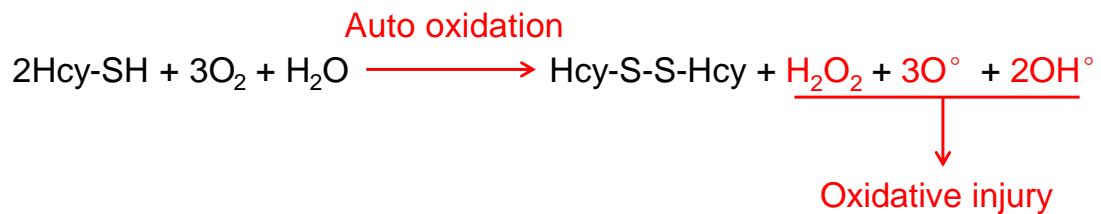


Figure 1.3. Homocysteine autooxidation.

Hcy can be auto-oxidized with another Hcy molecule to generate disulfide and ROS to induce oxidative injury. Hcy-SH, free homocysteine; Hcy-S-S-Hcy, homocysteine (disulfide); O₂, oxygen; H₂O, water; H₂O₂, hydrogen peroxide; O[°], singlet oxygen; OH[°], hydroxyl radical.

2. We have proposed that hypomethylation is a key biochemical mechanism (M. E. Lee & Wang, 1999) by which Hcy causes vascular diseases (M. D. Jamaluddin et al., 2007;

Tan et al., 2006; H. Wang et al., 1997). This hypothesis is supported by several studies (Pogribny & Beland, 2009). In one such example, increased Hcy levels along with a reduced global lymphocyte DNA methylation pattern was reported in patients with renal functional impairment, a clinical condition that augments the risk for vascular diseases (Ingrosso et al., 2003). We have performed a series of studies to demonstrate that Hcy selectively induces SAH accumulation and subsequent cellular hypomethylation in EC, leading to EC specific growth inhibition (H. Wang et al., 1997). Hcy also causes an EC specific suppression of DNA methyltransferase 1 (DNMT1) activity, Ras protein carboxyl methylation and cyclin A promoter methylation (M. D. Jamaluddin et al., 2007; H. Wang et al., 2002; H. Wang et al., 1997). Studies from other labs also indicate that Hcy inhibits EC growth by downregulating FGF2 via hypermethylation of the FGF2 promoter (Chang et al., 2008) and that Hcy promotes EC dysfunction by upregulating p66shc via hypomethylation of the p66shc promoter (C. S. Kim et al., 2011).

3. Hcy could cause protein homocysteinylolation. Hcy converts to thiolactone in consequence of an error-editing function of some aminoacyl-tRNA synthetases (Jakubowski, Zhang, Bardeguet, & Aviv, 2000), which is one of characteristic of Hcy metabolism that may account for adverse effects of elevated Hcy levels. Plasma proteins incubated with Hcy thiolactone spontaneously form homocysteinylated proteins. Protein homocysteinylolation by thiolactone may contribute to Hcy toxicity in humans. Hcy-thiolactone and N-Hcy-protein can induce endoplasmic reticulum (ER) stress (Jakubowski, 2006).

Hcy metabolism and cellular methylation

Cellular methylation is conducted by methyltransferases which transfer the methyl group from SAM to DNA, RNA, proteins and other important biochemical molecules such as the creatine precursor.

DNA methylation usually occurs at the 5' position of the cytosine ring within CpG dinucleotide. The DNA methyltransferases (DNMTs) catalyze the transfer of a methyl group from SAM to DNA. In mammals, although five members of the DNMT family have been found: DNMT1, DNMT2, DNMT3a, DNMT3b and DNMT3L, only DNMT1, DNMT3a and DNMT3b possess methyltransferase activity. DNMT3A and DNMT3B are *de novo* methyltransferases that establish cytosine methylation patterns on unmethylated DNA during embryogenesis (Okano, Bell, Haber, & Li, 1999). DNMT1 functions to maintain the existing methylation pattern following DNA replication (Leonhardt, Page, Weier, & Bestor, 1992).

Protein methylation is conducted by protein methyltransferases which add a methyl group from the donor SAM to carboxyl groups of glutamate, leucine, and isoprenylated cysteine, or on the side-chain nitrogen atoms of lysine, arginine, and histidine residues (Clarke, 1993). Two families of enzymes have been identified that catalyze protein methylation, **(1)** histone methyltransferases, and **(2)** carboxyl methyltransferases.

DNA methylation and histone methylation are two key mechanisms of epigenetic regulation which plays vital role in embryonic development, genome stability, and development of various diseases, including cancer and CVD.

Since all methyltransferases involved in cellular methylation require SAM as the methyl group donor, biochemical regulation of SAM plays a crucial role in cellular methylation and requires special attention.

SAM is generated from the methionine-homocysteine metabolic cycle (**Figure 1.4**) which can be described in five major steps: **1)** SAM synthesis, **2)** methyl transfer reactions, **3)** SAH hydrolysis/synthesis, **4)** Hcy remethylation/methionine synthesis and **5)** Hcy transsulfuration.

Briefly, SAM is derived from methionine and can be converted to S-adenosyl-homocysteine (SAH) after donating its methyl group for cellular methylation. SAH is then hydrolyzed to adenosine and Hcy. Hcy can then be converted back to methionine via the remethylaiton pathway or then become cysteine via the transsufuration pathway (M. E. Lee & Wang, 1999).

1. SAM synthesis

Methionine adenosyltransferase (MAT) catalyzes the biosynthesis of SAM from methionine and ATP. Among three forms of MAT identified in mammalian tissues, MAT I and MAT III are encoded by MAT1A gene, and synthesized primarily in the liver. MAT II on the other hand, is encoded by MAT2A and is found in fetal liver as well as kidney, brain, testis and lymphocytes. The majority of the hypermethioninemia subjects with presumably MAT deficiency were clinically well while only a few showed neurological deficiency with severe loss of MAT activity (Mudd et al., 1995).

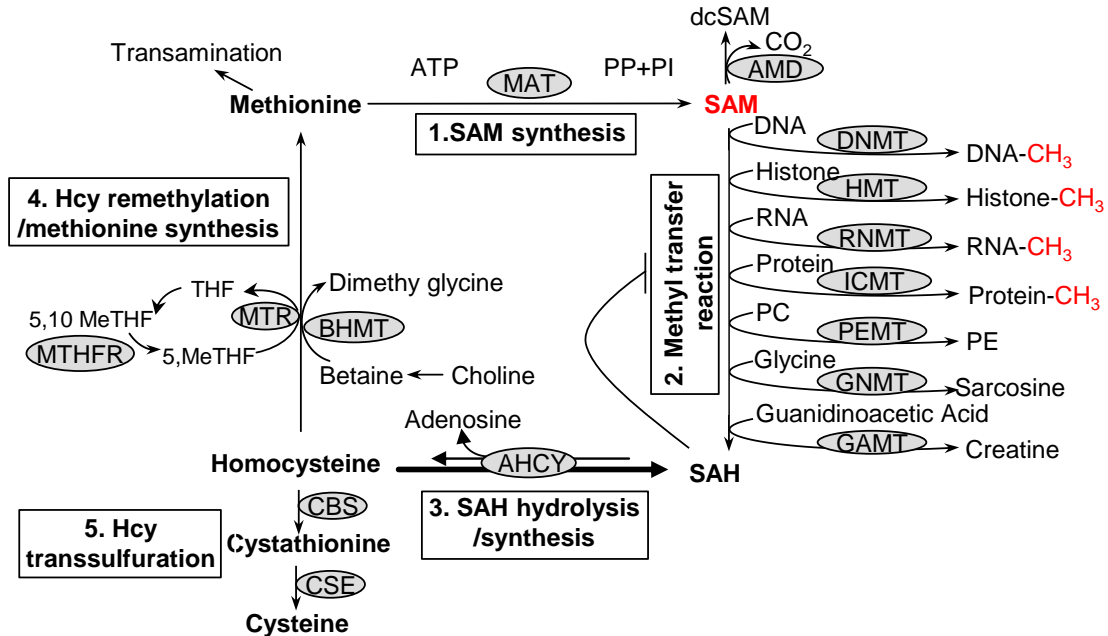


Figure 1.4. Methionine-homocysteine metabolic cycle and cellular methylation. SAM is the major methyl donor for cellular methylation and is an intermediate product in the methionine-homocysteine metabolism cycle, which has five key steps: 1. SAM synthesis; 2. Methyl transfer reaction which transfers methyl group to DNA, histone, RNA and protein as well as other molecules; 3. SAH hydrolysis/synthesis; SAH is a competitive inhibitor of SAM-dependent methyltransferases; SAH hydrolysis is a reversible reaction. Accumulation of Hcy leads to SAH production and inhibits cellular methylation; 4. Hcy remethylation to methionine; 5. Hcy transsulfuration into cysteine. There are 15 enzymes involved in methionine-homocysteine metabolism. AHCY, S-adenosylhomocysteine hydrolase; AMD, S-adenosylmethionine decarboxylase; BHMT, betaine:homocysteine methyltransferase; CBS, cystathionine- β -synthase; CSE, cystathionine- γ -lyase; DNMT, DNA methyltransferase; GAMT, guanidinoacetate N-methyltransferase; GNMT, glycine N-methyltransferase; HMT, histone methyltransferase; ICMT, isoprenylcysteine carboxyl methyltransferases; MAT, methionine adenosyltransferase; MTHFR, 5,10-

methylenetetrahydrofolate reductase; MTR, 5-methyltetrahydrofolate-homocysteine methyltransferase; PEMT, phosphatidylethanolamine N-methyltransferase; RNMT, RNA methyltransferase. Abbreviation: dcSAM, decarboxylated S-adenosylmethionine; Hcy, homocysteine; Met, methionine; 5,10MeTHF, 5-methylenetetrahydrofolate; 5MeTHF, 5-methyltetrahydrofolate; PC, phosphatidylcholine; PE, phosphatidylethanolamine; SAM, S-adenosylmethionine; SAH, S-adenosylhomocysteine; THF, tetrahydrofuran.

2. Methyl transfer reactions

SAM can be converted to SAH after donating its methyl group to DNA, RNA, protein, phospholipid or other biochemical molecules through methyltransferases (Niculescu & Zeisel, 2002). We profiled the tissue mRNA distribution of 12 enzymes involved in homocysteine metabolism and found that methyltransferases are differentially expressed in human and mouse tissues (N. C. Chen et al., 2010).

DNMT1 is important for maintenance of DNA methylation while DNMT3a and DNMT3b are essential for de novo methylation during development. HMTs mediate the histone methylation. Because DNMT and HMT deficiencies usually lead to embryonic lethal phenotype (E. Li, Bestor, & Jaenisch, 1992; Yu, Hanson, Hess, Horning, & Korsmeyer, 1998) and severe development hindrance (Okano et al., 1999) in mice, it can be concluded that their function is more important in development than in metabolism and methylation regulation.

Isoprenylcysteine carboxymethyltransferase (ICMT) catalyzes the transfer of methyl groups from SAM to the α -carboxyl of isoprenylcysteine residues. The small G-proteins, such as Ras and Rho, are important substrates of ICMT and their binding to the cell membrane to conduct signal transduction is triggered by carboxyl methylation via ICMT. In fact, ICMT deficiency in mice leads to embryonic lethality (Bergo et al., 2001), indicating that protein carboxyl methylation mediated by ICMT is crucial for embryonic development.

Phosphatidylethanolamine N-methyltransferase (PEMT) catalyzes phosphatidylcholine to phosphatidylethanolamine. *Pemt*^{-/-} mice display a relatively normal phenotype (Zhu,

Song, Mar, Edwards, & Zeisel, 2003), indicating that PEMT is not critically involved in methylation regulation at least in mice.

Glycine N-methyltransferase (GNMT) catalyzes the transfer of methyl group to glycine to synthesize sarcosine. Another enzyme guanidinoacetate methyltransferase (GAMT) catalyzes the transfer of methyl group to guanidinoacetate to form creatine. Among all methylation reactions, synthesis of creatine/creatinine normally consumes 75%-80% of the total SAM generated in young adult (Mudd & Poole, 1975).

3. SAH hydrolysis/synthesis

SAH is hydrolyzed to adenosine and Hcy by S-adenosylhomocysteine hydrolase (AHCY) (Baric et al., 2004). SAH hydrolysis serves not only to sustain the flux of methionine sulfur toward cysteine, but also plays a critical role in the regulation of methylation. This reaction is reversible but favors the SAH formation. Under physiologic conditions, adenosine and Hcy is rapidly removed, driving the reaction towards SAH hydrolysis. However, in pathological conditions such as during high levels of Hcy, this reaction is reversed, leading to SAH accumulation. Importantly, this reaction is regulated in a cell type specific manner. When EC and VSMC are both treated with pathologically relevant concentration of Hcy (50 μ M), intracellular SAH levels are significantly elevated only in EC but not in VSMC (H. Wang et al., 1997). This induction is associated with EC specific growth inhibition via DNA hypomethylation on CDE (suppressor binding site) of the cyclin A promoter (M. D. Jamaluddin et al., 2007). Consistent with these findings, elevated Hcy levels in patients are linked to increased SAH levels and impaired erythrocyte membrane protein methylation (Perna et al., 1993). Consistently, increased

plasma Hcy levels are associated with increased hepatic SAH and decreased SAM levels in *Cbs*^{+/-} mice (Z. Chen et al., 2001). The SAH-related hypomethylation change in EC may be major biochemical mechanism for Hcy-induced atherosclerosis (M. E. Lee & Wang, 1999; H. Wang et al., 1997).

The plasma levels of SAM, SAH and Hcy are critical for tissue maintenance of correct methylation status. Many studies have suggested that intracellular SAM/SAH ratio (J. M. Kim, Hong, Lee, Lee, & Chang, 2009) is an indicator of DNA methylation level. A higher SAM/SAH ratio represents higher methylation status. Others argue that SAH concentration (Caudill et al., 2001; Ulrey, Liu, Andrews, & Tollefsbol, 2005; Yi et al., 2000) alone is a better indicator of DNA methylation based on the correlation between DNA methylation level and SAH concentration. In light of this, it is recommended to use both SAH concentration and SAH/SAM ratio to determine cellular methylation status.

4. Hcy remethylation/methionine synthesis

Hcy remethylation can be catalyzed by 5-methyltetrahydrofolate-homocysteine S-methyltransferase (MTR), also called methionine synthase, which transfers a methyl group from 5-methyl-tetrahydrofolate to Hcy, generating tetrahydrofolate (THF) and methionine. MTR is extremely important in development as indicated by *Mtr* homozygous knockout embryos which die soon after implantation (Swanson et al., 2001). This lethality is probably due to its role in supplementing methionine synthesis and thus regulating the subsequent methyl-transfer reaction. The 5,10-methylenetetrahydrofolate reductase (MTHFR) catalyzes the conversion of 5,10-methylenetetrahydrofolate (5,10meTHF) to 5-methyltetrahydrofolate (5MeTHF), a co-substrate for Hcy

remethylation to methionine. Hcy remethylation is an essential biochemical process and highly regulated at the tissue level, with both MTR and MTHFR being broadly expressed in most of human and mouse tissues (N. C. Chen et al., 2010). In fact, *Mthfr*^{-/-} mice have increased plasma Hcy and SAH levels, as well as DNA hypomethylation in the liver and brain (Dayal et al., 2005). It is strongly suggested that deficiency or decreased activity of MTHFR reduces the methyl transfer to methionine and contributes to global DNA hypomethylation.

In addition, betaine-homocysteine methyltransferase (BHMT) converts betaine to dimethylglycine while remethylating Hcy to methionine. This reaction mostly takes place in the liver, where BHMT is primarily expressed in human and mice (N. C. Chen et al., 2010). In accordance, *Bhmt*^{-/-} mice had increased hepatic Hcy (6-8 fold) and SAH (3-fold) concentrations, and decreased SAM (43%) (Teng, Mehedint, Garrow, & Zeisel, 2011).

5. Hcy transsulfuration

The Hcy transsulfuration pathway involves two catabolic steps: **1)** Cystathionine- β -synthase (CBS) converts Hcy to cystathionine, and **2)** cystathionine- γ -lyase (CSE) converts cystathionine to cysteine. The CBS gene is expressed in almost all human tissue (N. C. Chen et al., 2010), therefore humans possess a higher level of tissue-specific regulation of the CBS reaction. In mice however, CBS is predominantly expressed in the liver and therefore is rather heavily dependent on liver metabolism. In clinic, CBS deficiency leads to HHcy ranging from 200 to 300 μ M compared to \sim 10 μ M in healthy individuals (L. Wang et al., 2005). Patients with CBS homozygous mutation develops

severe HHcy, CVD, thromboembolic diseases, lens dislocations and osteoporosis, and usually die before thirty years of age due to thromboembolism complications if not treated (Kraus et al., 1999). Similarly, the *Cbs*^{-/-} mice have severe HHcy with concentrations of over 200µM and die within 5 weeks postnatal (Watanabe et al., 1995), suggesting an important role of CBS during the postnatal development.

CSE is expressed predominantly in the liver in both human and mice. In fact, the CSE reaction is likely liver-dependent, and not critical for development nor growth-related metabolism. *Cse*^{-/-} mice do not exhibit any growth problem (G. Yang et al., 2008).

F-BAR protein family

F-BAR (Fes/CIP4 homology and Bin/amphiphysin/Rvs) proteins are important regulators of cell protrusion formation, migration, and endocytosis. These processes depend on the concerted action of the plasma membrane and cytoskeleton, and F-BAR proteins are modular molecules that serve as multivalent adaptors physically and functionally linking both compartments.

Structure of F-BAR proteins

As shown in Figure 1.5, F-BAR proteins contain an F-BAR domain at the N-terminus and usually one or two Src-homology 3 (SH3) domains at the C-terminus. F-BAR domains were first identified as FER/CIP4 homology (FCH) domain, because of a region of sequence similarity between Fer kinase and CIP4 (Aspenstrom, 1997). The following studies expanded the FCH domain to F-BAR domain due to the sequence similarity between the larger domain and BAR domains (Itoh et al., 2005; Tsujita et al., 2006). F-BAR domains are banana-shaped alpha-helical bundles, existing as end to end dimers

(Shimada et al., 2007). The F-BAR domains bind strongly to phosphatidylserine and phosphatidylinositol 4,5-bisphosphate in the cell membrane's inner aspect of the lipid bilayer via electrostatic interactions (Tsujita et al., 2006). Through dimerization, they construct a scaffold at the membrane's edge (Frost, Unger, & De Camilli, 2009). Many F-BAR proteins also contain one or two C-terminal SH3 domains, which serve as the docking site for F-BAR binding proteins, such as Wiskott–Aldrich syndrome protein (WASP)/neuronal Wiskott–Aldrich Syndrome protein (N-WASP) and dynamin.

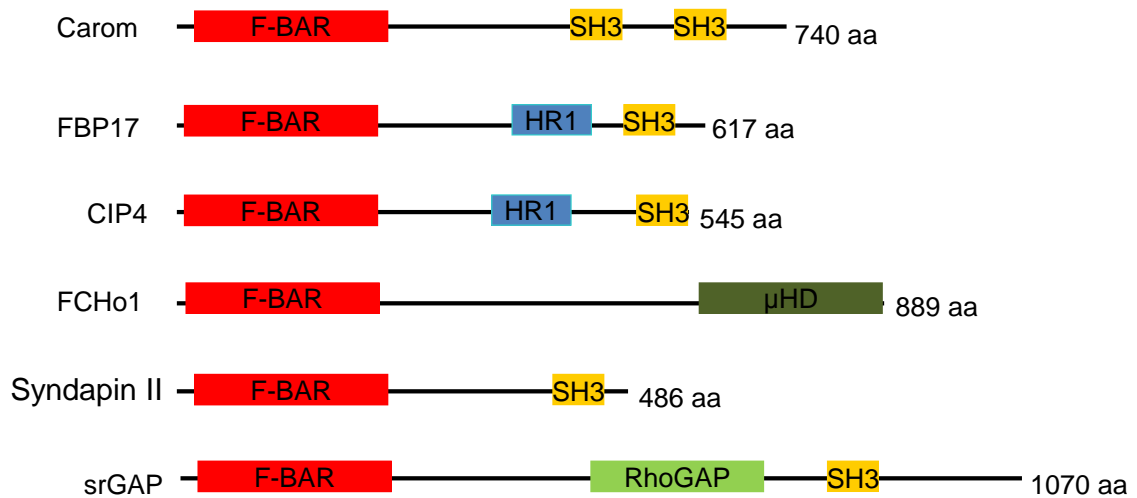


Figure 1.5. Diagram of the domain structures of selected F-BAR proteins. F-BAR: FES-CIP4 Homology and Bin/Amphiphysin/Rvs domain, SH3: Src Homology 3 domain, HR1: Protein kinase C-related kinase homology region 1 domain, μHD: μ-homology domain, RhoGAP: GTPase-activator protein (GAP) for Rho-like small GTPases domain.

Functions of F-BAR proteins

1. Endocytosis

The first studies of F-BAR proteins indicated that F-BAR domains strongly bind to phospholipids, induce *in vitro* tubulation of phospholipid vesicles, and cause membrane tubulation in cultured cells (Itoh et al., 2005; Kamioka et al., 2004; Tsujita et al., 2006). Combined with the observation that full length CIP4, Toca-1 and syndapin recruit WASP family members and dynamin via their SH3 domains (Itoh et al., 2005; Tsujita et al., 2006), these findings immediately suggest F-BAR proteins in the process of endocytosis.

Three following studies have identified the role of F-BAR proteins in endocytosis. One study showed that FCHo proteins define sites of endocytosis. The μ HD domain of membrane-bound FCHo2 recruits intersectin and Eps15 to initiate clathrin coated pit formation and knock-down of FCHo1 and FCHo2 blocks the formation of cortical clathrin spots, a very early step in endocytosis (Henne et al., 2010). The second elegant *in vitro* study, using a cell-free system, demonstrated that FBP17 is recruited after clathrin vesicle budding, to the neck of the budded vesicle (Wu et al., 2010). In a third study, FBP17 and Toca-1 were found to recruit N-WASP to endocytic vesicles, triggering subsequent Arp2/3 complex activation and internalization (Takano, Toyooka, & Suetsugu, 2008). Thus, lipid bilayer curvature can control Arp2/3-dependent F-actin nucleation via F-BAR proteins, perhaps explaining how F-actin nucleation occurs only at the proper stage of endocytosis. Taken together, these studies set the foundation for a model wherein F-BAR proteins play roles in multiple steps of endocytosis.

2. Cell protrusion and migration

There are several types of protrusive structures in cells. Most of these structures contain actin filaments, presumably for their stability and mechanical strength required for the force execution for cell motility or the uptake of extracellular materials. The best-characterized cellular protrusions are filopodia and lamellipodia.

Filopodia are membrane projections that contain long parallel actin filaments arranged in tight bundles. These particular structures act as sensors of motile stimuli. Classically, the formation of filopodia is regulated by activation of the small GTPase Cdc42 that associates with WASPs. Lamellipodia are cytoplasmic protrusions that form at the leading edge of spreading or migrating cells (Small, Stradal, Vignal, & Rottner, 2002). These protrusions are approximately 1 to 5 μm wide and approximately 2 μm thick. The formation of lamellipodia is associated with important actin polymerization involving Rac and Arp2/3 complex. The formation of filopodia and lamellipodia is essential for cell migration. Protrusive structures driven by actin polymerization are also observed in phagocytosis. During phagocytosis, the protruding lamellipodia-like structure surrounds the material that is incorporated into the cell.

The F-BAR domain of srGAP2 was reported to induce membrane invagination in vitro, with the same geometry as found in membrane protrusions, such as filopodia. The overexpression of the F-BAR domain-containing fragment of srGAP2 induced filopodia-like protrusions without actin filament localization (Guerrier et al., 2009).

FBP17 recruitment of WASP and dynamin-2 is necessary for podosomes formation (Tsuboi et al., 2009). TOCA-1 recruits N-WASP, followed by Arp2/3 and actin, then by formins, VASP and fascin, leading to filopodia formation (K. Lee, Gallop, Rambani, &

Kirschner, 2010). In breast cancer cells, CIP4 is a regulator of invadopodia formation (Hu et al., 2011; Pichot et al., 2010), and promotes invadopodia formation through activation of N-WASP (Pichot et al., 2010). WASP could cause actin to polymerize away from the plasma membrane, parallel to it, or toward it (Chitu & Stanley, 2007; Takenawa & Suetsugu, 2007). F-BAR protein variants without an SH3 domain (such as PSTPIP2 or FCHo) may preferably enhance specific processes such as filopodia (Chitu et al., 2005).

Syndapin, also called protein kinase C and casein kinase II interacting protein (PACSIN), is a member of F-BAR protein family. Syndapin was reported to play a role in cell migration and spreading through the Ras/Rac signalling cascade regulating actin dynamics and the formation of membrane protrusions. HeLa cells transiently transfected with syndapin I and II proteins formed actin-rich filopodia localizing with the Arp2/3 complex enriched at the tips of actin polymerization and turnover (Qualmann & Kelly, 2000). Endogenous syndapin II in HeLa cells localizes to vesicular tubular structures and this distribution is regulated by microtubules. Syndapin II SH3 domain interacts directly with the C-terminus of Rac1 and colocalizes on intracellular tubular structures, early endosomes and peripheral membrane protrusions. Silencing of syndapin II by siRNA increases the levels of Rac1-GTP and promotes cell spreading and migration in a wound healing assay (de Kreuk et al., 2011).

Carom, an F-BAR protein, is up-regulated by Hcy in EC.

Our laboratory has demonstrated that Hcy selectively inhibits EC proliferation, arrests the EC Cell cycle at the G₁/S Transition (H. Wang et al., 1997). To further explore the mechanisms of Hcy-induced EC growth inhibition, we showed that Hcy inhibits DNMT-

1 activity, but not DNMT-3A/B, and selectively reduces cyclin A mRNA expression by induction of hypomethylation of cyclin A promoter (M. D. Jamaluddin et al., 2007; H. Wang et al., 2002).

Considering that DNMT-1 plays a vital role in maintaining the existing methylation pattern following DNA replication, Hcy-inhibited DNMT-1 activity could lead to hypomethylation not only in cyclin A promoter, but also in other genes. Thus, there are probably some genes which expression levels are changed in response of Hcy treatment in EC.

To find Hcy-responsive genes in EC, we performed differential display and identified a novel gene, Carom. The human Carom gene is located on chromosome 11 (chr11:72547790-72853143). Its cDNA length is 4507 bp, encoding a protein of 740aa. The Carom protein contains 1 N-terminal F-BAR (FES-CIP4 Homology and Bin/Amphiphysin/Rvs) domain and 2 C-terminal SH3 domains (Figure 1.6), providing it with the Genebank name of Carom is FCHSD2. Carom is a member of F-BAR protein family.

With protein BLAST alignment, Human FCHSD2 and its murine homologs Fchsd2 are 96.5% identical at the amino acid level. Human FCHSD2 has 20 exons and four F-BAR encoding alternative splice forms. FCHSD2a (mRNA ID: NM_014824) is a 740aa full length protein. FCHSD2b (mRNA ID: AB018312) is alternatively spliced at exons 1 and 2, resulting in an N terminus truncated FCHSD2 protein of 684aa in length. The FCHSD2c (mRNA ID: AK296376) is highly similar to *Mus musculus* Fchsd2, with 604aa. FCHSD2d (mRNA ID: BC010394) containing one F-BAR domain, one SH3

domain and one Variant SH3 domain, is 530aa. FCHSD2e (mRNA ID: AA831767) only contains a truncated F-BAR domain with 221aa.

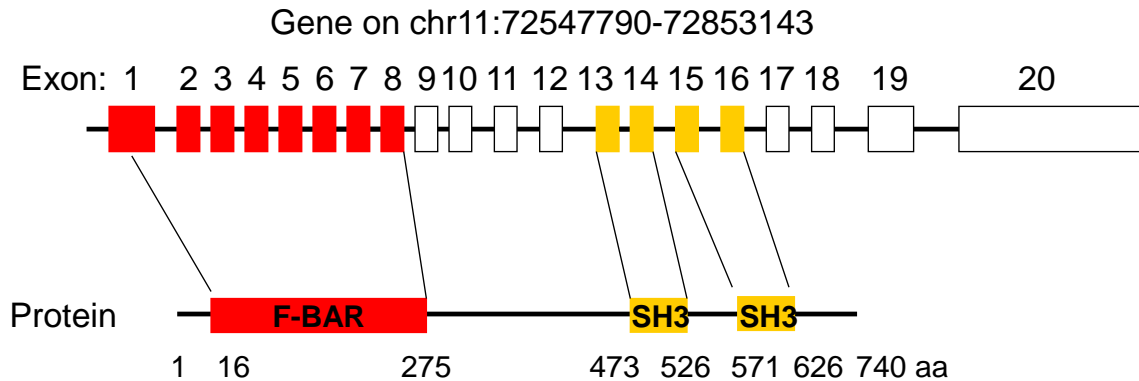


Figure 1.6. Carom gene and protein. Human Carom gene locates on chromosome 11. Totally 20 exons encode mature Carom mRNA. Carom protein is 740 aa long, containing 1 F-BAR domains in N-terminus and 2 SH3 domains in C-terminus.

Carom was first identified as a membrane-associated guanylate kinase (MAGUK)-interacting protein in 2003 (Ohno et al., 2003). The MAGUK proteins play central roles in the molecular organization of epithelial junctions, which are implicated in the signal transduction that regulates cell proliferation. MAGI-1 is a member of the MAGUK family and involved in epithelial tight junction. In search of the MAGI-1-interacting protein, Ohno et al. obtained a protein, which is a KIAA0769 gene (an aberrant human FCHSD2 cDNA) product, through the yeast two-hybrid screening using MAGI-1 as bait, and named it Carom. Furthermore, they found Carom binds to the fifth PDZ domain of MAGI-1 via a PDZ-binding motif in its C-terminus. Then they tested the interaction of

Carom with a variety of PDZ proteins including CASK, and CASK was shown to interact with Carom through the calmodulin kinase domain (Ohno et al., 2003).

In 2004, Carom was identified as FCHSD2 (Katoh & Katoh, 2004). Since then, there are only two publications about Carom. One study showed that overexpression of Carom increased chemoresistance, while Carom shRNA enhanced chemosensitivity in U937 cells. The average Carom expression level in acute myeloid leukemia (AML) patients with complete remission was significantly lower than that in non-responder patients. These data suggest that Carom could be a predictor of outcome for AML patient (Han et al., 2012). Another study found that Carom expressed in mouse hair cell and stimulates F-actin assembly (Cao et al., 2013).

Nwk, a Carom ortholog, was first identified in *Drosophila* where mutations of *nwk* gene cause excessive growth of neuromuscular junctions (NMJ), resulting in seizure-like spasms and paralysis (Coyle et al., 2004). Nwk modulates F-actin dynamics or endocytosis via binding to F-actin regulatory proteins Wsp, Dynamin, Dap160, and Snx16 (O'Connor-Giles, Ho, & Ganetzky, 2008; Rodal et al., 2011; Rodal, Motola-Barnes, & Littleton, 2008).

Angiogenesis and EC Migration

Blood vessels supply oxygen and nutrients and provide gateways for immune surveillance. Endothelial cells line the inner surface of vessels to support tissue growth and repair. As this network nourishes all tissues, angiogenesis is required in many physiological and pathological conditions, including embryonic development, wound healing, tissue regeneration, and tumor growth. In the adult, vessels are quiescent and rarely form new branches. Insufficient vessel growth or maintenance can lead to stroke, myocardial infarction, ulcerative disorders and neurodegeneration, and abnormal vessel growth or remodelling fuels cancer, inflammatory disorders, pulmonary hypertension and blinding eye diseases (Carmeliet, 2003; Folkman, 2007).

Formation of Blood Vessels

Endothelial cells derive from the successive differentiation of mesodermal cells into hemangioblasts, which leads to the formation of the first vascular structures that are called primitive blood islands. The hemangioblasts from the center of the islands give rise to the hematopoietic stem cells, whereas the peripheral hemangioblasts differentiate into angioblasts, the precursors of mature endothelial cells. Under the influence of vascular endothelial growth factor (VEGF), the angioblasts and newly formed endothelial cells migrate on a matrix constituted mainly of collagen and hyaluronan, allowing the fusion of the blood islands, their remodeling into tubular structures, and the formation of the first primitive vascular plexus. These tubules remodel through vasculogenesis into larger vessels, leading to vascularization of the embryo (Swift & Weinstein, 2009). Subsequent vessel sprouting creates a network that remodels into arteries and veins, known as

angiogenesis (Adams & Alitalo, 2007). Arteriogenesis then occurs, in which endothelial cell channels become covered by pericytes or VSMCs, which provide stability and control perfusion (Jain, 2003).

Angiogenesis Process

In a healthy adult, quiescent endothelial cells have long half-lives and are protected against insults by the autocrine action of maintenance signals such as VEGF, NOTCH, angiopoietin-1 (ANG-1) and fibroblast growth factors (FGFs). Because vessels supply oxygen, endothelial cells are equipped with oxygen sensors and hypoxia-inducible factors — such as prolyl hydroxylase domain 2 (PHD2) and hypoxia-inducible factor-2 α (HIF-2 α), respectively — which allow the vessels to re-adjust their shape to optimize blood flow. Quiescent endothelial cells form a monolayer of phalanx cells with a streamlined surface, interconnected by junctional molecules such as VE-cadherin and claudins. These endothelial cells are ensheathed by pericytes, which suppress endothelial cell proliferation and release cell-survival signals such as VEGF and ANG-1. Endothelial cells and pericytes at rest produce a common basement membrane. When a quiescent vessel senses an proangiogenic signal, such as VEGF, VEGF-C, ANG-2, FGFs or chemokines, released by a hypoxic, inflammatory or tumour cell, pericytes first detach from the vessel wall (in response to ANG-2) and liberate themselves from the basement membrane by proteolytic degradation, which is mediated by matrix metalloproteinases (MMPs). Attracted by proangiogenic signals, ECs become motile and invasive and protrude filopodia. These so-called tip cells spearhead new sprouts and probe the environment for guidance cues. Following tip cells, stalk cells extend fewer filopodia but establish a lumen and proliferate to support sprout elongation. Tip cells anastomose with

cells from neighboring sprouts to build vessel loops. The initiation of blood flow, the establishment of a basement membrane, and the recruitment of mural cells stabilize new connections (Adams & Alitalo, 2007; Carmeliet & Jain, 2011; Potente, Gerhardt, & Carmeliet, 2011).

EC Migration in Angiogenesis

As described, EC migration is the key step during angiogenesis. The constant remodeling of the actin cytoskeleton into filopodia, lamellipodia, and stress fibers is essential to drive the several steps of actin-based endothelial cell: (1) sensing of the motogenic signal by filopodia; (2) formation and protrusion of lamellipodia and pseudopodia-like forward extension; (3) attachment of the protrusions to the extracellular matrix (ECM); (4) stress fiber-mediated contraction of the cell body to allow forward progress; (5) rear release; and (6) recycling of adhesive and signaling materials (Lamallice, Le Boeuf, & Huot, 2007).

Endothelial cell migration involves 3 major mechanisms: chemotaxis, the directional migration toward a gradient of soluble chemoattractants; haptotaxis, the directional migration toward a gradient of immobilized ligands; and mechanotaxis, the directional migration generated by mechanical forces (S. Li, Huang, & Hsu, 2005). EC migration during angiogenesis is the integrated resultant of these 3 mechanisms. Typically, chemotaxis of endothelial cells is driven by growth factors such as VEGF and basic fibroblast growth factor (bFGF), whereas haptotaxis is associated with increased EC migration activated in response to integrins binding to ECM component (Giroux et al., 1999; Klemke et al., 1997). Because of their location at the inner face of blood vessels,

endothelial cells are constantly in contact with shear stress, which contributes to activate migratory pathways. In fact, there is now accumulating evidence that fluid shear stress initiates mechanotaxis and modulates the various steps of migration including extension at the leading edge, adhesion to the matrix, and release of adhesions at the rear (S. Li et al., 2005). Hence, endothelial cell migration is a mechanically integrated molecular process that involves dynamic, coordinate changes in cell adhesion, signal transduction, and cytoskeletal dynamics and organization.

Angiogenesis and CVD

The role of angiogenesis in CVD is controversial. Although angiogenic cytokines such as VEGF or FGFs has been widely used to stimulate collateral blood vessel formation in the ischemic heart disease and to enhance arterioprotective functions of the endothelium (Simons & Ware, 2003), some studies suggest that neovascularization contributes to the growth of atherosclerotic lesions (Kamat, Galli, Barger, Lainey, & Silverman, 1987; Sueishi et al., 1997; Williams, Armstrong, & Heistad, 1988; Zamir & Silver, 1985; Y. Zhang, Cliff, Schoefl, & Higgins, 1993) and the angiogenic cytokine VEGF promotes atherosclerosis (Celletti et al., 2001). Noteworthy, there is no evidence indicating that vasa vasorum significantly contributes to the disease process and it is very difficult to attribute the effects of VEGF on atherosclerosis to angiogenesis alone because VEGF causes a complex array of other biological responses, including increased vascular permeability, monocyte chemotaxis, vasodilatation, and hypotension (Ferrara, Gerber, & LeCouter, 2003).

Key Knowledge Gaps

HHcy has been established as an independent risk factor of CVD. EC injury, EC dysfunction, monocyte activation, thrombosis activation, and VSMC proliferation have all been suggested as mechanisms by which elevated Hcy mediates pathological cardiovascular changes. Vascular disease may be initiated by endothelial injury resulting from insult to the vessel wall. Endothelial injury subsequently leads to platelet aggregation, coagulation, VSMC proliferation, and atherosclerosis. EC dysfunction is an early event in the development of atherosclerosis, occurring before morphological changes in the endothelium can be detected. HHcy has already been demonstrated to induce EC injury and EC dysfunction. However, the molecular mechanisms underlying these EC disorders are not well understood.

Our laboratory has demonstrated that Hcy selectively inhibits EC proliferation, arrests the EC cell cycle at the G₁/S Transition (H. Wang et al., 1997). Furthermore, we found that Hcy selectively reduces cyclin A expression in EC through demethylation of cyclin A promoter, which results in EC growth inhibition (M. D. Jamaluddin et al., 2007; H. Wang et al., 2002). However, cyclin A inhibition in EC occurs after 24h treatment of Hcy. The early events in the Hcy signaling pathway of EC growth inhibition remain to be elucidated.

We reported that Hcy selectively inhibits cyclin A transcription and EC growth through a hypomethylation related mechanisms, which block cell cycle progression and endothelium regeneration. Hcy can use adenosine, a normal constituent of all body fluids, to form SAH, a potent inhibitor of cellular methylation. We found that elevated Hcy

increases SAH level and inhibits DNMT-1 activity in EC (M. D. Jamaluddin et al., 2007; H. Wang et al., 1997). Hcy-induced DNMT-1 inactivation leads to cyclin A promoter CDE demethylation, and the reduction of MBP and increased bindings of ACH3 and ACH4 on cyclin A promoter (M. D. Jamaluddin et al., 2007). Cyclin A promoter remodeling may facilitate the function of CDE suppressor and result in cyclin A suppression, which finally leads to EC growth inhibition. It is also reported that Hcy causes hypomethylation of CpG sites 6 and 7 of P66shc promoter, which leads to increased P66shc expression, causing oxidative stress and endothelial dysfunction (C. S. Kim et al., 2011). HHcy-induced EC disorders are complicated multi-step processes, in which various genes could be involved. Moreover, Hcy-inhibited DNMT-1 activity may lead to hypomethylation throughout the whole genome of EC, leading the transcription activation or inactivation of Hcy-responsive genes. However, the list of Hcy-responsive genes so far is too short. More genes regulated by Hcy to mediate pathological changes in EC which contribute to CVD still remain unclear.

Hypothesis of Dissertation

Encouragingly, our lab has found an early Hcy-induced gene – Carom, using differential display to screen mRNA samples from EC following 12h Hcy-treatment. Carom is a member of the F-BAR protein family, it interacts with CASK in epithelial cells (Ohno et al., 2003). There are only two studies about Carom function. One showed that Carom expression negatively correlates with chemotherapy outcome in AML patients (Han et al., 2012). Another found that Carom is expressed in mouse hair cell and stimulates F-actin assembly (Cao et al., 2013). Beyond these, the function of Carom is largely unknown. Recent studies demonstrate that CASK, the Carom-interacting protein, plays a role in cell

cycle progress. Overexpression of CASK in ECV304 cells inhibited cell growth, while blocking CASK promoted cell proliferation. Furthermore, CASK upregulates the mRNA and protein expression level of p21, a potent cyclin-dependent kinase inhibitor, which binds to and inhibits the activity of cyclin-CDK2 or -CDK4 complexes, and thus functions as a regulator of cell cycle progression at G₁ (Sun et al., 2009). Knockdown of CASK leads to increased proliferation in cultured keratinocytes. Accelerated cell cycling in CASK knockdown cells is associated with upregulation of Myc and hyperphosphorylation of Rb (Ojeh, Pekovic, Jahoda, & Maatta, 2008). Considering the interaction between Carom and CASK, it is possible that Carom plays a role in cell growth inhibition via CASK. We have already found that Hcy selectively inhibits EC proliferation, reduces cyclin A expression and induces upregulation of Carom expression prior to downregulation of cyclin A in EC. These data suggest that Carom may be involved in the Hcy signaling pathway which that leads to EC proliferation inhibition. In addition, Carom is a member of F-BAR protein family, which plays a role in cell migration. Carom-interacting protein MAGI1 has been indicated to inhibit the cancer cell migration and invasion of hepatocellular carcinoma via regulating PTEN (G. Zhang & Wang, 2011). Furthermore, CASK was also found to play an inhibitory role in MDCK cell migration (Marquez-Rosado, Singh, Rincon-Arano, Solan, & Lampe, 2012). Since Hcy has been demonstrated to inhibit EC migration both in vitro and in vivo (Jacovina et al., 2009; Tan et al., 2006), Carom may mediate Hcy-induced EC migration inhibition. Thus, we **hypothesize** that Hcy upregulates Carom gene to inhibit EC proliferation or EC migration (Figure 1.7). This hypothesis will be examined by using following three specific aims:

Specific aim 1: Confirm Carom induction by Hcy and characterize Carom function in EC.

Study 1: Confirm Hcy-induced Carom expression in cultured EC.

Study 2: Examine Carom expression in EC from Hyperhomocysteinemia mice.

Study 3: Characterize Carom's function in EC.

Specific aim 2: Determine the mechanisms underlying Carom induction.

Study 1: Determine the role of methylation in Carom expression.

Study 2: Map the methylation status changes in Carom gene induced by Hcy in EC.

Specific aim3: Identification of signaling molecules mediating Carom's function.

Study 1: Identify Carom regulated signaling molecules in EC.

Study 2: Determine the role of Carom regulated molecules in EC biology.

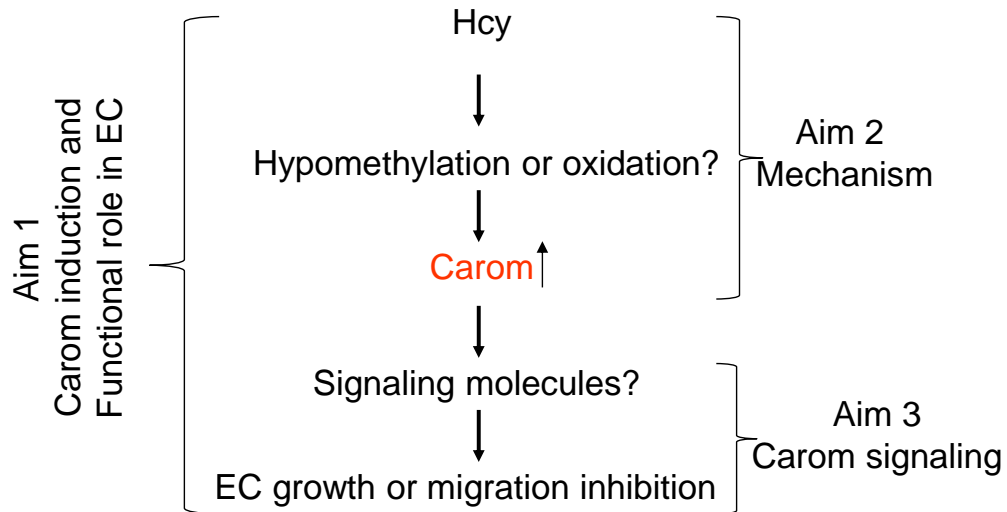


Figure 1.7. Hypothesis and specific aims. The central hypothesis is that Hcy up-regulates Carom gene via hypomethylation or oxidation to trigger downstream signaling molecules which contribute to the inhibition of EC migration or proliferation. There are three specific aims. Aim 1: Confirm induction of Carom by Hcy and determine the role of Carom in EC biology; Aim 2: Determine the mechanisms underlying Carom induction; Aim3: Identification of signaling molecules mediating Carom’s function.

CHAPTER 2

MATERIALS AND METHODS

Tissue Expression Profiling of Carom Gene in Human and Mouse

A data mining strategy was used as previous described (N. C. Chen et al., 2010; Huang et al., 2013) to establish the tissue expression profiles of Carom gene. 21 human and 20 mouse tissues were given tissue ID numbers and examined for mRNA expression by mining human and mouse expression sequence tag (EST) databases deposited in the NIH UniGene database. The EST database is created via cDNA cloning from various tissue cDNA libraries followed by DNA sequencing. As previous described, we used relative mRNA expression units (REU) of Carom, normalized by the transcript per million (TPM) of Carom with that of β -actin (left-side y axis). Further, we determined median REU (mREU) of the human and mouse tissues in order to compare the gene expression. The ratio of REU/mREU is expressed as tissue median adjusted mRNA expression units and is presented in Figure 3.2 (right-side y axis). Confidential interval of the gene expression was generated using mean REU and 2 times the standard deviation (SD) [mean + 2SD] of the REU of 3 randomly selected housekeeping genes [pituitary tumor-transforming 1 interacting protein (PTTG1IP), pyruvate kinase muscle (PKM2), and heterogeneous nuclear ribonucleoprotein K (HNRNPK)] in 21 human or 20 mouse tissues, normalized by β -actin in given tissues. If the expression variation of Carom gene in the tissues was larger than the upper limit of the confidential interval of the housekeeping genes, the high expression levels of genes in the tissues were considered statistically significant.

Chemicals and Antibodies

All chemicals were purchased from Sigma-Aldrich (St Louis, MO) unless stated. Anti-FLAG antibody was purchased from Sigma-Aldrich (St Louis, MO). Anti- β -actin, Horseradish Peroxidase (HRP) conjugated anti-mouse and anti-rabbit immunoglobulin G (IgG) antibodies were purchased from Cell Signaling Technology (Beverly, MA). IRDye 800CW anti-Rat IgG was purchased from Li-Cor (Lincoln, NE). Anti-CXCL10 and Anti-CXCL11 neutralizing antibodies were purchased from R&D Systems (Minneapolis, MN). Radiolabelled [^3H]Thymidine was purchased from Perkin Elmer (Waltham, MA). Fetal bovine serum (FBS) was from Gibco (Carlsbad, CA).

Animals

The transgenic mice, Tg-hCBS, were established as previously described (L. Wang et al., 2005; D. Zhang et al., 2009). All mice are in a C57BL/6 background. Pups were genotyped at day 10 for both human transgene CBS and mouse Cbs gene. These mice were fed with 25 mM ZnSO₄ containing water for the first four weeks postnatal. ZnSO₄ was withdrawn after weaning at 1 month of age. For ZnSO₄ water therapy group, mice were fed with two weeks of ZnSO₄ water beginning at 10 weeks to lower their Hcy levels. Experimental animals were group-housed (5 per cage) on a 12-h light-dark cycle with access to food and water in a temperature and humidity controlled environment. Animals were fed with standard rodent chow diet (0.67% methionine; 5001; Labdiet, Saint Louis, MO). Age-matched male littermates were selected for experiments. Control

mice for all experiments were sibling transgene-positive mice that were in *Cbs*^{+/+} background.

The mouse protocols were approved by the Temple University Institutional Animal Care and Use Committee.

Mouse Genotyping

Mouse toes were cut at postnatal day 10 and digested with a lysis buffer (100 mM Tris-Cl pH 8.0, 5 mM EDTA, 0.2% SDS, 200 mM NaCl, 400 µg/mL proteinase K) and supernatant were extracted and precipitated using 100% ethanol. DNA was finally dissolved in TE buffer and used for PCR.

Genotyping for the mouse *Cbs* allele was performed using a three primer PCR system developed by the Loscalzo Laboratory. The three primers used are 5'-GAAGTGGAGCTATCAGAGCA-3' (forward primer), 5'-TGGCTCTTGGTTCTGAAACC-3' (reverse primer, WT), 5'-GAGGTCGACGGTATCGATA-3' (reverse primer, KO). The PCR condition is 94°C for 1 min, 60°C for 1 min and 72°C for 1 min for a total of 30 cycles. The wild-type allele gives an 800 bp product, whereas the deleted allele gives a 450 bp product. Human CBS allele was examined using a primer pair developed by the Kruger Laboratory. The two primers used are 5'-ATGTAGTTCCGCACTGAGTC-3' (forward primer), 5'-AGTGGGCACGGGCGGCACCA-3' (reverse primer). The human CBS gene product is 380 bp. The PCR condition is 94°C for 30s, 60°C for 30s and 72°C for 30s for a total of

30 cycles. The PCR products were separated by 2% agarose gel and examined by a Foto analyst image system (Hartland, WI).

Cell Culture

Human umbilical vein endothelial cells (HUVEC, Lonza CC2517) and human aortic endothelial cells (HAEC, Lonza CC2535) were cultured in M199 medium (Hyclone, Logan, UT) supplemented with 20% fetal bovine serum, 50 µg/mL EC growth supplement (BD Biosciences, Franklin Lakes, NJ), 50 µg/mL heparin, and 100 U/mL penicillin, 100 U/mL streptomycin, and 0.25 µg/mL amphotericin (Invitrogen, Carlsbad, CA). In some experiments, 40 µM adenosine and 10 µM erythro-9-(2-hydroxy-3-nonyl)-adenine (EHNA) were added to the medium.

Differential Display

Differential Display is the technique by which a researcher can compare and identify changes in gene expression at the mRNA level between any pair of eukaryotic cell samples (Liang & Pardee, 1992). As shown in Figure 2.1, Differential Display starts from RNA extraction from cell with treatment and control group. Then total RNA is reverse transcribed to cDNA, and this cDNA is amplified with an anchored oligo-dT primer and a set of short primers of arbitrary sequences by PCR. The PCR products are displayed by agarose gel electrophoresis. Side-by-side comparisons of such complementary DNA patterns between relevant RNA samples indicate differences in gene expression.

Differentially expressed cDNA bands can be retrieved and sequenced for further molecular characterization.

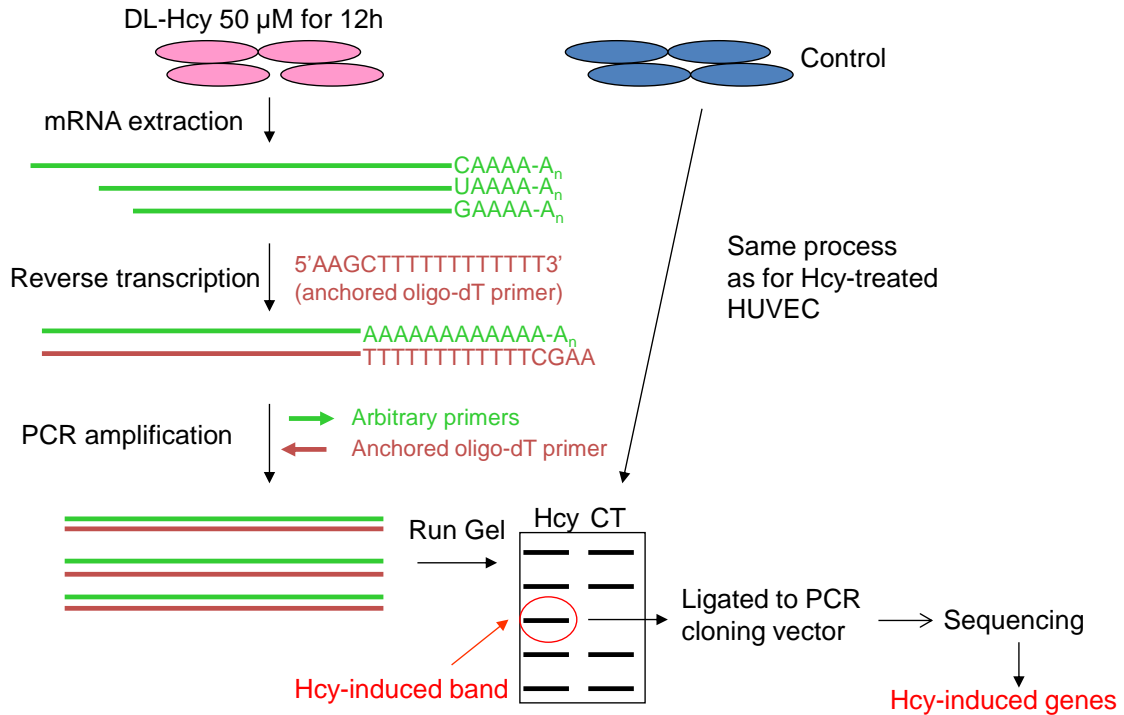


Figure 2.1. Differential Display to identify Hcy-induced genes in HUVECs. This schematic diagram shows the main steps of Differential Display. Total RNA from Hcy-treated HUVECs is extracted and reverse transcribed to cDNA. Then cDNA is amplified with an anchored oligo-dT primer and a set of short primers of arbitrary sequences by PCR. The PCR products are displayed by agarose gel electrophoresis. Side-by-side comparisons of such complementary DNA patterns between RNA samples from Hcy group and control group indicate differences in gene expression. Differentially expressed cDNA bands can be retrieved and sequenced for further molecular characterization.

Total RNA was obtained from Hcy-treated HUVECs by guanidinium isothiocyanate extraction and centrifugation through cesium chloride. First-strand oligo(dT)-primed cDNA synthesis was performed in 50 µl reactions consisting of 1 µg RNA, 50 mM Tris-HCl (pH 8.3), 50 mM KCl, 4 mM MgCl₂, 0.1 mM each dNTP, 20 mM DTT, 6 µM oligo(dT) primer [5' -AAGC(T)₁₂-3'], 20 units RNasin (Promega, Madison, WI) and 40 units Moloney murine leukemia virus reverse transcriptase (Pharmacia, Sweden). Reactions were incubated at 37°C for 90 min and then heated to 60°C for 10 min. The mix was centrifuged through a Sephadex G-25 column (Pharmacia, Sweden) and adjusted to 100 µl. For PCR amplification, 2 µl of the cDNA template was used in 25 µl reactions containing 10 mM Tris-HCl (pH 8.3), 25 mM KCl, 2 mM MgCl₂, 0.1 mM each dNTP, 0.5 µM decamer primer (Operon Technologies, Alameda, CA) and 0.5 mM oligo(dT) primer (as for first-strand cDNA synthesis). Forty-five amplification cycles (1 min at 94°C, 1 min at 40°C, 2 min at 72°C) were performed in a Perkin-Elmer thermal cycler. Reaction products were resolved on a 1.4% agarose gel, visualized by ethidium bromide staining, and excised for cloning. The differentially amplified bands was gel purified and cloned in the TA Cloning Kit (Invitrogen, Carlsbad, CA), and then sequenced. The sequences of differential displayed clones were analyzed with Basic Local Alignment Search Tool (BLAST, <http://blast.ncbi.nlm.nih.gov/Blast.cgi>) to identify Hcy-induced genes.

Generation of Rabbit antibody against Carom

1. Antigen Analysis

To generate specific anti-Carom antibody, the antigen to be injected into animals should be the common region among most isoforms of Carom protein, should be hydrophilic enough to expose to immune cells, and be highly antigenic to induce an adaptive immune response. We used AceView (<http://www.ncbi.nlm.nih.gov/iebr/research/acembly/>) to align all public mRNA sequences of human Carom, and found that exons 2-8 of the human whole length Carom mRNA (NM_014824) cover most of alternative transcript variants (Figure 2.2). Exons 2-8 encode the fragment from aa21 to aa230 of Carom protein. This fragment is part of F-BAR domain, and named as CaromAg. Then we used Lasergene software (DNASTAR, Madison, WI) to analyze the hydrophilicity and antigenicity of Carom protein, as shown in Figure 2.2.

2. Production of GST-CaromAg Fusion Protein as the Antigen

The gene encoding CaromAg was inserted into Sal I site of the Glutathione S-transferase (GST) expression vector pGEX-6P2 (GE Healthcare Life Sciences, Piscataway, NJ) to generate pGEX-6P2-CaromAg vector to express GST-CaromAg fusion protein. pGEX-6P2-CaromAg was transformed to *E. coli* BL21 (GE Healthcare Life Sciences, Piscataway, NJ) to express fusion protein. GST-CaromAg fusion protein was then purified through Glutathione Sepharose 4B (GE Healthcare Bio Sciences, Sweden).

3. Production and Purification of Rabbit anti-Carom Antibody

Purified GST-CaromAg fusion protein was injected to 2 rabbits (1 mg/rabbit, 1 prime injection and 3 boosters) by Pacific Immunology (Ramona, CA), antisera were collected. Antisera in a series of dilution were incubated with total HUVEC proteins transferred to nitrocellulose membranes in Mini-PROTEAN II multiscreen apparatus (Bio-Rad, Hercules, CA). The membranes were then blotted with HRP-conjugated anti-rabbit IgG (Cell Signaling, Beverly, MA), detected with SuperSignal West Pico Chemiluminescent Substrate (Pierce Biotechnology, Rockford, IL), and exposed to film.

Anti-Carom antibody was purified from the crude anti-Carom rabbit sera of high specificity with cross-linked Glutathione-GST and Glutathione-GST-CaromAg sepharoses as described (Bar-Peled & Raikhel, 1996).

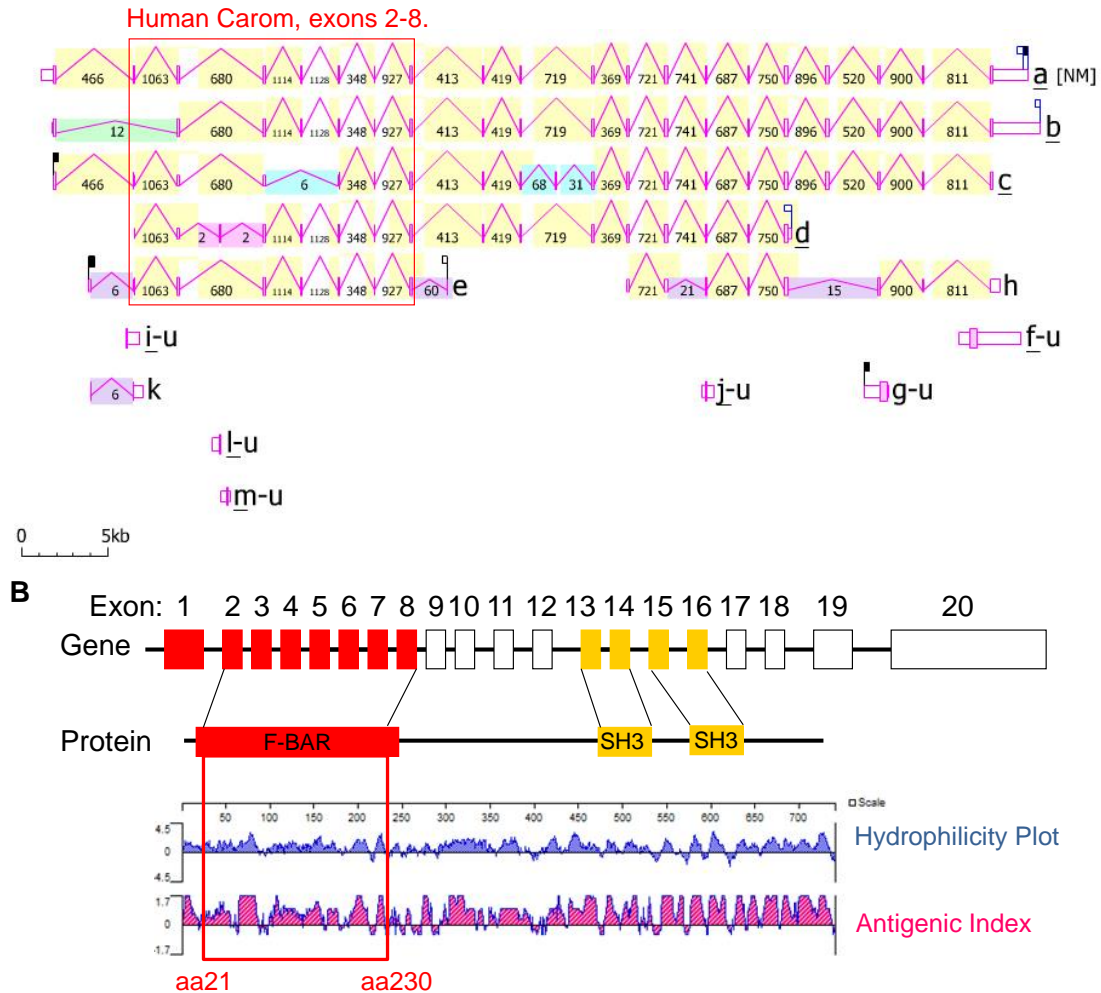


Figure 2.2. Antigen analysis for production of anti-Carom antibody.

A. Alignment of human Carom mRNA isoforms with AceView (<http://www.ncbi.nlm.nih.gov/iebr/research/acembly/>). Exons 2-8 of the human whole length Carom mRNA (NM_014824) cover most of alternative transcript variants. B. Hydrophilicity and antigenicity of Carom protein. Exons 2-8 encode the fragment from aa21 to aa230 of Carom protein. This fragment covers most of the F-BAR domain on Carom protein. The hydrophilicity and antigenicity of Carom protein was analyzed with Lasergene software (DNASTAR, Madison, WI).

Plasma and intracellular SAM, SAH, and Hcy measurement

2.3×10^6 (80% confluence) HAECs P8 were seeded in 10 cm dishes and treated with Hcy for 24 hr. Then cells were washed with PBS and cell pellets were harvested. Then cell pellets were directly dissolved in 100 μ L 0.1 M perchloric acid (PCA) and frozen in liquid nitrogen. Hcy, SAM, and SAH concentrations were measured by liquid chromatography/electrospray tandem mass spectrometry methods as described previously (Liao et al., 2006).

Protein Extraction and Western Blot Analysis

Cultured cells were homogenized in lysis buffer (50 mM Tris-Cl pH 6.8, 100 mM NaCl, 1 mM DTT, 1 mM EDTA, 1 mM PMSF, 1% SDS, 3.25% glycerol and protease inhibitor), boiled for 10 min and followed with sonication. 25 μ g protein was solubilized in sample buffer (0.1 M Tris-Cl, 2% SDS, 1% glycerol, 0.1% bromophenol blue, and 100 mM DTT), boiled for 10 min and loaded in SDS polyacrylamide gel. Proteins were separated by gel electrophoresis and transferred onto nitrocellulose membranes. Blots were stained with 1% Ponceau S for loading controls. Then blots were blocked with 5% nonfat milk in TBST (TBS + 0.1% Tween) for 1 hr at room temperature and probed with primary antibody overnight or longer time at 4°C. Blots were then washed 4 times with TBST for 10 min. HRP conjugated anti-mouse, rabbit or goat secondary antibodies were incubated for 1 hr at room temperature. Blots were washed for 4 times with TBST for 10 mins. Then antigen-antibody complexes were detected by film exposure and development.

Densities were calculated with Image Gauge software (Fujifilm Medical Systems, Stamford, CT).

Primary Mouse Lung EC Isolation

Tg-hCBS Cbs^{-/-}, *Tg-hCBS Cbs^{+/-}* and *Tg-hCBS Cbs^{+/+}* (*Wt*) mice (n = 5 in each group) at 13-14 weeks old were anesthetized by sodium pentobarbital and lungs were dissected and digested with 1 mg/mL collagenase type I for 45 min at 37°C. Then the single cell suspension was labeled and selected with sheep anti-rat magnetic beads coated with rat anti-mouse CD31 antibody. Then selected cells were homogenized in lysis buffer (50 mM Tris-Cl pH 6.8, 100 mM NaCl, 1 mM DTT, 1 mM EDTA, 1 mM PMSF, 1% SDS, 3.25% glycerol and protease inhibitor), boiled for 10 min and followed with sonication. The cell lysate was then subject to Western blot with anti-Carom antibody.

[³H]-Thymidine Incorporation

Cells were plated onto 24-well plates and grown to 70–80% confluence. The cells were incubated with fresh medium containing 50 mM adenosine and 10 mM EHNA for 24 h and exposed to treatments. Cells were metabolically labeled with 1 mCi/ml [methyl-³H]-thymidine (Perkin Elmer, Waltham, MA) for the last 3 h. After labeling, the cells were washed with phosphate-buffered saline, fixed with cold 10% trichloroacetic acid, and then washed with 95% ethanol. Incorporated [methyl-³H]thymidine was extracted in 0.2 N NaOH and measured in a liquid scintillation counter.

RNA Extraction and Real-Time PCR

Total mRNA was extracted from cultured cells using Trizol (Invitrogen, Carlsbad, CA) followed with chloroform extraction and isopropyl alcohol precipitation. The mRNA was reverse transcribed into cDNA using High-Capacity Reverse Transcription Kits (Applied Biosystems, Foster City, CA). The mRNA levels of target genes were determined by quantitative Real-time PCR, a SYBR-green PCR system (SABiosciences, Frederick, MD) was used, and the Real-time PCR was ran on StepOnePlus real-time PCR system (Applied Biosystems, Foster City, CA). As shown in Table 1, Real-time PCR primers for the target genes were designed with Primer Premier 5 (Premier Biosoft, Palo Alto, CA) and synthesized by Integrated DNA Technologies (Coralville, IA).

Table 2.1. Real-time PCR Primers of Target Human Genes.

Gene Name	Primers Sequences
Carom	Forward: 5' GGAGTTTTCCCATCGGTGC 3' Reverse: 5' TGGAGGCAGGGAGGCG 3'
β -Actin	Forward: 5' ATTGCCGACAGGATGCAGA 3' Reverse: 5' CTCGTCATACTCCTGCTTGCTG 3'
CCL5	Forward: 5'TGCCACATCAAGGAGTATTT3' Reverse: 5'ACTCCCGAACCCATTTCTTC3'
CXCL10	Forward: 5'AGAATCGAAGGCCATCAAGAA3' Reverse: 5'CCTCTGTGTGGTCCATCCTTG3'
CXCL11	Forward: 5'CAGCAACAGCAAAAAACAAACA3' Reverse: 5'GGCCTATGCAAAGACAGCG3'

Cytokine Array

A human cytokine array was purchased from R&D Systems. The nitrocellulose membranes pre-spotted with 40 cytokines and chemokines antibodies were first blocked with 1× blocking buffer for 1hr. Then cell lysates or supernatant together with reconstituted antibody cocktail were directly added to the membrane and incubated overnight at 4°C. Then membranes were washed with 1× wash buffer three times and incubated with Streptavidin-HRP for 30 min at room temperature, then wash three times with 1× wash buffer. Finally antigen-antibody complexes were detected by film exposure and development.

Northern Blot Hybridization

Total RNA was obtained from cultured HUVECs by guanidinium isothiocyanate extraction and centrifugation through cesium chloride. The RNA was fractionated on a 1.3% formaldehyde-agarose gel and transferred to nitrocellulose filters. The filters were hybridized at 68°C for 2 h with ³²P-labeled human Carom cDNA probe in QuikHyb solution (Stratagene, La Jolla, CA). The hybridized filters were then washed in 30 mM sodium chloride, 3 mM sodium citrate, and 0.1% SDS solution at 55°C and autoradiographed with Kodak XAR film at -80°C for 16–24 h or stored on phosphor screens for 6–8 h. The filters were washed in a 50% formamide solution at 80°C and rehybridized with an oligonucleotide probe complementary to 18s ribosomal RNA to correct for loading differences.

Construction of Recombinant Adenoviruses and Adenovirus Infection

1. Adv-Carom to transduce human Carom in EC

A full length cDNA clone of human Carom was obtained from Open Biosystems (Huntsville, AL). The whole open reading frame of Carom was amplified by PCR and cloned into the pShuttle-IRES-hrGFP-1 vector (Stratagene, La Jolla, CA). The Carom-pShuttle-IRES-hrGFP-1 plasmid DNAs was linearized and transfected into BJ5183 *Escherichia coli* containing adenoviral backbone pAdEasy-1 vector (Stratagene) to allow homologous recombination of the two vectors to generate recombinant adenoviral plasmid - pAd-Carom, which encodes adenovirus overexpressing Carom. Construction of pAd-Carom plasmid was identified by restriction enzyme digestion and DNA sequencing. pAd-Carom plasmid DNA was linearized with Pac I (New England Biolabs, Ipswich, MA), and then transfected into 293A cells (Invitrogen, Carlsbad, CA), a packaging cell line that supplies the Adenoviral E1 function in transfection. Virus from cytopathic 293 cells were harvested after 48 hours of virus infection, collected by 3 freeze-thaw cycles followed by centrifugation, and purified by gradient cesium chloride (62%, 36%, and 51%) centrifugation at 35 000g for 2 hours. Viral titers were determined by plaque assay on 293A cells as described (H. Wang et al., 2002). HAECs at 50% confluence were infected with purified adenovirus at indicated multiplicity of infection (MOI) (plaque-forming unit [PFU]/cell). Western blotting (with anti-Carom and anti-FLAG antibodies) was carried out to examine ectopic gene expression.

2. Adv-Carom-shRNAs to transduce Carom shRNAs in EC

As shown in Table 2, four shRNAs (shRNA 1, 2, 3 and 4) targeted against human Carom were designed with BLOCK-iT RNAi Designer (Invitrogen, Carlsbad, CA). Recombinant adenoviruses expressing four Carom shRNAs and control shRNA were constructed using the Block-iT Adenoviral RNAi system (Invitrogen, Carlsbad, CA) as described (Behrend, Mohr, Dick, & Zwacka, 2005). The recombinant adenoviruses have been amplified, purified and titrated as described above. HAECs at 50% confluence were infected with purified adenovirus at 20 MOI for 48 hours. Infected HAECs were treated with or without Hcy after another 24 hours. Western blotting (with anti-Carom antibody) and Real-time PCR (with Carom primers) were carried out to examine Carom gene expression.

Table 2.2. Carom shRNAs targeting sequences

shRNA	Targeting sequence	Location on Carom mRNA
shRNA 1	GAGGTGTTAGAAGTGATTGAAGATGGAGA	1551bp-1579bp
shRNA 2	CAGAAGTTGGCTAGTCAATACCTGAAGAG	243bp-271bp
shRNA 3	CAGTTCCAGCCTTGTGACAGTGATACTAG	969bp-997bp
shRNA 4	GCGAAGAGTTTGAAGATAACA	1408bp-1428bp
control	GCTGGACTTCCAGAAGAACA	N/A

Bisulfite Next-Generation Sequencing

Genomic DNA was extracted from HUVECs after treatment and then modified by bisulfite, which converts unmethylated cytosine to uracil as described (Olek, Oswald, & Walter, 1996). This conversion was performed at the University of Pennsylvania's Next-Generation Sequencing Core (NGSC) according to protocol (ngsc.med.upenn.edu). Services of the NGSC were then enlisted to perform comparative next-generation sequencing of DNA from HUVEC treated with and without Hcy analyzed for whole genome methylation patterns.

Analysis of Transcription Factor Binding Frequencies

Carom promoter sequence was used as input into the University of Pennsylvania's Transcription Element Search System (TESS): <http://www.cbil.upenn.edu/cgi-bin/tess/tess>. TESS outputs a ranked list of predicted transcription factor binding sites for the inputted DNA sequence.

Scratch Wound Assay

The migration of HAEC was assessed by scratch wound assays (Su, Sorenson, & Sheibani, 2003). HAECs of 70% confluence were cultured on 6-well plates and exposed to treatment for 2 days. Cells were wounded by scratching with a micropipette tip, rinsed with PBS, and then incubated with consistent treatment for 16 h. Wound closure was monitored through the use of digital photography and measured using the Axiovision

software (Zeiss, Germany). Cell migration was expressed as the percentage of distance migrated divided by the length of the initial wound.

Tube Formation Assay

We used tube formation on Matrigel as in vitro angiogenesis model (Arnaoutova & Kleinman, 2010). Matrigel Basement Membrane Matrix (BD, Bedford, USA) was thawed on ice at 4°C overnight and all pipettes and 96-well flat bottom plate (Corning Costar, Tewksbury, MA) were precooled before use. 96-well plates were coated with 30 µl Matrigel per well. HAECs with or without treatment were seeded at 4×10^3 cells per well in 80 µl EC growth media. Each group was in triplicate. After 6h of incubation, tube-like structures were photographed using inverted microscope (Zeiss, Germany). The total tube length and branch number were quantified using Image J software (NIH, Bethesda, MD).

Statistical analysis

Data were analyzed using a Student's t-test. Statistical significance was determined at the alpha level of 0.05. Results are expressed as the mean±SEM. Statistical comparisons between 2 groups were performed via Student t test. One-way ANOVA was used to compare the means of multiple groups. $P < 0.05$ was considered significant.

CHAPTER 3

RESULTS

Carom is identified as an early induced gene by Hcy in EC

Previously we found that Hcy inhibits EC growth via cyclin A inhibition (H. Wang et al., 2002). However, this inhibition occurs after 24h treatment of Hcy. To identify the early genes induced by Hcy in EC, we employed differential display assay. HUVECs P8 were treated with 50 μ M Hcy in presence of 40 μ M adenosine and 10 μ M EHNA for 12 hours. Then Total RNA was extracted and subjected to differential display. 50 cDNA clones were obtained from differential display. After sequencing and gene BLAST alignment, 15 clones were identified as Carom gene (Table 3.1 and Figure 3.1).

Table 3.1. Carom cDNA clones are identified with Differential Display. HUVECs P8 were cultured in EC growth media containing 40 μ M adenosine and 10 μ M EHNA. At 70%-80% confluence, HUVECs were exposed to 50 μ M DL-Hcy for 12 hours. Total RNA were extracted and subjected to differential display (DD). Fifty cDNA clones were identified; fifteen clones out of fifty were Carom cDNA clones.

cDNA clones from DD	Length (bp)	Location on Carom cDNA
A2=A28=A4=A5=A22	180	2249bp-2425bp
A12=A13=A31=A27	190	2607bp-2794bp
A14=A15=A33	200	2836bp-3031bp
A19=A26	280	3893bp-4169bp
A6	300	4211bp-4507bp

A

Homo sapiens FCH and double SH3 domains 2 (FCHSD2), mRNA

Sequence ID: [reflNM_014824.2](#) Length: 4507 Number of Matches: 1

Range 1: 2249 to 2425 [GenBank](#) [Graphics](#) ▼ Next Match ▲ Previous Match

Score	Expect	Identities	Gaps	Strand
285 bits(154)	9e-74	172/180(96%)	4/180(2%)	Plus/Plus
Query 3		GTACTTTCCTCCCGGTCTCCTTCAGCAAACGAAAAAGCCTTCATGCTGAGTCACCAGGATT		62
Sbjct 2249		GTACTTTCCTCCCGGTCTCCTTCAGCAAACGAAAAAGCCTTCATGCTGAGTCACCAGGATT		2308
Query 63		CATCACAGGCATCAAGGCATACCTCCTGACGACCTCATATGGCAAACGCGACCTGTCCG		122
Sbjct 2309		C-TCACAGGCATCAAGGCATAC-TCCTGA-GACCTCATATGGCAAACGCGACCTGTCCG		2365
Query 123		GGCACGTCCCCCTCCACCTACACAGAATCACCGAAG-CCACGAGAGAAGATTGAAGATGT		181
Sbjct 2366		GGCAGCTCCCCCTCCACCTACACAGAATCACCGAAGGCCAGCAGAGAAGATTGAAGATGT		2425

B

Homo sapiens FCH and double SH3 domains 2 (FCHSD2), mRNA

Sequence ID: [reflNM_014824.2](#) Length: 4507 Number of Matches: 1

Range 1: 2607 to 2794 [GenBank](#) [Graphics](#) ▼ Next Match ▲ Previous Match

Score	Expect	Identities	Gaps	Strand
335 bits(181)	9e-89	186/188(99%)	2/188(1%)	Plus/Minus
Query 6		TGCACATGATCAGTAATTTAGGGACTGTGCCCTGGAATGAGGCCTGTTCTTGAGTCTCAT		65
Sbjct 2794		TGCACATGATCAGTAATTTAGGGACTGTGCCCTGGAATGAGGCCTGTTCTTGAGTCTCAT		2735
Query 66		ATAAAAAACAGACCACCTGTTAGGCATGAGGGCTGCCCCCTCTTTGCTCCTAGGGTCCGCT		125
Sbjct 2734		ATAAAAAACAGACCACCTGTTAGGCATGAGGGCTGCCCCCTCTTTGCTCCTAGGGTCCGCT		2675
Query 126		AG-ATTTGTGCTATGGTAGGAGAAATGACATAGAAAATGACAACAAAAAAAAA-GGCACG		183
Sbjct 2674		AGGATTTGTGCTATGGTAGGAGAAATGACATAGAAAATGACAACAAAAAAAAAAGGCACG		2615
Query 184		AAATATTC 191		
Sbjct 2614		AAATATTC 2607		

Figure 3.1. BLAST result of cDNA clones A2 and A12 obtained from differential display of HUVECs with 12h Hcy treatment. HUVECs P8 were cultured in EC growth media containing 40 μ M adenosine and 10 μ M EHNA. At 70%-80% confluence, HUVECs were exposed to 50 μ M DL-Hcy for 12 hours. Total RNA were extracted and subjected to differential display. 50 cDNA clones were obtained and sequenced. DNA sequences of 50 clones were aligned with BLAST (<http://blast.ncbi.nlm.nih.gov/Blast.cgi>). **A.** Alignment result of clone A2. **B.** Alignment result of clone A12.

Carom gene is differentially expressed in Human and Mouse tissues

Tissue mRNA expression profiles of Carom gene in 21 human and 20 mouse tissues are presented in Figure 3.2. Confidential intervals are generated based on mRNA expression levels of 3 housekeeping genes (PTTG1IP, PKM2, and HNRNPK), which have relatively consistent mRNA levels across the selected tissues in both human and mouse. In Figure 3.2A, PTTG1IP expression profiles are presented as representative of housekeeping genes. The confidential intervals of the housekeeping gene expression are $X + 2SD = 3.24$ in human tissues and $X + 2SD = 3.32$ in mouse tissue, and not significantly different between species. Lines indicating an upper limit of the confidence interval are put in all bar graphs of tissue profile to establish the significance of gene expression. mRNA expression levels of Carom in the tissues higher than the upper limit of the confidential interval of the housekeeping genes are considered statistically significant higher expression.

As shown in Figure 3.2B, in humans, Carom gene is highly expressed in lymph node, pituitary gland and nerve. The expression of Carom in vascular tissue is not significantly higher to other tissues.

In mouse tissues, Carom gene is highly expressed in blood, eye, lymph node, spleen and ovary. Carom expression data is not available in EST database.

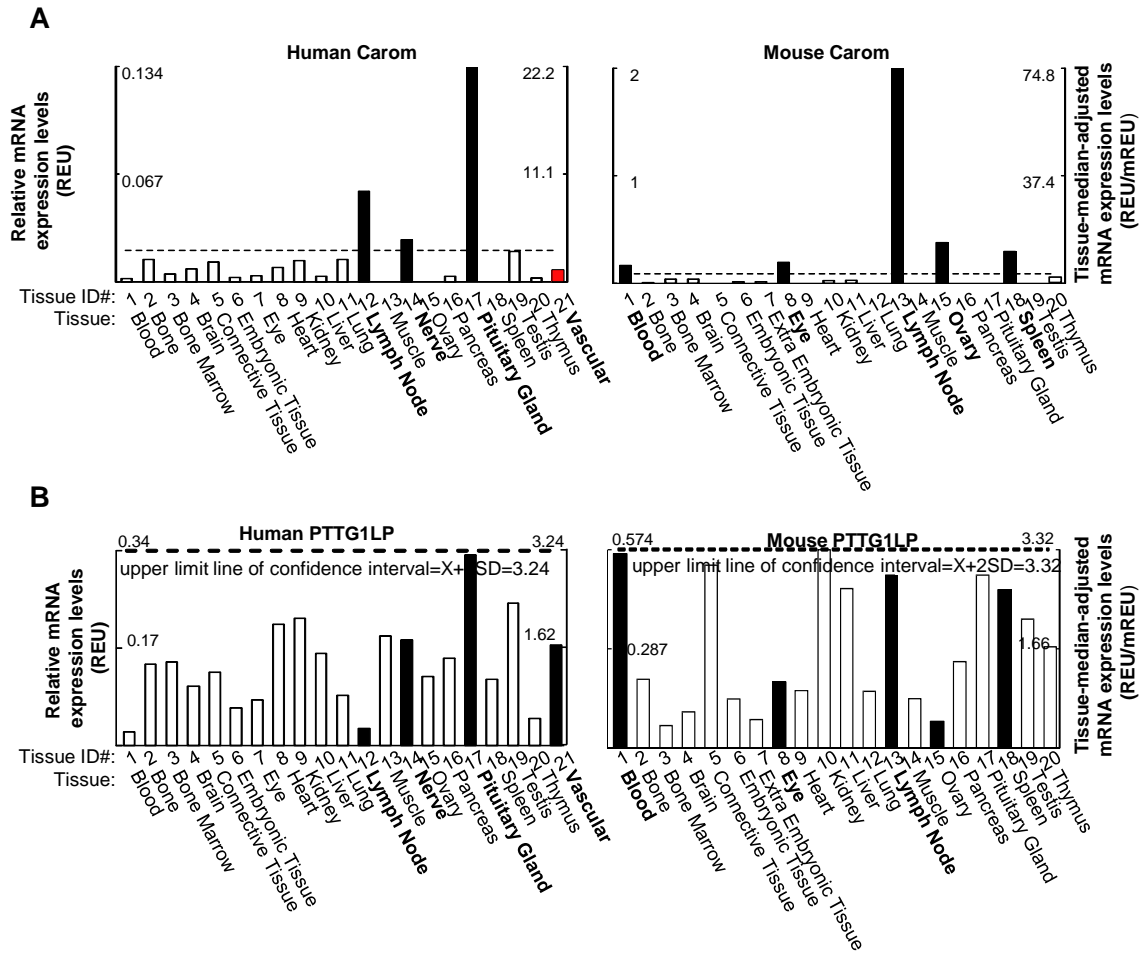


Figure 3.2. Tissue mRNA Expression Profile of Carom Gene. Twenty one human and twenty mouse tissues were given tissue ID numbers and examined for mRNA expression by mining human and mouse expression sequence tag (EST) databases deposited in the NIH UniGene database. Left and right Y-axis represents relative mRNA expression (REU) and tissue-median adjusted mRNA expression levels (REU/mREU) respectively. REU of the genes is acquired by normalization of gene transcript per million (TPM) with that of β -actin. Dashed lines indicates upper limit of the confidence intervals of the three housekeeping genes (PTTG1IP, PKM2, and HNRNPK). mRNA expression levels of Carom in the tissues higher than the upper limit of the confidential interval of the

housekeeping genes are considered statistically significant higher expression. **A.** Tissue mRNA expression profile of Carom gene in human and mouse. **B.** Representative tissue mRNA expression profile of housekeeping gene PTTG1P in human and mouse.

Hcy up-regulates both mRNA and protein expression levels of Carom in EC

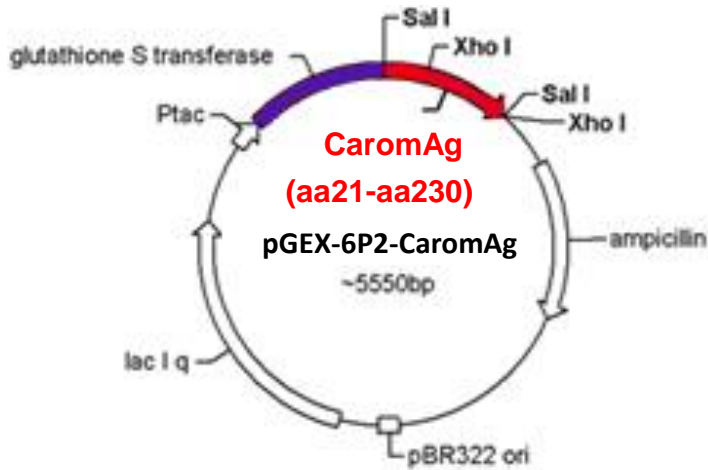
Generation of rabbit anti-Carom antibody

Carom is a novel gene and there was no commercial anti-Carom antibody available. To examine Carom protein expression in EC, we successfully generated rabbit anti-Carom antibody.

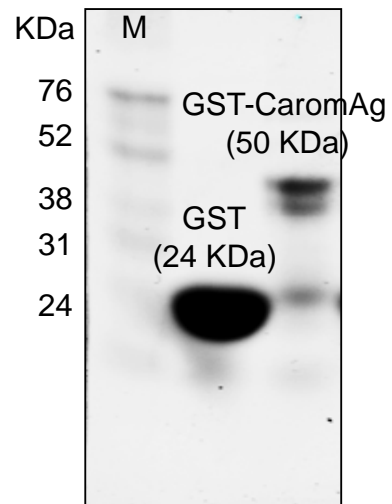
After alignment of all public mRNA sequences of human Carom with AceView (<http://www.ncbi.nlm.nih.gov/iebrsearch/acembly/>), we found that exons 2-8 of the human whole length Carom mRNA (NM_014824) cover most of alternative transcript variants (Figure 2.2). Exons 2-8 encode the fragment from aa21 to aa230 of Carom protein. This fragment is part of F-BAR domain, and named as CaromAg. Carom protein entire sequence was analyzed with Lasergene software (DNASTAR, Madison, WI), the hydrophilicity and antigenicity of CaromAg were good for antibody induction, as shown in Figure 2.2.

As shown in Figure 3.3A, the gene encoding CaromAg was inserted into Sal I site of the GST expression vector pGEX-6P2 (GE Healthcare Life Sciences, Piscataway, NJ) to generate pGEX-6P2-CaromAg vector to express GST-CaromAg fusion protein. pGEX-6P2-CaromAg vector was transformed to *E. coli* BL21 (GE Healthcare Life Sciences, Piscataway, NJ) to express fusion protein. GST-CaromAg fusion protein was then purified through Glutathione Sepharose 4B (GE Healthcare Bio Sciences, Sweden). Purification products were loaded to SDS-PAGE gel and separated with electrophoresis. The molecular weights of GST-CaromAg and GST are 50 KDa and 26 KDa respectively.

A Map of GST-CaromAg vector



B Expression of GST-CaromAg fusion protein



C Titration of rabbit antisera against Carom Antisera

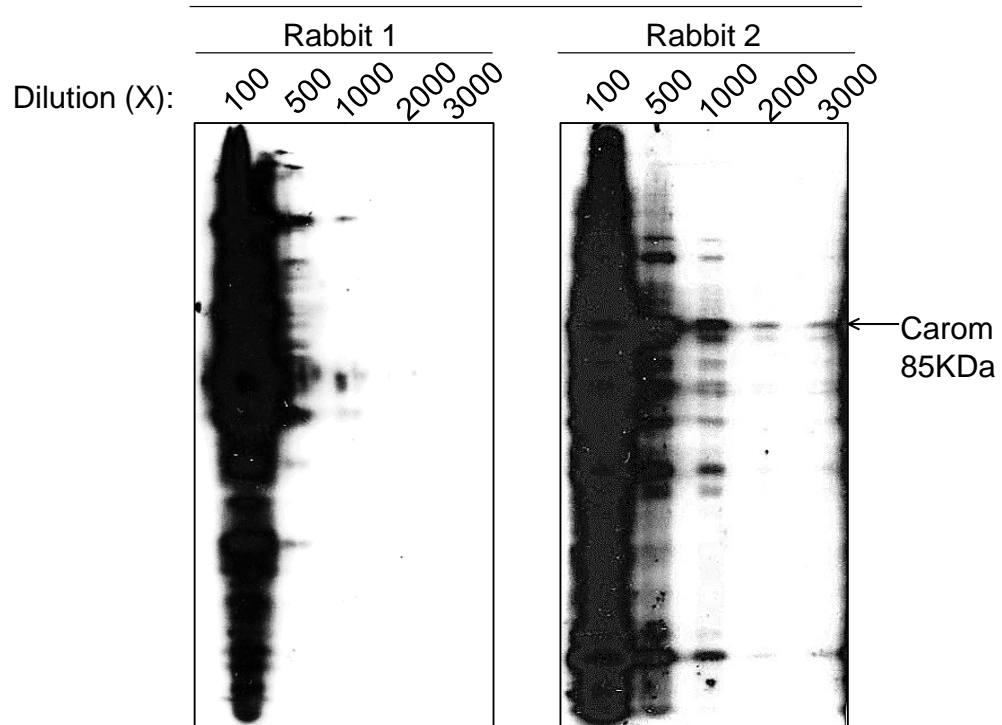


Figure 3.3. Generation of Rabbit Anti-Carom Antibody. A. Construction of GST-CaromAg fusion protein expression vector. The gene encoding CaromAg was inserted into Sal I site of the GST expression vector pGEX-6P2 (GE Healthcare Life Sciences,

Piscataway, NJ) to generate pGEX-6P2-CaromAg vector to express GST-CaromAg fusion protein. **B.** Expression and purification of GST-Carom fusion protein. pGEX-6P2-CaromAg vector was transformed to *E. coli* BL21 (GE Healthcare Life Sciences, Piscataway, NJ) to express fusion protein. GST-CaromAg fusion protein was then purified through Glutathione Sepharose 4B (GE Healthcare Bio Sciences, Sweden). Purification products were loaded to SDS-PAGE gel and separated with electrophoresis. After electrophoresis, the gel was stained with coomassie blue. GST purification was loaded as control (M, protein molecular weight marker). **C.** Titration of rabbit anti-Carom antibody. Purified GST-Carom was injected to two rabbits to generate anti-Carom antibody. After 1 prime injection and 3 boosters, the antisera were collected. Antisera from 2 rabbits in a series of indicated dilution were incubated with the nitrocellulose membrane transferred with 200 µg of total HAECs P8 proteins and subjected to western blot for titration with anti-Rabbit antibody.

Figure 3.3B presents the coomassie blue staining result of purification product of GST-CaromAg and GST as control. The size of purified GST-CaromAg on the SDS-PAGE gel is around 50 KDa, as predicted.

Purified GST-CaromAg fusion protein was injected to 2 rabbits (1 mg/rabbit, 1 prime injection and 3 boosters) by Pacific Immunology (Ramona, CA), antisera were collected. Antisera in a series of dilution were incubated with the nitrocellulose membrane transferred with total HUVEC proteins and subjected to western blot for titration. Figure 3.3C shows the titration results. In the lane of 3000X dilution of antisera from rabbit 2, a specific band of 85 KDa appeared. This band stood for Carom protein. However, there were no specific bands in the lanes of rabbit 1.

Purification of anti-Carom antibody

GST-CaromAg is a GST fusion protein. It could induce either anti-Carom or anti-GST antibodies. To remove anti-GST antibody in anti-Carom antisera, we used columns of Glutathione Sepharose 4B cross-linked with GST and GST-CaromAg. As shown in Figure 3.4A, crude antisera of rabbit 2 were loaded to GST column to pull down anti-GST antibody and the flow through was then loaded to GST-Carom column to pull down anti-Carom antibody. Then the antibodies bound to GST and GST-Carom columns were eluted and named as 1st Elution and 2nd Elution respectively. 1st Elution and 2nd Elution were used as primary antibody to detect GST and GST-Carom fusion protein with western blot. Figure 3.4B shows that 1st Elution (anti-GST) recognizes both GST and GST-Carom proteins, while 2nd Elution (anti-Carom) only recognizes GST-Carom but not GST. Then the purified anti-Carom antibody (2nd Elution) was titrated against total proteins from HAECs. As shown in Figure 3.4C, at dilution of 1000X, purified anti-Carom antibody generates only one band around 85 KDa, which is Carom protein.

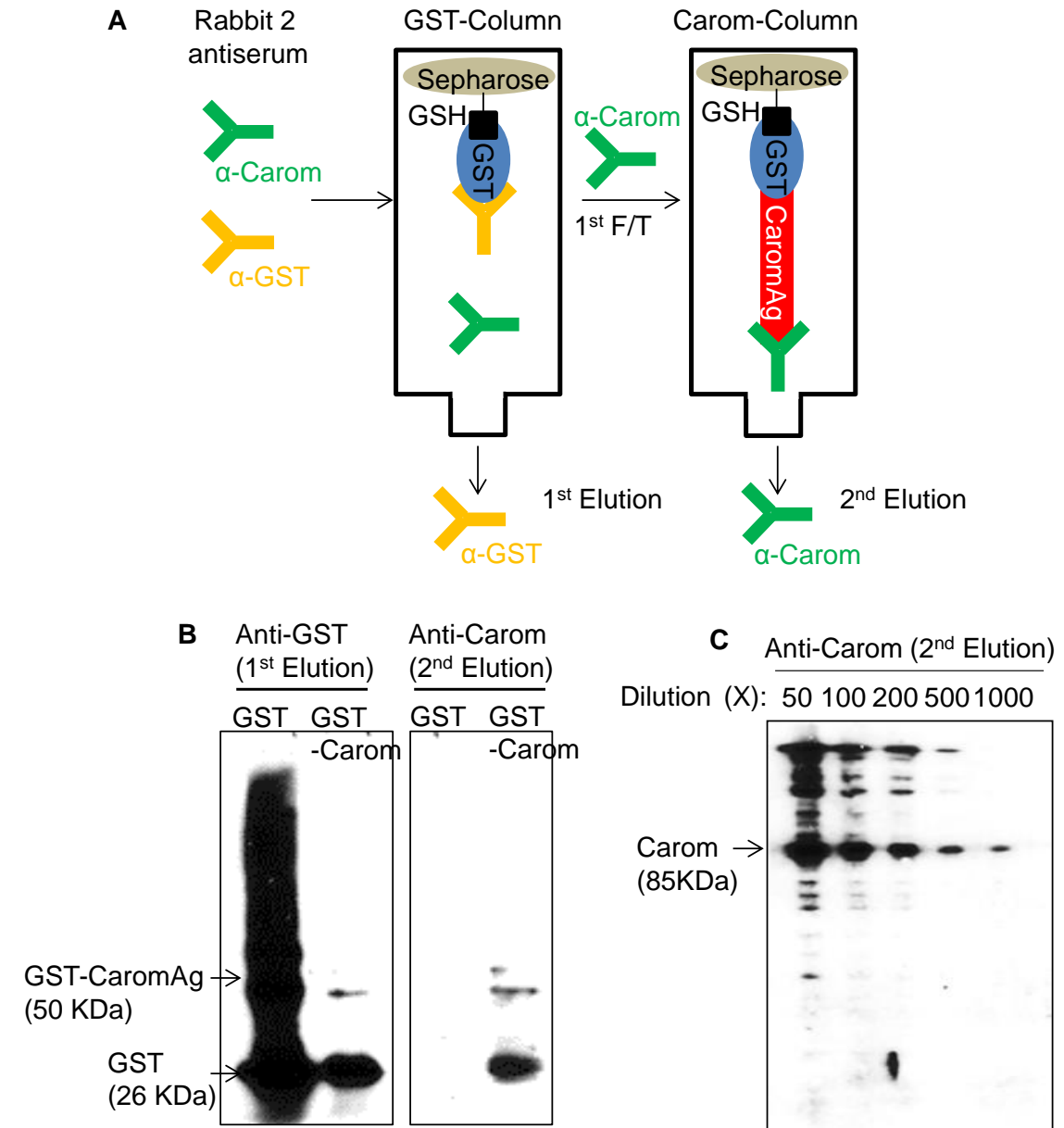


Figure 3.4. Purification of anti-Carom antibody. **A.** Schematic diagram of anti-Carom antibody purification. Crude Rabbit 2 antisera were loaded to columns filled with cross-linked GST- and GST-Carom-Glutathione Sepharose sequentially. Then the antibodies bound to GST and GST-Carom columns were eluted and named as 1st Elution (anti-GST) and 2nd Elution (anti-Carom) respectively. **B.** Purified GST and GST-Carom proteins were blotted with eluted GST and Carom antibody (1000x dilution). **C.** Eluted Carom antibody was titrated against total proteins from HAECs P8.

Hcy up-regulates Carom mRNA expression in cultured human EC

We have identified Carom as an early induced gene in Hcy-treated EC. To confirm mRNA induction of Carom by Hcy, we used Northern Blot and Real-time PCR assay to examine Carom mRNA levels in HUVEC or HAEC in response to Hcy. RNA was harvested from HUVECs treated with 50 μ M of Hcy for 12 hours, 24 hours and 48 hours, then analyzed by Northern blotting with 32 P labeled Carom cDNA clone A12 which obtained from differential display (Figure 3.5A). The Carom mRNA increased by 45% with 50 μ M Hcy for 12 hours, by 34% for 24 hours, and by 35% for 48 hours.

Real-time PCR was also used to confirm Hcy-induced Carom mRNA expression in HAECs. Total RNA of HAECs treated with 50 μ M of Hcy for 12 hours, 24 hours and 48 hours, was analyzed by Real-time PCR (Figure 3.5B). The Carom mRNA was increased by 50 μ M of Hcy to 1.91 -fold for 12 hours, to 2.76 -fold for 24 hours, and to 2.52 -fold for 48 hours.

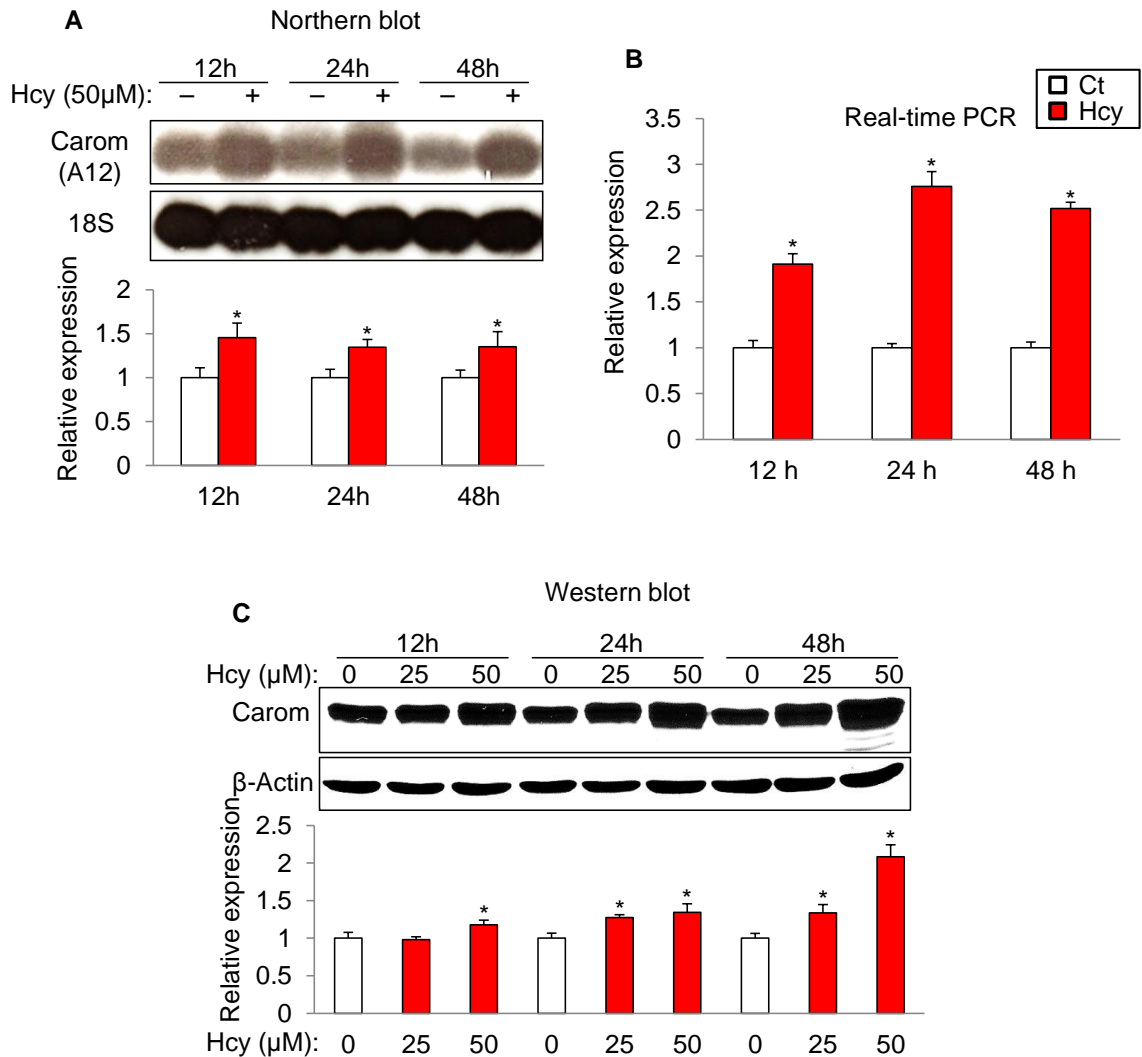


Figure 3.5. Hcy induces Carom expression in cultured human endothelial cells.

HUVECs or HAECs were cultured in media containing 40 μ M adenosine and 10 μ M EHNA to 70% -80% confluence. **A.** Carom mRNA level in Hcy-treated HUVECs. HUVECs P8 were exposed to 50 μ M DL-Hcy for the indicated time. Total cellular RNA (10 μ g) was used for Northern blot analysis with 32 P-labeled Carom cDNA A12 which was identified by Differential Display. 18S RNA was used as endogenous transcriptional control. Northern blot image was analyzed with Image J software to quantify the relative expression levels of Carom. **B.** Carom mRNA level in Hcy-treated HAECs. HAECs P9

were exposed to 50 μ M DL-Hcy for the indicated time. Total cellular RNA was used for Real-time PCR assay with Carom primers. Carom mRNA levels were assessed using real-time PCR by $\Delta\Delta C_T$ comparison to β -Actin. (C). Carom protein expression level in Hcy-treated HAECs. HAECs P9 were treated with 25 μ M or 50 μ M DL-Hcy for the indicated time. Total protein was extracted and analyzed by Western Blot with the purified homemade rabbit anti-Carom antibody. Relative expression levels of Carom protein was quantified with Image J software compared to β -Actin. Values represent mean (\pm SD) from 3 separate experiments (n = 3). *P < 0.05 versus non-Hcy control.

Hcy up-regulates Carom protein expression in cultured human EC

To assess whether Hcy induced increases in Carom mRNA levels were reflected increases in protein levels, we performed Western blot analysis. HAECs were treated with 25 μ M or 50 μ M Hcy in a time course (12 hours, 24 hours and 48 hours). Protein lysates were detected with purified anti-Carom antibody (Figure 3.5C). Hcy increased Carom protein expression in a dose dependent manner. 50 μ M Hcy increased Carom protein to 1.18-fold for 12 hours, to 1.34-fold for 24 hours, and to 2.08-fold for 48 hours. This time course suggests that 48 hours treatment of 50 μ M Hcy is good for the maximal induction of Carom protein.

Carom protein expression is increased in EC from HHcy mice

It is known that genetic deficiency of the key enzymes such as CBS and MTHFR leads to high levels of plasma Hcy. *Cbs*^{-/-} mice have a plasma Hcy level reaching up to 200 μ M and most die within 5 weeks postnatal (Watanabe et al., 1995). To circumvent this problem, a transgenic human CBS mouse was created in Dr. Kruger's laboratory in Fox Chase Cancer Center. In these mice, the human CBS cDNA is controlled by a zinc-inducible metallothionein promoter. A *Tg-hCBS Cbs*^{-/-} mouse model was created by crossing *Tg-hCBS* mice with *Cbs*^{-/-} mice. Mice were fed with water supplemented with 25 mM zinc sulfate (ZnSO₄) during pregnancy and lactation to induce human CBS gene expression.

Tg-hCBS Cbs^{-/-} mice and their WT or heterozygous control mice were used to examine Carom *in vivo* expression levels (genotype shown in Figure 3.6A). They were provided with 25 mM ZnSO₄ containing water during the first month after birth and then replaced with common drinking water to induce HHcy status. At the end of fourteen weeks, *Tg-hCBS Cbs^{-/-}* mice had plasma total Hcy (tHcy) level ranging from 50~100 μM with mean plasma Hcy level about 80 μM (Figure 3.6B). The WT mice and heterozygous littermates all had Hcy level less than 10 μM.

Mice of 13-14 weeks old were anesthetized by sodium pentobarbital and lungs were dissected and digested with 1 mg/mL collagenase type I for 45 min at 37°C. Then the single cell suspension was labeled and selected with sheep anti-rat magnetic beads coated with anti-CD31 antibody. Total proteins were extracted from bead-bound mouse ECs. Carom expression was then examined by Western blot. As shown in Figure 3.6C, Hcy also increased EC expression of Carom protein *in vivo*.

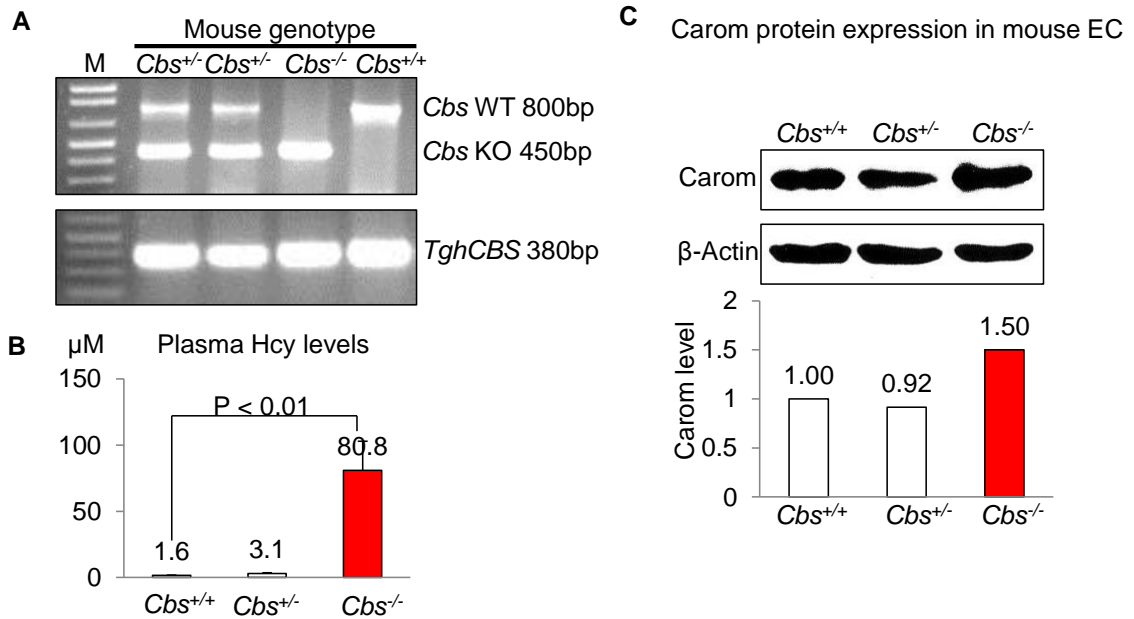


Figure 3.6 Carom protein expression in HHcy mice EC. *Tg-hCBS Cbs*^{-/-}, *Tg-hCBS Cbs*^{+/-} and *Tg-hCBS Cbs*^{+/+} (*Wt*) mice (n = 5 in each group) at 13-14 weeks old were sacrificed, and tissues were subjected to measurement. **A.** Genotyping of human CBS transgene and mouse *Cbs* gene by PCR analysis. DNA was extracted from mouse toe. PCR products were separated by 1.2% agarose gel. The mouse wild type *Cbs* band is 800 bp while the KO *Cbs* band is 450 bp. Transgene human CBS is 380 bp. CBS, cystathionine β-synthase; KO, knockout; M, molecular marker. **B.** Total plasma Hcy levels. EDTA anti-coagulant mouse plasma was collected and the total plasma Hcy levels were measured by High-performance liquid chromatography (HPLC). Values represent mean (± SD). **C.** Carom protein expression in mouse lung endothelial cells (MLECs). The lungs of each group were dissected and digested together with 1 mg/mL collagenase type I for 45 min at 37°C. Then the single cell suspension was labeled and selected with sheep anti-rat magnetic beads coated with anti-CD31 antibody. Total proteins of the bead-bound endothelial cells were extracted and Carom expression was examined by Western

blot with anti-Carom antibody. Relative expression levels of Carom protein was quantified with Image J software compared to β -Actin.

Carom inhibits EC migration

Construction of recombinant adenovirus expressing Carom

Since cultured primary EC are poorly transfected by conventional transfection methods, an adenoviral-mediated approach was used to overexpress the Carom protein in order to determine the role of Carom in EC biology. Adenoviral vector pAd-Carom encoding recombinant adenovirus Adv-Carom which expresses full length Carom protein fused with 3x FLAG tag at N-terminus was successfully constructed. As shown in Figure 3.7A, Carom expression is driven by a CMV promoter, and followed by the IRES-initiated GFP protein to monitor viral infection efficiency in host cells. pAd-Carom plasmid DNA was linearized and then transfected into 293A cells to pack Adv-Carom. Adenovirus Adv-Ct, which only expresses GFP but not any other foreign gene, was also packed as infection control of Adv-Carom. After viral package, Adv-Carom was amplified, purified and titrated.

HAECs were infected with Adv-Carom for 48 hours and the protein expression of Carom was examined with Western blot. As shown in Figure 3.7B, Adv-Carom induced Carom protein expression in a dose-dependent manner, 20 multiplicity of infection (MOI) Adv-Carom increased Carom level to 2.12-fold, which was similar to 50 μ M Hcy treatment of 48 hours (2.08-fold). Anti-FLAG antibody detected a 85 KDa band, consistent with the size of Carom protein. Moreover, the level of this FLAG-tagged protein was also increased by Adv-Carom dose-dependently. Adv-Carom expressed GFP was examined with fluorescent microscope and flow cytometer. GFP fluorescence appeared in most of Adv-Carom infected HAECs (Figure 3.7C).

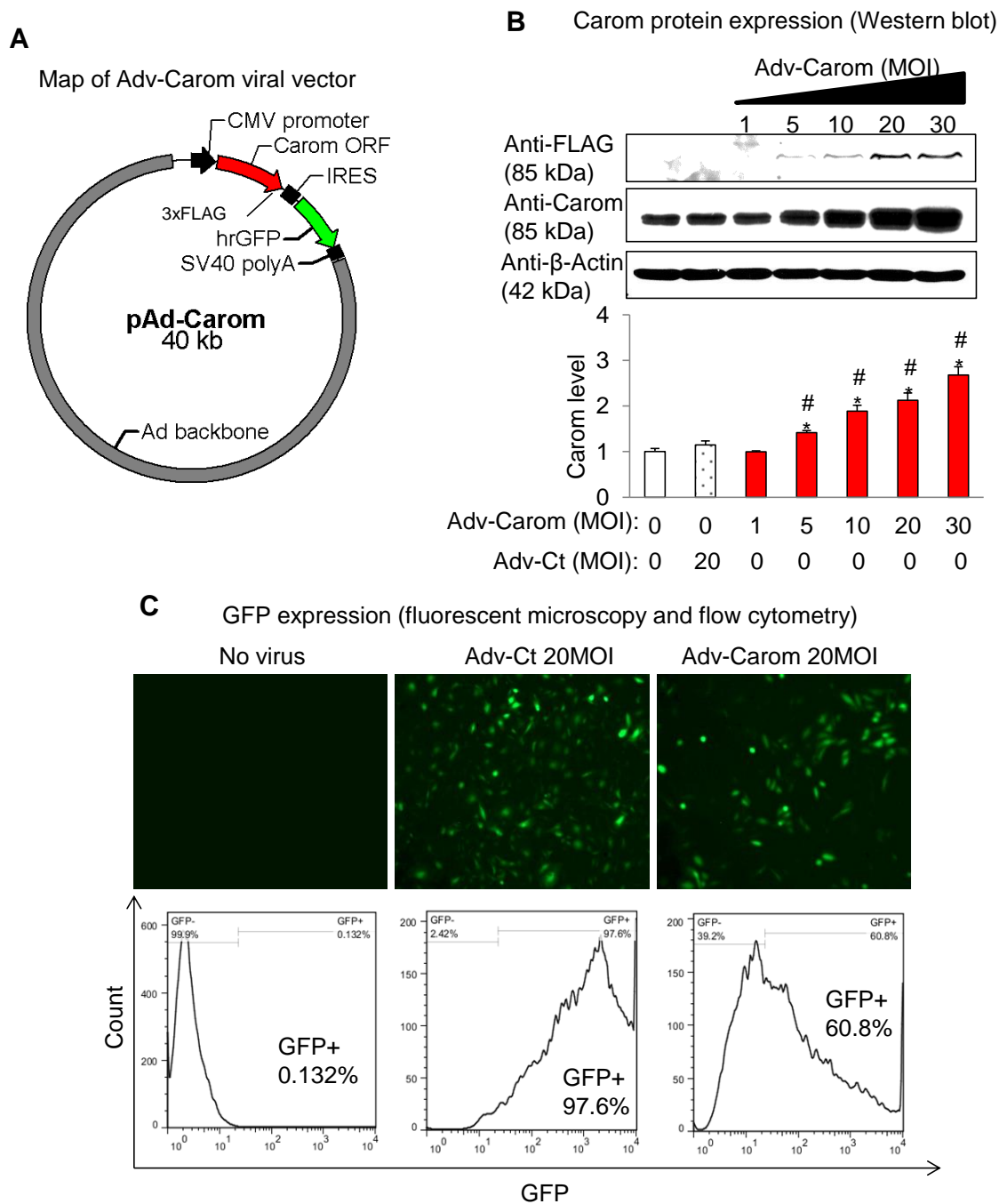


Figure 3.7. Generation of recombinant adenovirus Adv-Carom to express Carom.

A. Map of adenoviral vector pAd-Carom. pAd-Carom encodes recombinant adenovirus Adv-Carom which expresses full length Carom protein fused with 3x FLAG tag at N-

terminus. Carom expression is driven by a CMV promoter, and followed by the IRES-initiated GFP protein. **B.** Carom protein expression in HAECs P8 with 48 hours infection of Adv-Carom at indicated multiplicity of infection (MOI). Carom protein expression was examined by western blot with anti-Carom antibody, Carom-FLAG protein expression was examined by Western blot with anti-FLAG antibody. **C.** GFP expression in HAECs P8 with 48 hours infection of 20 MOI Adv-Carom. GFP fluorescence was examined with fluorescent microscope and flow cytometer. Relative expression levels of Carom protein was quantified with Image J software. Values represent mean (\pm SD) from 3 separate experiments ($n = 3$). * $P < 0.05$ versus nonviral control, # $P < 0.05$ versus Adv-Ct control.

Construction of recombinant adenovirus expressing Carom shRNAs

To knock down the Carom gene in EC, we generated recombinant adenoviruses Adv-shRNAs to express Carom shRNA. As shown in Figure 3.8A, four shRNAs (shRNA 1, 2, 3 and 4) targeted against the indicated sites on human Carom mRNA were designed with BLOCK-iT RNAi Designer (Invitrogen, Carlsbad, CA). Recombinant adenoviruses Adv-Carom-shRNAs expressing four Carom shRNAs and Adv-Ct-shRNA expressing control shRNA (Lamin-shRNA not targeting against any of mammalian genes) were constructed using the Block-iT Adenoviral RNAi system (Invitrogen, Carlsbad, CA). Transcription of shRNAs is driven by U6 promoter and terminated by RNA Polymerase III terminator. The recombinant adenoviruses were amplified, purified and titrated. HAECs at 50% confluence were infected with Adv-Carom-shRNAs at 20 MOI for 24 hours, and then treated with or without Hcy after another 48 hours. As shown in Figure 3.8B, four Adv-Carom-shRNAs all decreased Carom mRNA expression in HAECs, and Adv-Carom-shRNA4 decreased Carom mRNA to the lowest level (28%), while control virus Adv-Ct-shRNA did not affect Carom mRNA level much (84%), as expected. Adv-Carom-shRNA4 most decreased Carom protein expression (36%) among Adv-Carom-shRNAs, and Adv-Ct-shRNA also did not affect Carom protein level much (91%) (Figure 3.10C). As shown in Figure 3.8C, induction of Carom protein expression by Hcy (1.96-fold) was reversed by Adv-Carom-shRNAs, and Adv-Carom-shRNA4 blocked down Hcy-induction most (0.7-fold). These data suggest that Adv-Carom-shRNA4 is the best virus to block down Carom expression in EC.

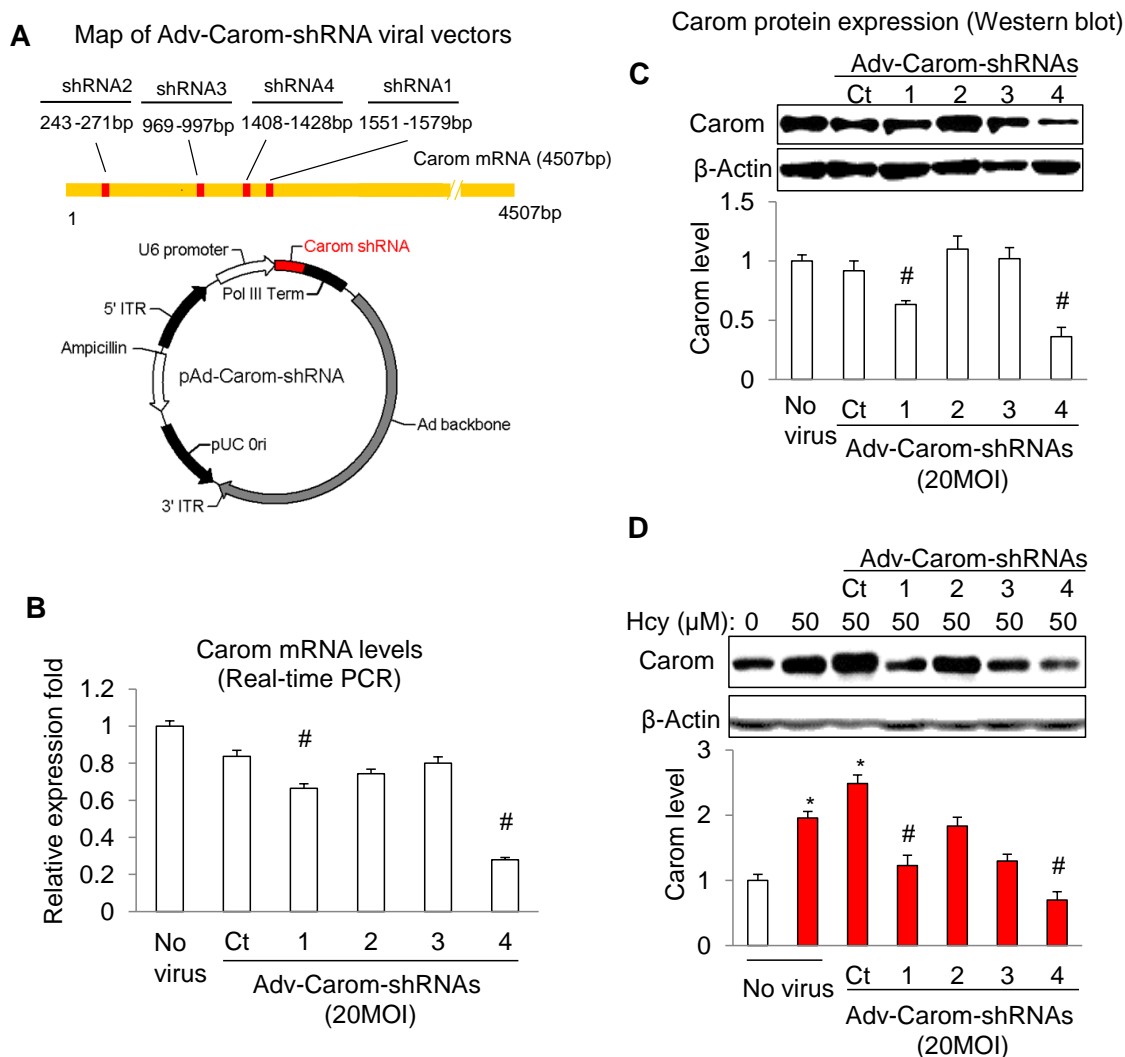


Figure 3.8. Generation of recombinant adenoviruses Adv-Carom-shRNAs to express Carom shRNAs. **A.** Map of adenoviral vector pAd-Carom-shRNA. Four shRNAs (shRNA1, 2, 3 and 4) targeted against human Carom mRNA were designed with BLOCK-iT RNAi Designer (Invitrogen). pAd-Carom-shRNAs encode recombinant adenoviruses Adv-Carom-shRNAs which express Carom shRNAs. **B-D.** HAECs P9 were cultured in media containing 40 μ M adenosine and 10 μ M EHNA to 50% confluence, and infected with 20 MOI Adv-Carom-shRNAs for 24 hours, and then treated with or

without 50 μ M DL-Hcy after another 48 hours. **B.** Carom mRNA levels in Adv-Carom-shRNAs infected HAECs. Total cellular RNA was used for Real-time PCR assay with Carom primers. Carom mRNA levels were assessed using real-time PCR by $\Delta\Delta C_T$ comparison to β -Actin. **C and D.** Carom protein expression levels of HAECs infected with Adv-Carom-shRNAs. Carom protein expression was examined by Western blot with anti-Carom antibody. **C.** Carom protein expression of HAEC in absence of Hcy. **D.** Carom protein expression of HAEC in presence of Hcy. Western blot results were analyzed with Image J software to quantify relative expression level of Carom. Values represent mean (\pm SD) from 3 separate experiments (n = 3). *P < 0.05 versus non-Hcy and nonviral control, [#]P < 0.05 versus Adv-Ct-shRNA control.

Carom does not affect EC growth

Our laboratory has demonstrated that Hcy selectively inhibits EC proliferation, arrests the EC cell cycle at the G₁/S Transition (H. Wang et al., 1997). Furthermore, we found that Hcy selectively reduces cyclin A expression in EC through demethylation of cyclin A promoter, which results in EC growth inhibition (M. D. Jamaluddin et al., 2007; H. Wang et al., 2002). However, cyclin A inhibition in EC occurs after 24h treatment of Hcy. The early events in the Hcy signaling pathway of EC growth inhibition remain to be elucidated. We performed Differential Display to identify early Hcy-induced genes in HUVECs, and Carom was found. The function of Carom is largely unknown. Studies show that CASK, a Carom-interacting protein, plays a role in cell proliferation inhibition (Ojeh et al., 2008; Sun et al., 2009). So we hypothesize that Carom may be induced by Hcy to inhibit EC growth.

To determine the role of Carom in EC growth, we used Adv-Carom and Adv-Carom-shRNA4 to perform gain-of-function and loss-of-function studies in EC proliferation respectively. As shown in Figure 3.9, Hcy-inhibited EC proliferation was confirmed, whereas adenovirus-transduced Carom expression neither increased nor decreased DNA synthesis in EC. In addition, Carom-shRNA expressed by adenovirus did not rescue EC growth in Hcy-treated EC.

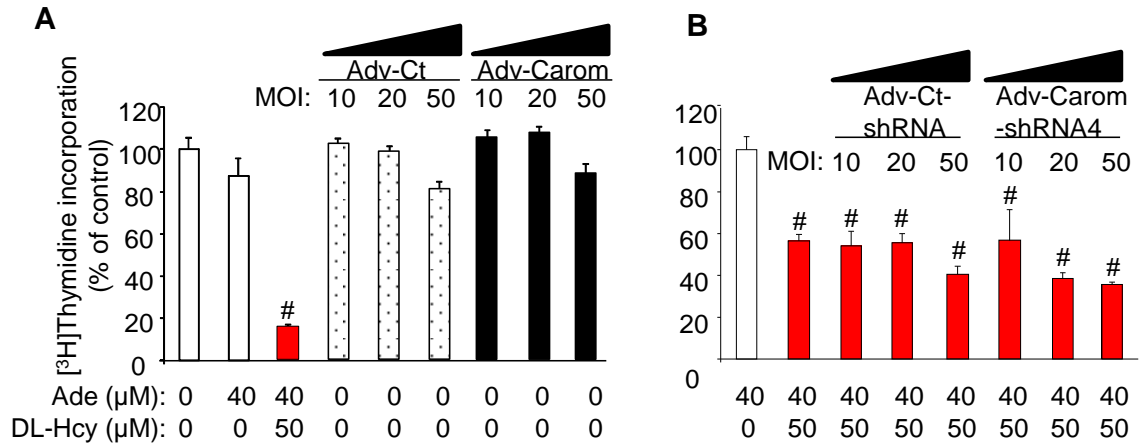


Figure 3.9. The effects of adenovirus-transduced Carom gene and Carom shRNA genes on DNA synthesis in HUVECs. HUVECs P8 of 70% confluence were infected with Adv-Carom or Adv-Ct at indicated MOI for 48 hours, or cultured in EC growth media for 24 hours and then treated with 50μM DL-Hcy in the presence of 40 μM adenosine for another 24 hours (**A**). HUVECs P8 of 50% confluence were infected with Adv-Carom-shRNA or Adv-Ct-shRNA at indicated MOI for 48 hours and then treated with 50μM DL-Hcy in the presence of 40 μM adenosine for another 24 hours (**B**). **A and B.** [³H]-Thymidine uptake. Cells were metabolically labeled with 1 μCi (0.037 MBq)/mL [³H]-thymidine during the last 3 hours. [³H]-thymidine incorporation was measured in a liquid scintillation counter. Values represent mean (± SD) from 3 separate experiments with triplicates (n = 9). *P < 0.05 versus non-Hcy and non-Ade control, #P < 0.05 versus Ade and non-Hcy control.

Carom mediates Hcy-induced suppression of EC migration

Hcy has already been found to inhibit EC growth, induce EC dysfunction, trigger thrombosis and activate monocytes. Although we ruled out the role of Carom in EC growth, Carom may function in EC migration.

To determine the role of Carom in EC migration, the scratch-wound assay, a well-established *in vitro* cell migration model, was performed. Figure 3.10A shows that the relative migration distance compared to non-treated HAECs dropped from 83.4% in adenosine group to 39.9% in Hcy and adenosine group, confirming Hcy inhibition on EC migration again. Mimicking Hcy, 20 MOI Adv-Carom decreased migration from 95.7% in Adv-Ct group to 64.9%. Moreover, blocking Carom rescued EC migration in the presence of Hcy. As shown in Figure 3.10B, 50 MOI Adv-Carom-shRNA4 increased migration from 59.6% in Hcy group to 80.3%, while Adv-Ct-shRNA did not.

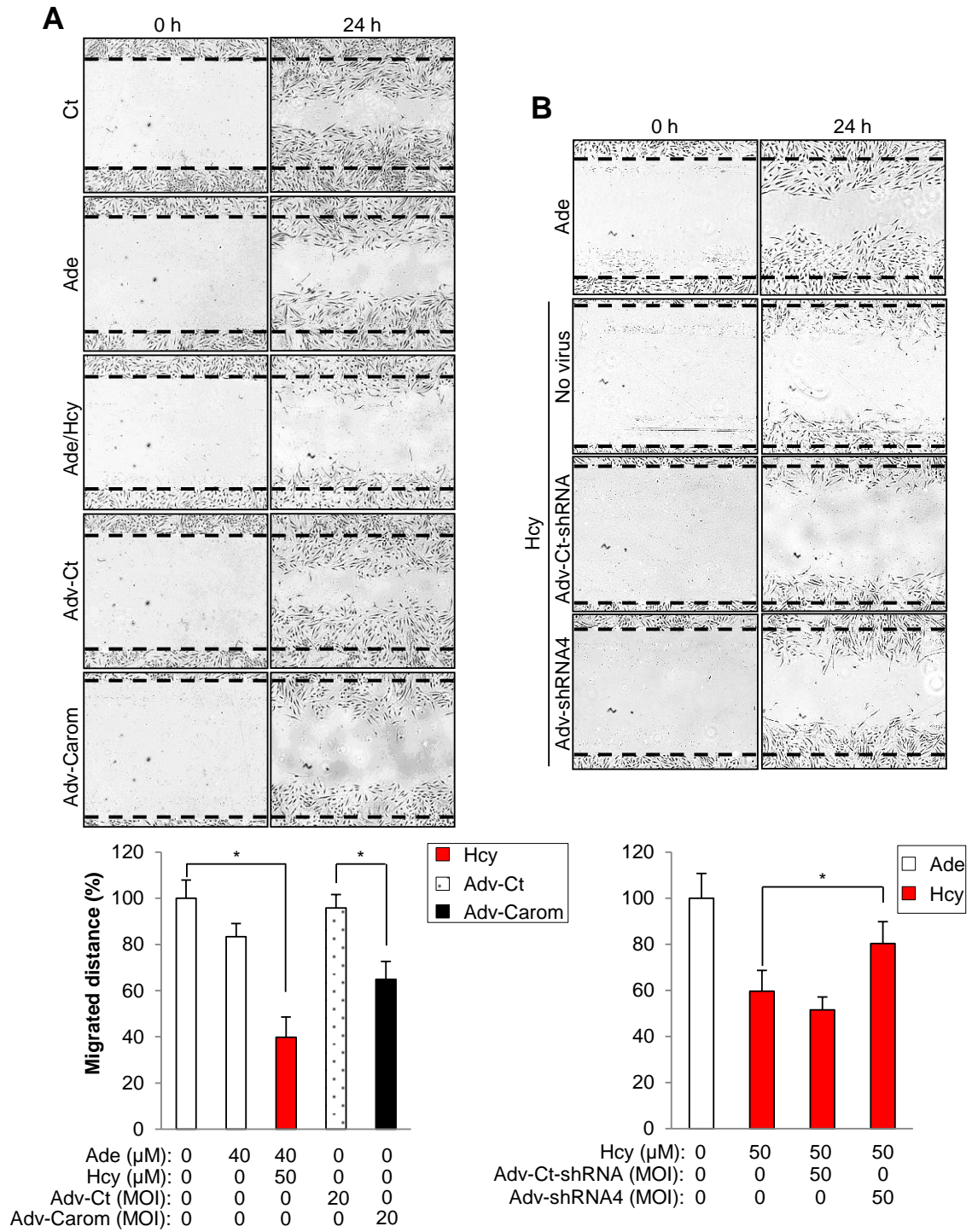


Figure 3.10. The effects of adenovirus-transduced Carom gene and Carom shRNA genes on EC migration. HAECs P9 of 70% confluence were infected with Adv-Carom or Adv-Ct at 20 MOI for 48 hours, or cultured in EC growth media for 24 hours and then

treated with 50 μ M DL-Hcy in the presence of 40 μ M adenosine for another 24 hours (**A**). HAECs P9 of 50% confluence were infected with Adv-Carom-shRNA or Adv-Ct-shRNA at 50 MOI for 48 hours and then treated with 50 μ M DL-Hcy in the presence of 40 μ M adenosine for another 24 hours (**B**). **A and B**. Cell migration. Cells were wounded by scratching with a micropipette tip. Cell migration was monitored 24 hours after wounding. Representative images of wound area (0 h) and wound closure (24 h) are shown. Cell migration distance was quantified with Axiovision software. Values represent mean (\pm SD) from 3 separate experiments, *P < 0.05.

Hcy up-regulates Carom expression through DNA hypomethylation

We have found that Hcy increases both mRNA and protein expression of Carom in EC. However, the mechanism of Carom induction by Hcy is totally unknown. Since hypomethylation and oxidation are the two main mechanisms of Hcy-induced EC disorder, we examined which mechanism affects Carom induction.

Hcy increases intracellular SAH level and decreases SAM/SAH ratio in EC

In the presence of adenosine and SAH synthetase, homocysteine accumulation could increase the level of SAH, a potent inhibitor of methyl transfer reactions involving SAM. The ratio of SAH to SAM represents a measure of cellular methylation status. To examine the intracellular methylation status after Hcy treatment, intracellular SAM and SAH levels in HAECs were measured by HPLC-MS, we found that 50 μ M Hcy significantly increased SAH level, slightly increased SAM, and significantly decreased SAM/SAH ratio, indicating that Hcy contributes to a hypomethylation status, see Figure 3.11A.

AZC, a DNMTs inhibitor, up-regulates Carom expression in EC

Hcy increases Carom gene transcription in the presence of adenosine in EC. This is associated with an increase in SAH, a potent inhibitor of methyltransferase. To test the susceptibility of Carom transcription to modulation by DNA methylation, we treated HAECs with AZC, a potent DNA demethylating agent that can be incorporated into newly synthesized DNA and form covalent complexes between cytosine-specific methyltransferases and the modified DNA, thereby inhibiting DNA methylation. We

found that AZC significantly increased expression of Carom protein, in a dose-dependent manner (Figure 3.11B).

Hcy alone without adenosine does not induce Carom expression

Adenosine is necessary for conversion of Hcy to SAH in cultured cells. Therefore, hypomethylation may not occur in EC treated with Hcy alone. Moreover, oxidation has been proposed as a primary biochemical mechanism responsible for Hcy pathogenesis when Hcy concentrations close to or higher than 1 mM (Jamaluddin, Yang, & Wang, 2007). To examine whether oxidation could modulate Carom expression, we treated HAECs with high dose of Hcy. As shown in Figure 3.11C, Hcy alone does not induce any significant change in term of Carom expression, even at the dose of 500 μ M, which is approximately 25-fold higher than the elevated Hcy levels (15–20 mM) observed in patients in the general population.

H₂O₂ decreases Carom expression in EC

Hcy can be auto-oxidized with another Hcy molecule, to generate disulfide and reactive oxygen species (ROS) to induce oxidative stress in EC. To mimic Hcy produced ROS in EC, H₂O₂ was used to treat HAECs. As shown in Figure 3.11D, H₂O₂ decreased Carom expression in HAECs in a dose-dependent manner. With the treatment of 750 μ M H₂O₂, Carom expression was totally abolished.

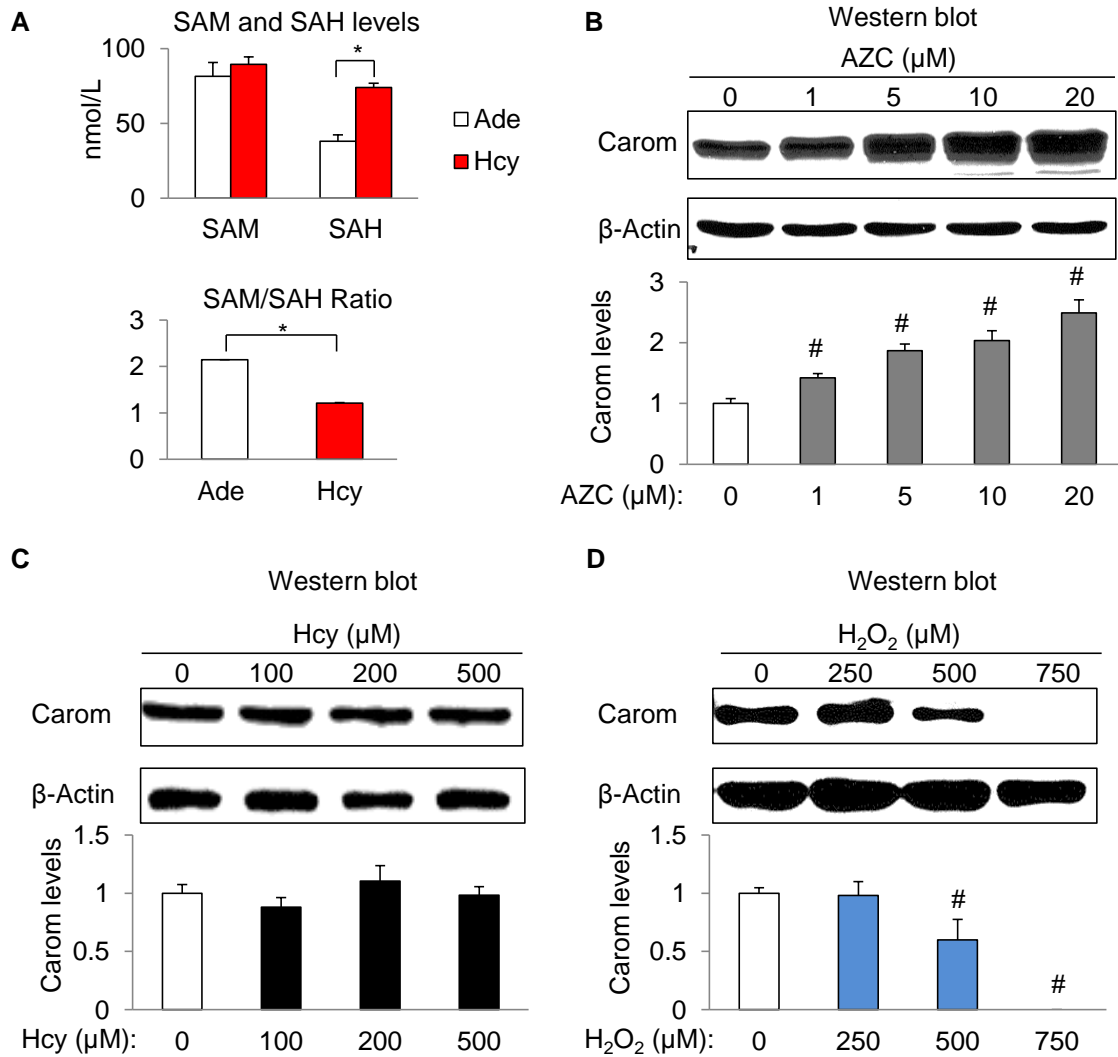


Figure 3.11. DNA methylation inhibitor upregulates Carom expression in EC. A. Intracellular levels of SAM, SAH, and SAM/SAH ratio of Hcy-treated HAECs. HAECs P8 were cultured in EC growth media containing 40 μ M adenosine and 10 μ M EHNA. At 70%-80% confluence, HAECs were exposed to 50 μ M DL-Hcy for 24 hours. Intracellular levels of SAM and SAH were measured with HPLC. **B.** Carom protein expression of AZC-treated HAECs. HAECs P8 were exposed to AZC of indicated concentration for 24 hours. Carom expression was measured by Western blot with anti-

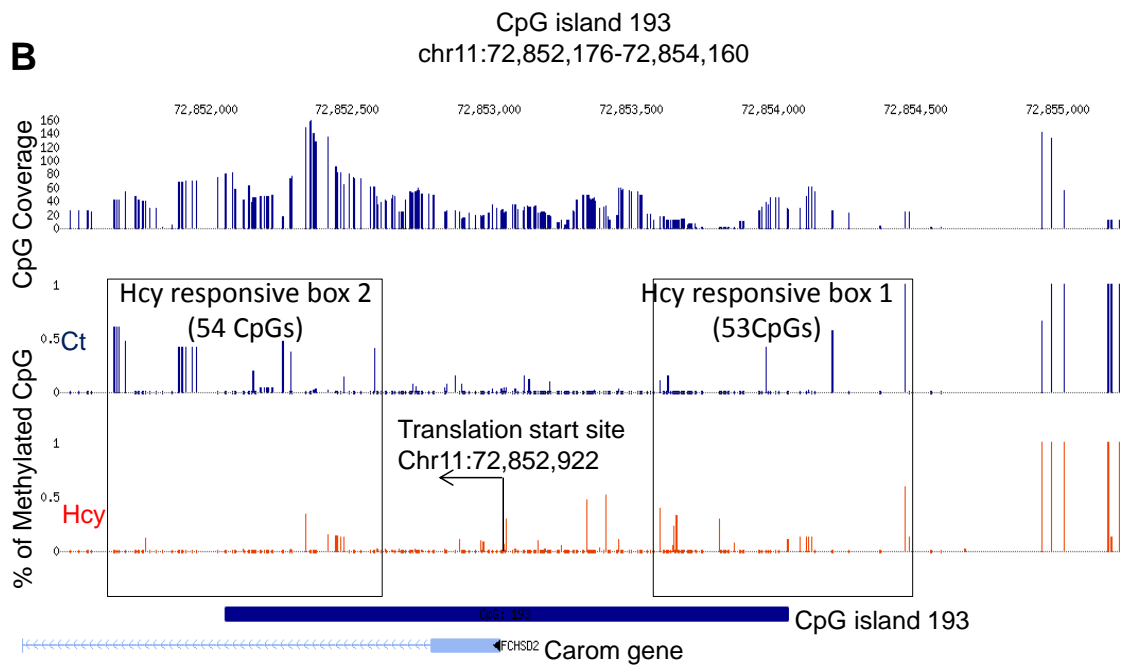
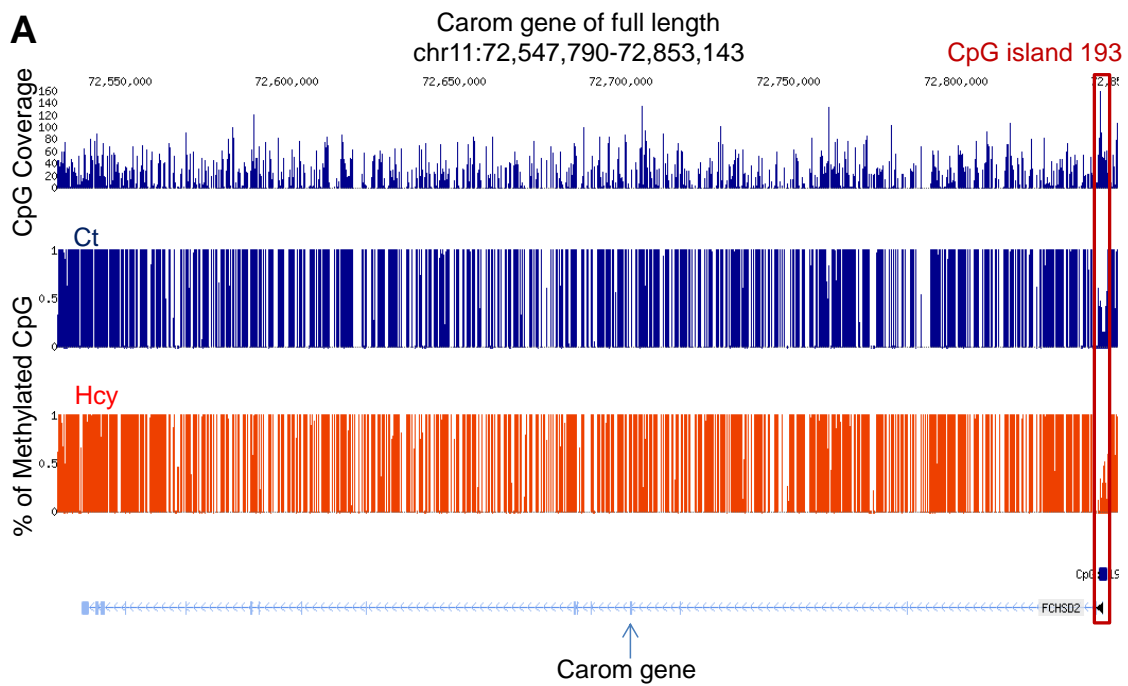
Carom antibody. **C.** Carom protein expression of HAECs treated with Hcy alone. HAECs P8 were cultured in EC growth media **without** Adenosine and EHNA. At 70%-80% confluence, HAECs were exposed to DL-Hcy at the indicated dose for 48 hours. Carom expression was measured by western blot with anti-Carom antibody. **D.** Carom protein expression of HAECs treated with H₂O₂. HAECs P8 were cultured in EC growth media to confluence of 70%-80%, and then exposed to H₂O₂ at the indicated dose for 24 hours. Carom expression was measured by western blot with anti-Carom antibody. . Relative expression levels of Carom protein was quantified with Image J software. Values represent mean (\pm SD) from 3 separate experiments (n = 3). *P < 0.05 versus non-Hcy control, #P < 0.05 versus non-AZC or non-H₂O₂ control.

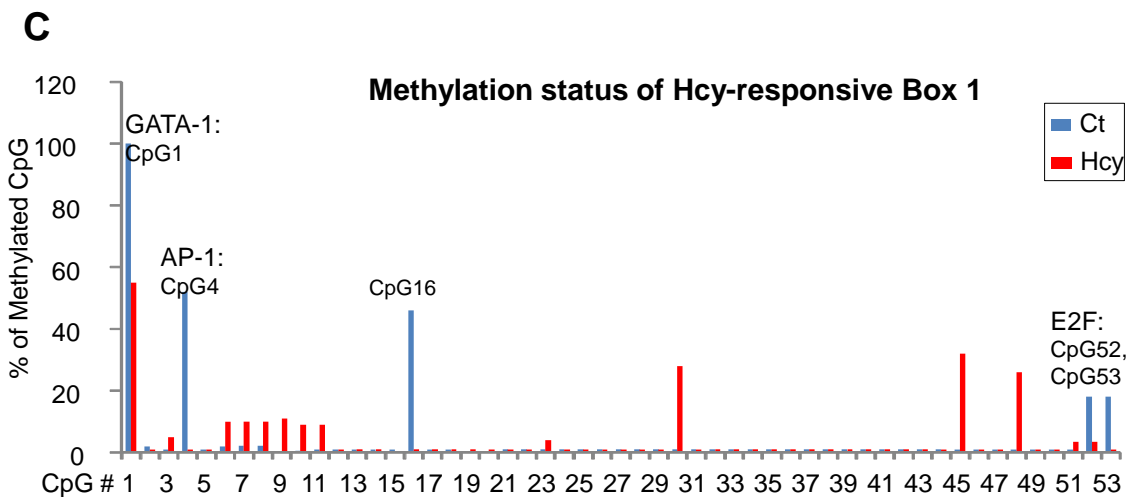
Hcy hypomethylates Carom promoter in EC

We found that Hcy increases Carom expression and SAH level in EC. This indicates a correlation between Carom expression and methylation. Furthermore, the DNA methyltransferase inhibitor-AZC also increases Carom expression in EC. Therefore, we hypothesize that DNA hypomethylation may be the mechanism of Carom induction by Hcy in EC. DNA methylation usually occurs at the 5' position of the cytosine ring within CpG dinucleotide. CpG sites are concentrated either in CpG islands (CGIs), which are short (approximately 1kb) CpG-rich DNA regions located in about 60% of human gene promoters, in the gene body, or in regions of large repetitive sequences, such as centromeres and retrotransposon elements (Toole et al., 2004). Methylation of CGIs in promoter regions mostly blocks transcription initiation, whereas gene body methylation is common in ubiquitously expressed genes and is positively correlated with gene expression (Hellman & Chess, 2007). Therefore, we examined the Carom promoter methylation status in Hcy-treated EC.

HUVECs P7 were treated with DL-Hcy 50 μ M for 24hours and genomic DNA was directly extracted and modified by bisulfite, which converts unmethylated cytosine to uracil. Comparative next-generation sequencing of DNA from HUVECs treated with and without Hcy analyzed for whole genome methylation patterns. Carom promoter sequence was also analyzed to predict transcription factor binding sites. As shown in figure 3.12A, there was no significant change of methylation status throughout the gene body of Carom in Hcy-treated cells compared to control cells. Only one CpG island is predicted on Carom gene. This CpG island 193 is located on the promoter region. Then the promoter region was enlarged to examine methylation changes induced by Hcy. Two Hcy-

responsive boxes containing enriched hypomethylated CpG sites were identified, box 1 (-1371bp – -594bp) located on the upstream of Carom translation starting site, and box 2 (439bp – 1356bp) on the downstream (Figure 3.12B). The DNA sequences of two boxes were analyzed to predict transcriptional factor binding sites. As shown in Figure 3.8C, five hypomethylated CpG sites were identified in box1. Three of them were located on transcriptional factor binding sites: CpG1 on GATA-1, CpG4 on AP-1 and CpG53 on E2F. Five CpG sites out of sixteen hypomethylated CpG sites in box 2 were located on transcriptional factor binding sites: CpG24 on MZF2, CpG25 on SP1, CpG39 on MEF1, CpG41 on AP-1 and CpG53 on GATA-1 (Figure 3.12D).





-1371

1 **GATA-1** 2 **deltaE** 3 **USF** 4 **AP-1** 5 **AP-1** 6 **AP-1** 7 **USF** 8 **Oct-1**

9 **Nkx-2** 10 **CG** 11 **CG** 12 **CG** 13 **CG** 14 **CG** 15 **CG** 16 **CG** 17 **C-Myb** 18 **CG** 19 **CG** 20 **CG** 21 **CG** 22 **E2F** 23 **CG** 24 **CG** 25 **CG** 26 **CG** 27 **CG** 28 **CG** 29 **CG** 30 **CG** 31 **MZF1** 32 **CG** 33 **CG** 34 **CG** 35 **CG** 36 **CG** 37 **CG** 38 **CG** 39 **CG** 40 **CG** 41 **CG** 42 **CG** 43 **CG** 44 **CG** 45 **Sp1** 46 **CG** 47 **CG** 48 **CG** 49 **CG** 50 **CG** 51 **CG** 52 **Egr-2** 53 **E2F** 54 **CG**

GATA-1 **AML-1a** **GATA-X** **GATA-1** **deltaE** **USF** **Oct-1** **Lyf-1** **AP-1** **Nkx-2** **C-Myb** **E2F** **HSF2** **MZF1** **Sp1** **Egr-2** **N-Myc** **E2F**

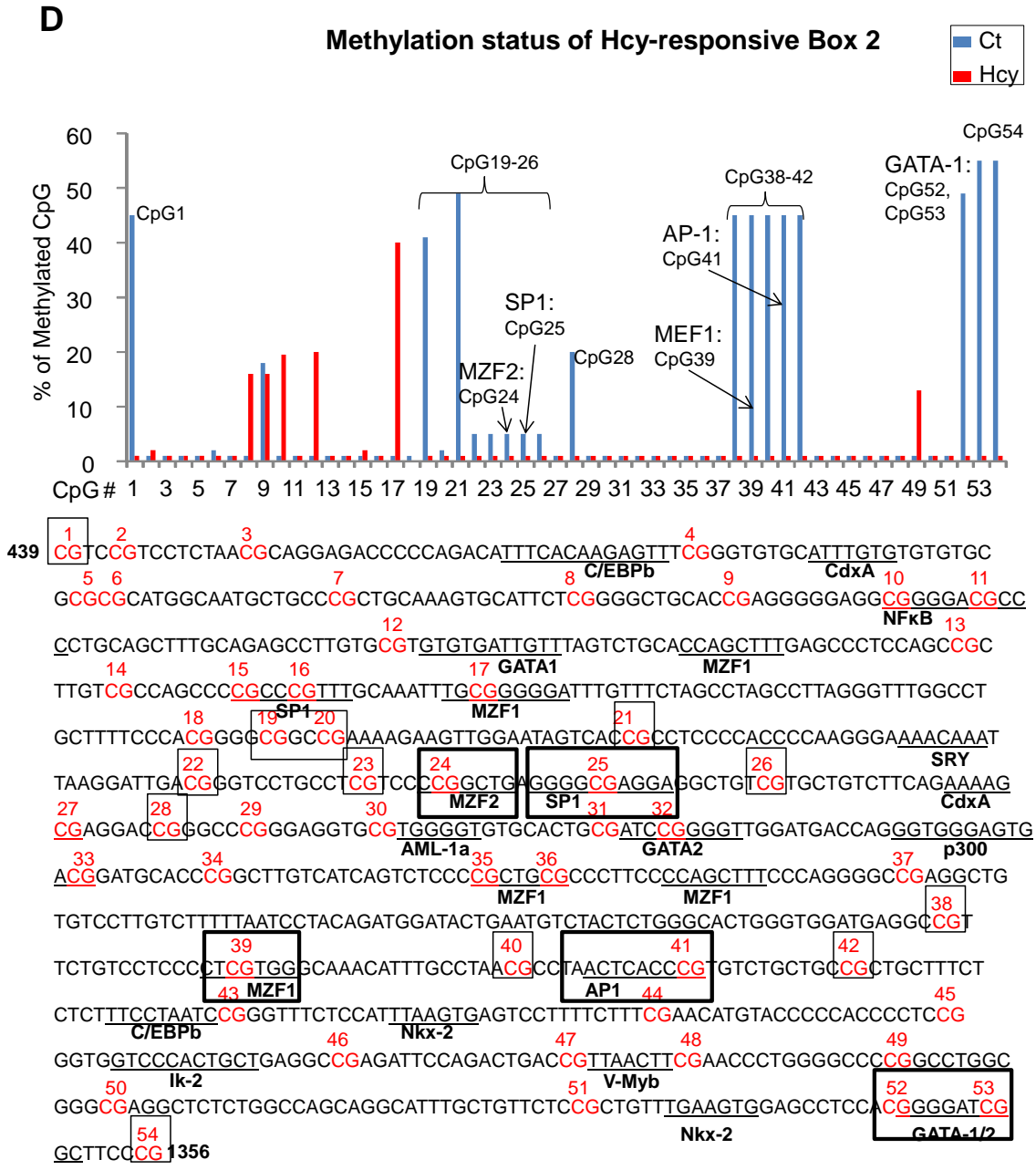


Figure 3.12. Hcy induces Carom promoter hypomethylation. HUVECs P7 were cultured in EC growth media containing 40 μ M adenosine and 10 μ M EHNA. At 80% confluence, HUVECs were exposed to 50 μ M DL-Hcy for 24 hours. Genomic DNA was directly extracted and modified by bisulfite, which converts unmethylated cytosine to uracil. Comparative next-generation sequencing of DNA from HUVECs treated with and without Hcy analyzed for whole genome methylation patterns. Sequencing data were

analyzed with BS Seeker software (UCLA, Los Angeles, CA). Cytosine of each CpG site is presented as a blue bar in the CpG coverage panel. Percentage of methylated cytosine on each CpG site is presented as a blue bar for control cells and as a red bar for cells with Hcy treatment in the % Methylated CpG panel. **A.** Methylation status of entire Carom gene. **B.** Methylation status of Carom promoter and two Hcy-responsive boxes which contain enriched hypomethylated CpG sites. **C-D.** Methylation status of Hcy-responsive box1 and box2. Sequences of box1 and box2 were analyzed with the University of Pennsylvania's Transcription Element Search System (TESS) to identify consensus elements of transcriptional factor binding sites. CpG sites were indicated as red in the DNA sequences and the consensus elements of transcriptional factor binding sites were underlined and marked.

Carom mediates Hcy-inhibited Angiogenesis via CXCL10 and CXCL11

Hcy up-regulates Carom to trigger the expression of CXCL10, CXCL11 and CCL5

Hcy has already been found to inhibit EC growth, induce EC dysfunction, trigger thrombosis and activate monocytes. Although we demonstrated that Carom inhibited EC migration, the downstream signaling molecules mediating this suppression were still unclear. Moreover, Carom may function in other Hcy-induced EC pathological changes.

Cytokines are small soluble proteins secreted by one cell that can alter the behavior or properties of the cell itself or of another cell. Each cytokine has a matching cell-surface receptor. Subsequent cascades of intracellular signaling then alter cell functions. Studies shows that ECs are not only targets but also able to secrete cytokines themselves in response to stimulations (Kofler, Nickel, & Weis, 2005; Krishnaswamy, Kelley, Yerra, Smith, & Chi, 1999). Therefore, identification of Carom-regulated cytokines could figure out the potential functions of Carom in EC. As shown in Figure 3.13A, adenovirus-expressed Carom at 100 MOI triggered secretion of CXCL10, CXCL11 and CCL5 in EC, while Adv-Ct did not. We then confirmed increase of mRNA levels of these three cytokines in HAECs infected with 20 MOI Adv-Carom, which expresses Carom protein to a similar level as 50 μ M Hcy (Figure 3.13B). In addition, the effect of Hcy on mRNA expression of CXCL10, CXCL11 and CCL5 was also examined. Figure 3.13C shows that Hcy increased all three cytokines' mRNA levels as early as 12 hours, CXCL10 and CCL5 were induced to the peak values (CCL5: 24.3-fold, CXCL10: 29.5-fold) at 24 hours, CXCL11 was increased to the highest level of 10.6-fold at 48 hours.

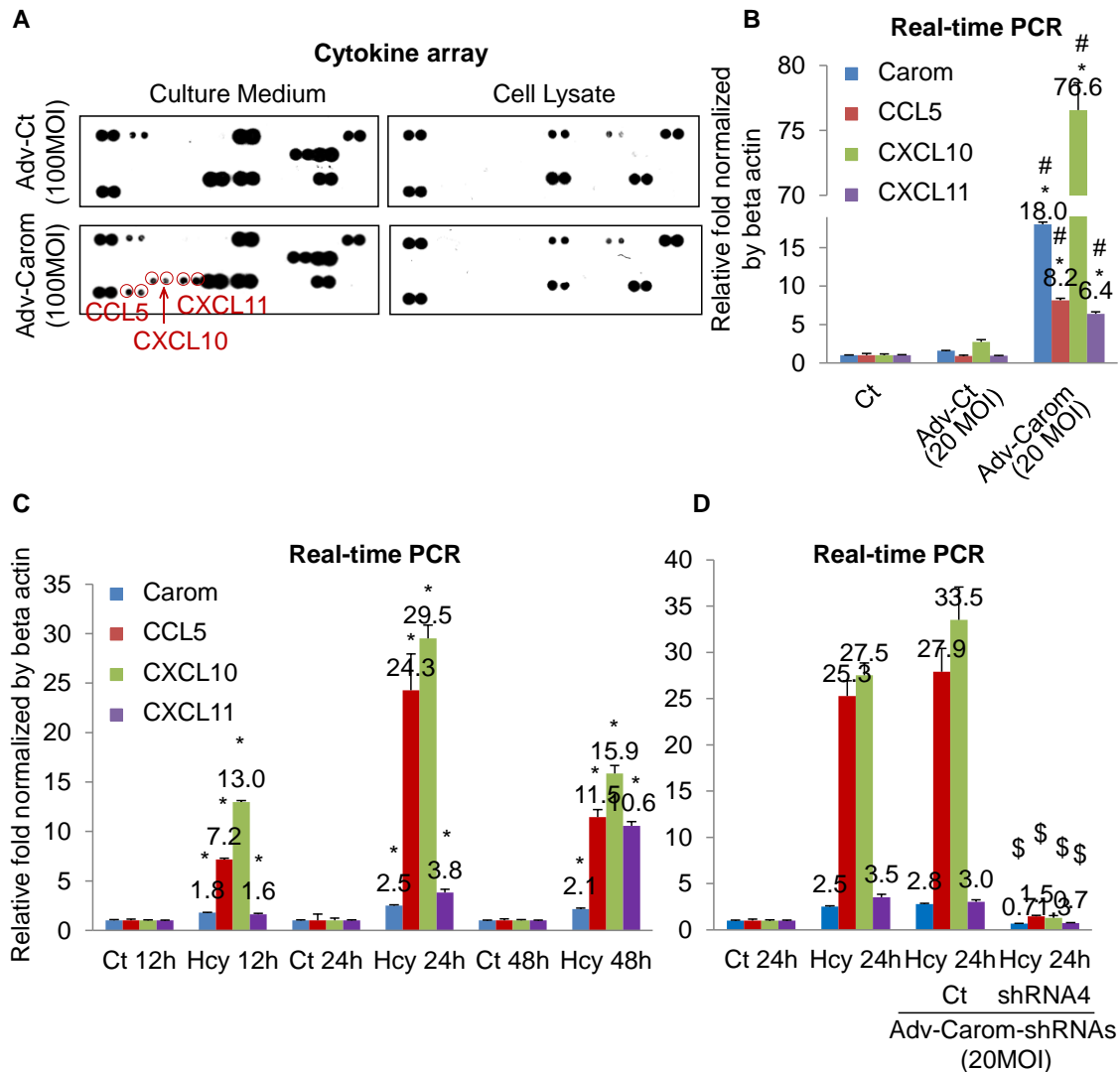


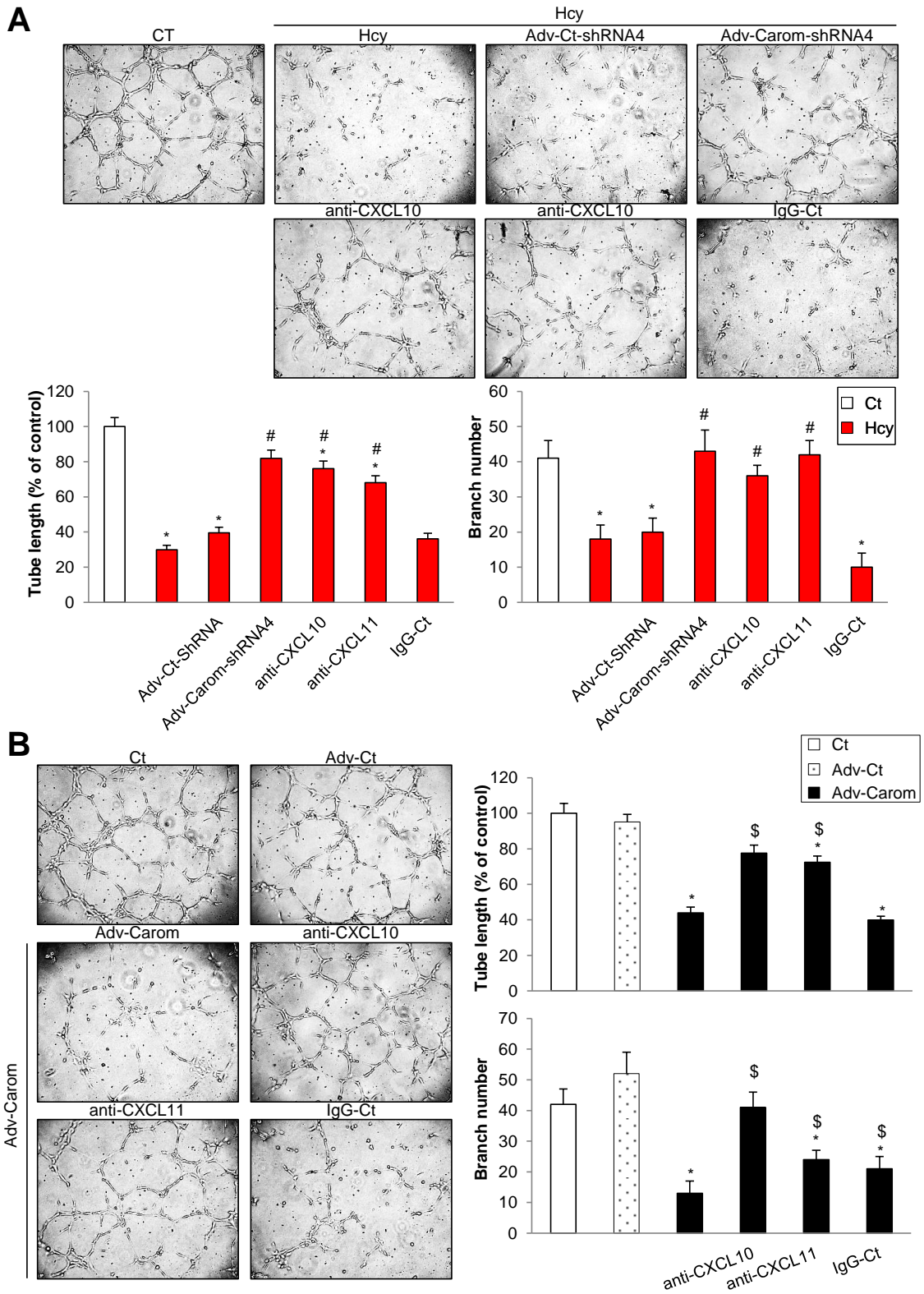
Figure 3.13. Hcy up-regulates Carom to trigger expression of CCL5, CXCL10 and CXCL11. **A.** Human cytokine array of HAECs infected with Adv-Carom. HAECs P9 of 80% confluence were infected with Adv-Carom 100 MOI for 48 hours. Cell lysate and culture medium were collected and subjected to Human Cytokine Array. **B.** mRNA levels of Carom, CXCL10, CXCL11 and CCL5 of HAECs P9 (80% confluence) infected with 20 MOI Adv-Carom or Adv-Ct for 48 hours. **C.** mRNA levels of Caorm, CXCL10, CXCL11 and CCL5 of HAECs P9 cultured in media containing 40 μ M adenosine and 10 μ M EHNA to 80% confluence, then exposed to 50 μ M DL-Hcy for indicated time. **D.**

mRNA levels of Caorm, CXCL10, CXCL11 and CCL5 of HAECs P9 cultured in media containing 40 μ M adenosine and 10 μ M EHNA to 50% confluence, then infected with 20 MOI Adv-Carom-shRNA4 for 48 hours and exposed to 50 μ M DL-Hcy for another 24 hours. **B-D.** Real-time PCR assay. Total cellular RNA was extracted from HAECs after treatment. mRNA levels of target genes were assessed using Real-time PCR by $\Delta\Delta C_T$ comparison to β -Actin. Values represent mean (\pm SD) from 3 separate experiments with triplicates (n = 9). *P < 0.05 versus non-Hcy and nonviral control, #P < 0.05 versus Adv-Ct control, \$P < 0.05 versus Adv-Ct-shRNA control.

Carom inhibits tube formation through CXCL10 and CXCL11

We have demonstrated that Carom induces three chemokines, CXCL10, CXCL11 and CCL5 in HAECs as well as Hcy. CXCL10 and CXCL11 belong to the CXC chemokine family which attracts neutrophils and lymphocytes, whereas CCL5 is a member of the CC chemokine family which primarily recruits monocytes, but also attracts lymphocytes, basophils, and eosinophils. Beyond their classical function in leukocyte recruitment, CXC chemokines also play a critical role in both physiologic and pathologic angiogenesis (Mehrad, Keane, & Strieter, 2007). CXCL10 and CXCL11 are non-ELR (Glu-Leu-Arg, a motif immediately preceding the first Cys residue) CXC chemokines which inhibits angiogenesis. CXCL10 and CXCL11 have been reported to block VEGF-induced EC migration and tube formation (Bodnar, Yates, Rodgers, Du, & Wells, 2009; Bodnar, Yates, & Wells, 2006; Leloup et al., 2010; Yates-Binder et al., 2012). Therefore, we hypothesize that Carom could inhibit angiogenesis via CXCL10 and CXCL11.

We investigated the effect of Carom on angiogenesis using the tube formation assay. HAECs were cultured on Matrigel Matrix, a solid gel of mouse basement membrane proteins, which is EC's natural substrate, and form capillary-like structures with a lumen. Figure 3.14A shows that Hcy significantly decreased both the tube length and the branch numbers, while this inhibition was rescued by Adv-Carom-shRNA4 and neutralizing antibodies of CXCL10 and CXCL11. Similarly, transduction of Carom by adenovirus induced a suppression of tube formation, which was reversed by neutralization of CXCL10 and CXCL11, as shown in Figure 3.14B.



shRNA or Adv-Ct-shRNA at 20 MOI for 48 hours and then treated with 50 μ M DL-Hcy in the presence of 40 μ M adenosine for another 24 hours. HAECs without virus infection were co-incubated with 0.5 μ g/ml mouse anti-human CXCL10, CXCL11 neutralizing antibodies and mouse IgG control (IgG-Ct) when treated with Hcy (**A**). HAECs P9 of 70% confluence were infected with 20 MOI Adv-Carom for 24 hours, then incubated with 0.5 μ g/ml mouse anti-human CXCL10, CXCL11 neutralizing antibodies and mouse IgG control (IgG-Ct) for another 24 hours (**B**). **A** and **B**. Tube formation. HAECs were trypsinized immediately after treatments and seeded to 96-well plate pre-coated with matrigel matrix at a density of 4×10^3 /well with 80 μ l EC growth media. Tube-like structure was photographed after 6 hours. The total tube length and branch number were quantified using Image J software. Values represent mean (\pm SD) from 3 separate experiments (n = 3), *P < 0.05 versus non-Hcy and nonviral control, #P < 0.05 versus nonviral Hcy group, \$P < 0.05 versus Adv-Carom group.

CHAPTER 4

DISCUSSION

Cardiovascular disease (CVD) and its complications, such as myocardial infarction and cerebrovascular accident, are the leading causes of death worldwide. Clinical, epidemiology and meta-analysis studies have established hyperhomocysteinemia (HHcy) as an independent risk factor for CVD. Endothelial cell damage, impaired endothelial function, dysregulation of cholesterol and triglyceride biosynthesis, thrombosis activation, and vascular smooth muscle cell proliferation have all been suggested as mechanisms by which elevated Hcy mediates pathological cardiovascular changes. Vascular disease may be initiated by endothelial injury resulting from insult to the vessel wall. Endothelial injury subsequently leads to platelet aggregation, coagulation, VSMC proliferation, and atherosclerosis. However, the underlying molecular mechanism by which HHcy contributes to EC injury remains to be elucidated. This study seeks to explore the regulatory mechanisms of Hcy induced EC injury at cellular and molecular levels in order to better understand HHcy's role in CVD. We have made three major findings in this study: 1) Carom, a novel gene, is up-regulated by Hcy at a physiologically relevant level (50 μ M) in EC. Both mRNA expression and protein expression of Carom are increased by Hcy in EC. 2) Carom induction by Hcy is associated with promoter hypomethylation in EC. 3) Carom triggers two antiangiogenic chemokines, CXCL10 and CXCL11, to inhibit EC migration and tube formation as well as Hcy.

Carom is a novel Hcy-responsive gene in EC

To understand better the mechanism of EC injury caused Hcy, identification of the Hcy-responsive genes is the first step. We have found that cyclin A is a Hcy-responsive gene. Hcy suppressed cyclin A transcription via promoter hypomethylation to inhibit EC growth. Noteworthily, Hcy inhibited EC growth as early as 24 hours, though significant suppression of cyclin A occurred after 30 hours of Hcy treatment (H. Wang et al., 2002). Thus, we speculated that there were some early genes responsive to Hcy. Differential Display was then performed to identify such genes. Fifty cDNA clones from HUVECs with 12 hours Hcy treatment were obtained with Differential Display. Surprisingly, fifteen out of fifty clones were identified as Carom (Table 3.1 and Figure 3.1).

Carom was first identified as a membrane-associated guanylate kinase (MAGUK)-interacting protein in search of the MAGI-1-interacting protein in epithelial cells. It was named as Carom and shown to bind scaffolding proteins MAGI-1 and CASK and associate with cytoskeleton (Ohno et al., 2003). Carom was later identified as FCHSD2 because it contains 1 N-terminal F-BAR (FES-CIP4 Homology and Bin/Amphiphysin/Rvs) domain and 2 C-terminal SH3 domains (Katoh & Katoh, 2004). Carom is a member of the F-BAR protein family which is a class of cytosolic proteins that have the ability to bind plasma membranes and thereby to couple other proteins such as actin cytoskeleton with plasma membranes. Functionally, F-BAR proteins have been shown to interact with plasma membranes and are involved in F-actin modulation, which implicates them in many fundamental biological processes, such as endocytosis, exocytosis, cytoskeletal reorganization, and cell migration (Chitu & Stanley, 2007). To date, Carom function is relatively unknown.

We next examined the tissue expression of Carom both in human and mouse. Carom was found to be ubiquitously expressed in 21 human tissues and in 20 mouse tissues (Figure 3.2). Carom was highly expressed in human lymph node, nerve and pituitary gland. Carom was also abundant in mouse blood, eye, lymph node, ovary and spleen. Lymph node is the common tissue where Carom is highly expressed between human and mouse. Lymphocytes accumulate in lymph node and their migration can be largely accelerated upon the stimulation of antigens. Therefore, high expression level of Carom in lymph node suggests that Carom may be involved in lymphocyte migration. In human vascular tissue, Carom expression was relatively lower than other tissues, suggesting that it could be a strictly regulated gene in vascular cells and could be possibly induced in response to stimulation.

To further confirm and characterize the time course of Carom induction by Hcy, we used Northern blot with the radiolabeled Carom cDNA clone A12 obtained from Differential Display and Real-time PCR to examine Carom mRNA levels in HUVECs or HAECs treated with Hcy for 12 hours, 24 hours and 48 hours. Carom mRNA induction was confirmed at each time-point with Northern blot (Figure 3.5A). And Real-time PCR results suggest that Carom induction by Hcy was in a time-dependent manner (Figure 3.5B).

After mRNA induction was confirmed, we went further to examine the effect of Hcy on Carom protein expression. Because Carom is a novel gene, there was no commercial Carom antibody available. Thus, we generated our highly specific homemade rabbit anti-Carom antibody with a recombinant Carom-GST fusion protein as antigen (Figure 3.3) and purified antibody through antigen affinity purification (Figure 3.4). Then we

examined the effect of Hcy on Carom expression in HAECs (Figure 3.5C) and Carom expression in HHcy mouse EC (Figure 3.6) with Western blot and found that Hcy increased Carom protein expression in EC both *in vitro* and *in vivo*.

Taken together, these data suggests that Carom was induced by Hcy in EC. There are some Hcy-responsive genes in EC have already been identified. ER stress protein GRP78/BiP, transcription factor ATF4, elongation factors EF-1 α , -1 β and -1 δ , cell cycle arresters GADD153, GADD45, and ATP-dependent DNA helicase were found to be induced by 5mM Hcy in HUVECs (Kokame, Kato, & Miyata, 1998; Outinen et al., 1999). However, 5mM was a relatively high concentration of Hcy, above the levels that confer increased cardiovascular risk. The following studies focused on cultured EC with clinically observable concentrations of Hcy. MCP-1 (F. L. Sung, Slow, Wang, Lynn, & O, 2001) and SDF-1(M. L. Sung et al., 2009), sEH (D. Zhang, Xie, et al., 2012), PDGF (D. Zhang, Chen, et al., 2012), FGF (Chang et al., 2008), p66shc (C. S. Kim et al., 2011) and VCAM-1(Silverman et al., 2002) have been identified as Hcy-responsive genes in EC treated with Hcy ranging from 20 μ M to 200 μ M. Given that all the found Hcy-responsive genes are well characterized in function, our study is the first to identify a novel gene responsive to Hcy at clinically relevant concentration.

In addition, VSMCs are the other important cells in vasculature. Proliferation and migration of VSMC play a key role in atherosclerosis development. Although Hcy inhibits EC growth significantly, it has little effect on VSMC growth (H. Wang et al., 1997), suggesting the difference between EC and VSMC in response to Hcy. Therefore, the expression level of Carom in Hcy-treated VSMC should be examined to comprehensively determine the role of Carom in CVD.

Carom induction by Hcy is associated with promoter hypomethylation in EC

We have demonstrated that Hcy increased Carom mRNA and protein levels in the presence of adenosine. However, the mechanism of Carom regulation was unknown yet. In Hcy metabolism, SAH is hydrolyzed to Hcy and adenosine by S-adenosylhomocysteine hydrolase (AHCY). While this reaction could be reversed by elevated Hcy level, results in SAH accumulation. Since SAH is a potent inhibitor of cellular methyltransferases, hypomethylation is one important biochemical mechanism by which HHcy contributes to EC injury. We confirmed the increase of SAH and the decrease of SAM/SAH ratio, a measure of cellular methylation status, in HAECs treated with 50 μ M Hcy (Figure 3.11A). Moreover, our lab have found that Hcy inhibits DNMT-1 activity in EC (M. S. Jamaluddin et al., 2007). Therefore, we suspected that Carom expression could be modulated by DNA methylation. To address this hypothesis, we treated HAECs with AZC, a potent DNA demethylating agent that can be incorporated into newly synthesized DNA and form covalent complexes between cytosine-specific methyltransferases and the modified DNA, thereby inhibiting DNA methylation. We found that AZC significantly up-regulated Carom in a dose-dependent manner (Figure 3.11B). These data indicate the association between Carom induction by Hcy and DNA methylation.

In vitro studies found that some biologic effects of Hcy can be mimicked by hydrogen peroxide or other sulfhydryl-containing agents, are inhibited by catalase, and require oxygen (Eberhardt et al., 2000; Starkebaum & Harlan, 1986). These results have provided support to the proposal that increased oxidation mediated through the sulfhydryl group of Hcy is a major mechanism responsible for Hcy-induced vascular pathogenesis (Lentz,

1997; Mayer, Jacobsen, & Robinson, 1996). In addition, these effects typically require relatively high concentrations of Hcy. To test whether oxidation plays a role in Carom induction, we treated HAECs with high concentrations of Hcy (100 μ M-500 μ M) in absence of adenosine, and found that Hcy of high level alone did not affect Carom protein expression (Figure 3.11C). We further used hydrogen peroxide to mimic the oxidation mediated through the sulfhydryl group of Hcy in HAECs, and the result shows that hydrogen peroxide of 250 μ M did not induce any significant change in Carom expression, but huge decrease appeared at 500 μ M and Carom expression was even totally abolished at 750 μ M (Figure 3.11D).

Taken together, these data suggest that Hcy may induce Carom expression via a DNA hypomethylation associated mechanism but not oxidation. To further confirm the role of DNA hypomethylation in Carom induction, the effect of adenovirus transduction of DNMT-1 on Carom expression should be examined to determine whether restoration of DNA methylation reverses Carom induction by Hcy in EC in the future.

DNA methylation usually occurs at the 5' position of the cytosine ring within CpG dinucleotide. CpG sites are concentrated either in CpG islands (CGIs), which are short (approximately 1kb) CpG-rich DNA regions located in about 60% of human gene promoters, in the gene body, or in regions of large repetitive sequences, such as centromeres and retrotransposon elements. DNA methylation of CGIs in promoter regions regulates gene transcription by interference with transcription activator or suppressor binding, by attracting methyl-CpG-binding proteins (MBPs) to repress transcription via the recruitment of histone deacetylase (HDAC) which leads to chromatin condensation. Meanwhile, gene body methylation is common in ubiquitously

expressed genes and is positively correlated with gene expression (Hellman & Chess, 2007). Thus, we used bisulfite deep sequencing to profile the methylation status of every single CpG on Carom gene to identify the Hcy-responsive site. Surprisingly, there is only one CGI found throughout the whole gene of Carom, located on the promoter region. On gene body, little difference of methylation status between control HUVECs and Hcy-treated HUVECs were found. But obvious change of methylation pattern was identified in the promoter region covering the only CGI (Figure 3.12A). Two Hcy-responsive boxes containing enriched hypomethylated CpG sites in Carom promoter were further identified, box 1 (-1371bp – -594bp) located on the upstream of Carom translation starting site, and box 2 (439bp – 1356bp) on the downstream (Figure 3.12B). The DNA sequences of two boxes were analyzed to identify hypomethylated CpGs in transcriptional factor binding sites. Three hypomethylated CpGs were identified in box1: CpG1 in GATA-1, CpG4 in AP-1 and CpG53 in E2F (Figure 3.12C); other five sites were identified in box2: CpG24 in MZF2, CpG25 in SP1, CpG39 in MEF1, CpG41 in AP-1 and CpG53 in GATA-1 (Figure 3.12D). Future study to determine the functional importance of these Hcy-hypomethylated CpG on transcription factor binding sites in Carom promoter will verify the Hcy-responsive CpG for Carom induction.

Our lab is the first to propose that Hcy regulates target gene expression via promoter hypomethylation. We demonstrated that Hcy inhibited DNMT1 activity, leading to hypomethylation of the cell-cycle dependent element (CDE) on the cyclin A promoter to recruit a transcription suppressor, in consequence blocked cyclin A transcription (M. S. Jamaluddin et al., 2007). This proposal is supported by following studies. Hcy is reported to cause hypomethylation of CpG sites 6 and 7 of P66shc promoter, which leads to

increased P66shc expression, causing oxidative stress and endothelial dysfunction (C. S. Kim et al., 2011). Moreover, Hcy has been shown to demethylate ATF6 binding site in the promoter of soluble epoxide hydrolase (sEH) gene, which hydrolyzes epoxyeicosatrienoic acids and attenuates their cardiovascular protective effects, contributing to sEH up-regulation and endothelial activation (D. Zhang, Xie, et al., 2012). The present study provides new evidence to sustain the proposal that DNA methylation is one major molecular mechanism underlying Hcy induced EC disorder.

Carom mediates Hcy-induced inhibition of EC migration and angiogenesis through CXCL10 and CXCL11

In order to characterize Carom function in EC, we generated recombinant adenovirus Adv-Carom to transduce Carom for gain-of-function study and Adv-Carom-shRNAs to express Carom shRNAs for loss-of-function study. The virus-expressed Carom protein levels were examined and 20 MOI Adv-Carom increased Carom protein level to 2.12-fold, similar to 2.08-fold in HAECs treated with 50 μ M Hcy for 48 hours (Figure 3.7). 20 MOI Adv-Carom-shRNA4 decreased Carom mRNA and protein to 1/3 of control HAECs, the lowest level among the four Carom shRNA expressing viruses. In addition, Adv-Carom-shRNA4 of 20MOI also most reversed Carom induction by Hcy in HAECs (Figure 3.8).

Because Carom induction occurs at 12 hours, much earlier than EC growth inhibition (24 hours) and cyclin A suppression (30 hours) induced by Hcy, and the Carom-interacting protein CASK has been shown to inhibit cell proliferation, we first hypothesized that Carom may play a role in EC growth inhibition. However, neither did adenovirus-

transduced Carom expression mimic Hcy to inhibit DNA synthesis, nor did Adv-Carom-shRNA4 recover EC growth suppressed by Hcy in HAECs (Figure 3.9). These findings rule out the role of Carom in EC growth.

Because of that Hcy has been found to inhibit EC migration both *in vitro* and *in vivo*, and that F-BAR proteins play a role in cell migration, we hypothesized that Carom could be the Hcy-induced inhibitor of EC migration. The effect of Carom on EC migration was then examined by the scratch-wound assay. We found that Adv-Carom inhibited HAECs migration as well as Hcy and Adv-Carom-shRNA4 rescued EC migration that was suppressed by Hcy (Figure 3.10).

We found that Hcy up-regulates Carom to inhibit EC migration. However, it was still unknown that whether Carom was the final effector or it could trigger other downstream signaling molecules to induce suppression.

Cytokines play various roles in EC functions including migration. Hcy has also been reported to induce cytokines production in EC (Postea, Koenen, Hristov, Weber, & Ludwig, 2008; F. L. Sung et al., 2001; Tacheny et al., 2002). Therefore, identification of Carom-regulated cytokines could figure out the potential signaling molecules of Carom in EC. Encouragingly, we found that adenovirus-expressed Carom at 100 MOI triggered secretion of CXCL10, CXCL11 and CCL5 in HAECs with Human Cytokine Array (Figure 3.13A). We next confirmed increase of mRNA levels of these three cytokines in HAECs infected with 20 MOI Adv-Carom, which expresses Carom protein to a similar level as 50 μ M Hcy (Figure 3.13B). Then we examined whether Hcy could also induce these cytokines. Our results show that Hcy increased all three cytokines' mRNA levels as early as 12 hours, CXCL10 and CCL5 were induced to the peak values (CCL5: 24.3-fold,

CXCL10: 29.5-fold) at 24 hours, CXCL11 was increased to the highest level of 10.6-fold at 48 hours (Figure 3.13C).

CXCL10 and CXCL11 are two established anti-angiogenic chemokines and reported to block VEGF-induced EC migration and tube formation (Bodnar et al., 2009; Bodnar et al., 2006; Leloup et al., 2010; Yates-Binder et al., 2012). We further investigated the effect of Carom on angiogenesis using the tube formation assay. Hcy significantly decreased both the tube length and the branch numbers, while this inhibition was rescued by Adv-Carom-shRNA4 and neutralizing antibodies of CXCL10 and CXCL11. Similarly, transduction of Carom by adenovirus induced a suppression of tube formation, which was reversed by neutralization of CXCL10 and CXCL11 (Figure 3.14). Taken together, our study suggests that Carom mediates Hcy-induced inhibition of EC migration and tube formation through CXCL10 and CXCL11.

A few cytokines induced by Hcy in EC have been reported, including MCP-1 (Poddar et al., 2001; Silverman et al., 2002; H. S. Zhang, Cao, & Qin, 2003), IL8 (Geisel et al., 2003; Poddar et al., 2001), CXCL16 (Postea et al., 2008), IL12 and CXCL10 (Shastry, Tyagi, Hayden, & Tyagi, 2004). However, most of these cytokines were induced in cell lines or mouse EC. Our study is the first to demonstrate that Hcy of clinically relevant concentration induces CXCL10, CXCL11 and CCL5 in human primary endothelial cells. Although CXCL10 and CXCL11 are found to inhibit angiogenesis, their proinflammatory effects in recruitment of leukocytes should be taken into consideration in the future study of Carom function. Moreover, CCL5 play an important role in monocyte recruitment in atherosclerosis (Doring et al., 2014; Drechsler, Megens, van

Zandvoort, Weber, & Soehnlein, 2010; Koenen et al., 2009). Therefore, future study should examine Carom's role in monocyte recruitment in atherosclerotic model.

Recently F-BAR proteins have emerged as important regulators of cell protrusion formation and migration as well as endocytosis. These processes require the concerted action of the plasma membrane and the cytoskeleton and F-BAR proteins are modular molecules that serve as multivalent adaptors that physically and functionally link both compartments. F-BAR proteins contain one N-terminal F-BAR domain and most contain one or two SH3 domains at C-terminus. The F-BAR domain senses and shapes membrane curvature, while a majority of F-BAR proteins uses the C-terminal domains to interact with components and regulators of the actin cytoskeleton, e.g. actin nucleation promoting factors WASP and N-WASP, Arp2/3 and the large GTPase dynamin. Most of functional studies of F-BAR proteins focused on neural cell, though the function of F-bar proteins in EC remains to be elucidated. Recently, the F-BAR protein NOSTRIN has been indicated to be necessary for proper vascular development in postnatal retinal angiogenesis in mice (Kovacevic et al., 2012). NOSTRIN formed a complex with the GTPase Rac1 and its exchange factor Sos1 and interacted with fibroblast growth factor (FGF) receptor 1 in mouse lung endothelial cells (MLECs). NOSTRIN was required for fibroblast growth factor 2 dependent activation of Rac1 in MLECs and the angiogenic response to FGF 2 in the in vivo matrigel plug assay. This study proposed a new signal pathway in which NOSTRIN assembles a signaling complex containing FGFR1, Rac1 and Sos1 thereby facilitating the activation of Rac1 in endothelial cells during developmental angiogenesis. Thereby, Carom may facilitate angiogenesis inhibition

through a signaling complex. Future study to identify Carom-interacting protein will improve our understanding of the Hcy-Carom signaling.

We found that Hcy-induced DNA hypomethylation was associated with Carom induction and Carom mediated EC migration and tube formation. The effect of DNA hypomethylation on EC migration and tube formation should be examined to determine the biochemical mechanism by which Hcy inhibits EC migration and angiogenesis in the future.

To further determine the *in vivo* role of Carom in CVD, Carom conditional knockout mouse is in generation.

Conclusion and Future Directions

Our study aims to elucidate mechanisms for Hcy-induced endothelial disorder that may contribute to the development of CVD. First, we identified Carom, a novel gene, as an early Hcy-responsive gene HUVECs. The increase of Carom expression induced by Hcy in EC was confirmed in both *in vitro* and *in vivo*.

Second, our data suggest that Hcy up-regulates Carom expression by a DNA hypomethylation associated mechanism. We confirmed that Hcy increased intracellular SAH level and decreased SAM/SAH ratio, and found that the DNMTs inhibitor azacytidine significantly induced Carom expression in HAECs as well as Hcy, suggesting the association between DNA hypomethylation and Carom induction. Therefore, we profiled the methylation status of Carom gene in Hcy-treated cells and found that Carom promoter was hypomethylated by Hcy. In addition, several hypomethylated CpGs in the potential transcriptional factor binding sites were identified.

For future study, the effect of adenovirus transduction of DNMT-1 on Carom expression in Hcy-treated ECs should be examined to further confirm the role of DNA hypomethylation in Carom induction. Promoter assay to determine the functional importance of the Hcy-hypomethylated CpG on transcription factor binding sites in Carom promoter should be performed to identify Hcy-responsive CpG.

Third, our data show that Carom triggers CXCL10 and CXCL11 to inhibit EC migration and angiogenesis as well as Hcy. Carom was not found to play a role in EC growth inhibition. However, we found that Carom overexpression by virus induced two anti-angiogenic cytokines CXCL10 and CXCL11 as well as Hcy in EC. Moreover, we found that Adv-Carom inhibited HAECs migration as well as Hcy and Adv-Carom-shRNA rescued EC migration suppressed by Hcy. We further investigated the effect of Carom on angiogenesis using the tube formation assay. Hcy significantly decreased tube formation, while this inhibition was rescued by Adv-Carom-shRNA4 or neutralizing antibodies of CXCL10 and CXCL11. Similarly, Adv-Carom induced a suppression of tube formation, which was also reversed by neutralization of CXCL10 and CXCL11.

In conclusion, we found that Hcy up-regulates Carom expression through DNA methylation to induce CXCL10 and CXCL11, which contribute to inhibitions of EC migration and angiogenesis (Figure 4.1).

Several members of the F-BAR protein family have been implicated in the trafficking of trans-membrane receptors such as the EGF- and the PDGF-receptor (Hu et al., 2009; Toguchi, Richnau, Ruusala, & Aspenstrom, 2010). In addition, NOSRTIN, an F-BAR protein, also facilitates eNOS internalization. Thus, Carom may possibly influence the endocytosis of signaling molecules which plays key role in EC biology.

Moreover, the Carom-interacting protein MAGI1 is required for enhancement of VE-Cadherin-mediated EC junction, which is essential for inhibition of EC permeability to prevent transendothelial migration of monocyte and leukocyte (Sakurai et al., 2006). This suggests that Carom may interact with MAGI1 and inhibit its function in EC junction, leading to increase of EC permeability.

Furthermore, we found Adv-Carom significantly induced CCL5, a proatherogenic chemokine, which recruits inflammatory monocytes to endothelium during atherosclerosis development. Therefore, Carom may play a role in monocyte recruitment, which contributes to the increased risk of CVD in HHcy.

This study on Carom leads us to propose a working model for the mechanism underlying the inhibitory effects of Hcy on EC migration and angiogenesis and its impact in CVD (Figure 4.1). Future studies of Carom's roles in endocytosis, EC permeability, monocyte recruitment will further characterize the novel mechanisms for Hcy-induced EC disorder and contribute to the development of CVD.

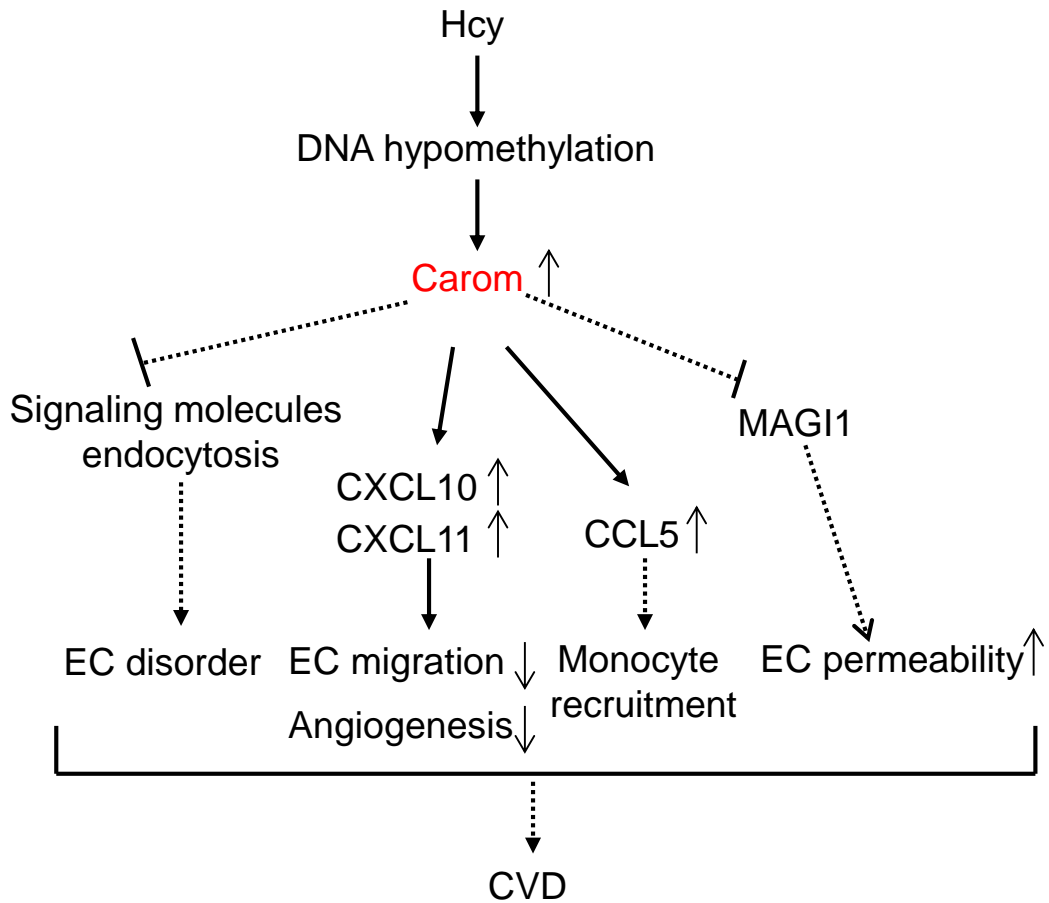


Figure 4.1. Working model of the mechanisms underlying Hcy-Carom induction and the impact on CVD. Solid lines are an experimentally confirmed mechanism and the dashed lines indicate potential mechanism to be confirmed. Hcy, homocysteine; EC, endothelial cells; CVD, cardiovascular disease.

REFERENCES CITED

- Adams, R. H., & Alitalo, K. (2007). Molecular regulation of angiogenesis and lymphangiogenesis. *Nat Rev Mol Cell Biol*, 8(6), 464-478. doi: 10.1038/nrm2183
- Arnautova, I., & Kleinman, H. K. (2010). In vitro angiogenesis: endothelial cell tube formation on gelled basement membrane extract. *Nat Protoc*, 5(4), 628-635. doi: 10.1038/nprot.2010.6
- Aspenstrom, P. (1997). A Cdc42 target protein with homology to the non-kinase domain of FER has a potential role in regulating the actin cytoskeleton. *Curr Biol*, 7(7), 479-487.
- Bar-Peled, M., & Raikhel, N. V. (1996). A method for isolation and purification of specific antibodies to a protein fused to the GST. *Anal Biochem*, 241(1), 140-142. doi: 10.1006/abio.1996.0390
- Baric, I., Fumic, K., Glenn, B., Cuk, M., Schulze, A., Finkelstein, J. D., . . . Mudd, S. H. (2004). S-adenosylhomocysteine hydrolase deficiency in a human: a genetic disorder of methionine metabolism. *Proc Natl Acad Sci U S A*, 101(12), 4234-4239. doi: 10.1073/pnas.0400658101
- Behrend, L., Mohr, A., Dick, T., & Zwacka, R. M. (2005). Manganese superoxide dismutase induces p53-dependent senescence in colorectal cancer cells. *Mol Cell Biol*, 25(17), 7758-7769. doi: 10.1128/MCB.25.17.7758-7769.2005
- Bergo, M. O., Leung, G. K., Ambroziak, P., Otto, J. C., Casey, P. J., Gomes, A. Q., . . . Young, S. G. (2001). Isoprenylcysteine carboxyl methyltransferase deficiency in mice. *J Biol Chem*, 276(8), 5841-5845. doi: 10.1074/jbc.C000831200
- Bodnar, R. J., Yates, C. C., Rodgers, M. E., Du, X., & Wells, A. (2009). IP-10 induces dissociation of newly formed blood vessels. *J Cell Sci*, 122(Pt 12), 2064-2077. doi: 10.1242/jcs.048793
- Bodnar, R. J., Yates, C. C., & Wells, A. (2006). IP-10 blocks vascular endothelial growth factor-induced endothelial cell motility and tube formation via inhibition of calpain. *Circ Res*, 98(5), 617-625. doi: 10.1161/01.RES.0000209968.66606.10
- Boushey, C. J., Beresford, S. A., Omenn, G. S., & Motulsky, A. G. (1995). A quantitative assessment of plasma homocysteine as a risk factor for vascular disease. Probable benefits of increasing folic acid intakes. *JAMA*, 274(13), 1049-1057.
- Cao, H., Yin, X., Cao, Y., Jin, Y., Wang, S., Kong, Y., . . . Xu, Z. (2013). FCHSD1 and FCHSD2 are expressed in hair cell stereocilia and cuticular plate and regulate actin polymerization in vitro. *PLoS One*, 8(2), e56516. doi: 10.1371/journal.pone.0056516
- Carmeliet, P. (2003). Angiogenesis in health and disease. *Nat Med*, 9(6), 653-660. doi: 10.1038/nm0603-653

- Carmeliet, P., & Jain, R. K. (2011). Molecular mechanisms and clinical applications of angiogenesis. *Nature*, *473*(7347), 298-307. doi: 10.1038/nature10144
- Caudill, M. A., Wang, J. C., Melnyk, S., Pogribny, I. P., Jernigan, S., Collins, M. D., . . . James, S. J. (2001). Intracellular S-adenosylhomocysteine concentrations predict global DNA hypomethylation in tissues of methyl-deficient cystathionine beta-synthase heterozygous mice. *J Nutr*, *131*(11), 2811-2818.
- Celletti, F. L., Waugh, J. M., Amabile, P. G., Brendolan, A., Hilfiker, P. R., & Dake, M. D. (2001). Vascular endothelial growth factor enhances atherosclerotic plaque progression. *Nat Med*, *7*(4), 425-429. doi: 10.1038/86490
- Chang, P. Y., Lu, S. C., Lee, C. M., Chen, Y. J., Dugan, T. A., Huang, W. H., . . . Lee, Y. T. (2008). Homocysteine inhibits arterial endothelial cell growth through transcriptional downregulation of fibroblast growth factor-2 involving G protein and DNA methylation. *Circ Res*, *102*(8), 933-941. doi: 10.1161/CIRCRESAHA.108.171082
- Chen, N. C., Yang, F., Capecci, L. M., Gu, Z., Schafer, A. I., Durante, W., . . . Wang, H. (2010). Regulation of homocysteine metabolism and methylation in human and mouse tissues. *FASEB J*, *24*(8), 2804-2817. doi: 10.1096/fj.09-143651
- Chen, Z., Karaplis, A. C., Ackerman, S. L., Pogribny, I. P., Melnyk, S., Lussier-Cacan, S., . . . Rozen, R. (2001). Mice deficient in methylenetetrahydrofolate reductase exhibit hyperhomocysteinemia and decreased methylation capacity, with neuropathology and aortic lipid deposition. *Hum Mol Genet*, *10*(5), 433-443.
- Cheng, Z., Jiang, X., Kruger, W. D., Pratico, D., Gupta, S., Mallilankaraman, K., . . . Wang, H. (2011). Hyperhomocysteinemia impairs endothelium-derived hyperpolarizing factor-mediated vasorelaxation in transgenic cystathionine beta synthase-deficient mice. *Blood*, *118*(7), 1998-2006. doi: 10.1182/blood-2011-01-333310
- Chitu, V., Pixley, F. J., Macaluso, F., Larson, D. R., Condeelis, J., Yeung, Y. G., & Stanley, E. R. (2005). The PCH family member MAYP/PSTPIP2 directly regulates F-actin bundling and enhances filopodia formation and motility in macrophages. *Mol Biol Cell*, *16*(6), 2947-2959. doi: 10.1091/mbc.E04-10-0914
- Chitu, V., & Stanley, E. R. (2007). Pombe Cdc15 homology (PCH) proteins: coordinators of membrane-cytoskeletal interactions. *Trends Cell Biol*, *17*(3), 145-156. doi: 10.1016/j.tcb.2007.01.003
- Clarke, S. (1993). Protein methylation. *Curr Opin Cell Biol*, *5*(6), 977-983.
- Coyle, I. P., Koh, Y. H., Lee, W. C., Slind, J., Fergestad, T., Littleton, J. T., & Ganetzky, B. (2004). Nervous wreck, an SH3 adaptor protein that interacts with Wsp, regulates synaptic growth in *Drosophila*. *Neuron*, *41*(4), 521-534.
- Dalton, M. L., Gadson, P. F., Jr., Wrenn, R. W., & Rosenquist, T. H. (1997). Homocysteine signal cascade: production of phospholipids, activation of protein kinase C, and the induction of c-fos and c-myc in smooth muscle cells. *FASEB J*, *11*(8), 703-711.

- Dayal, S., Brown, K. L., Weydert, C. J., Oberley, L. W., Arning, E., Bottiglieri, T., . . . Lentz, S. R. (2002). Deficiency of glutathione peroxidase-1 sensitizes hyperhomocysteinemic mice to endothelial dysfunction. *Arterioscler Thromb Vasc Biol*, *22*(12), 1996-2002.
- Dayal, S., Devlin, A. M., McCaw, R. B., Liu, M. L., Arning, E., Bottiglieri, T., . . . Lentz, S. R. (2005). Cerebral vascular dysfunction in methionine synthase-deficient mice. *Circulation*, *112*(5), 737-744.
- Dayal, S., & Lentz, S. R. (2005). ADMA and hyperhomocysteinemia. *Vasc Med*, *10 Suppl 1*, S27-33.
- de Kreuk, B. J., Nethe, M., Fernandez-Borja, M., Anthony, E. C., Hensbergen, P. J., Deelder, A. M., . . . Hordijk, P. L. (2011). The F-BAR domain protein PACSIN2 associates with Rac1 and regulates cell spreading and migration. *J Cell Sci*, *124*(Pt 14), 2375-2388. doi: 10.1242/jcs.080630
- De Vriese, A. S., Blom, H. J., Heil, S. G., Mortier, S., Kluijtmans, L. A., Van de Voorde, J., & Lameire, N. H. (2004). Endothelium-derived hyperpolarizing factor-mediated renal vasodilatory response is impaired during acute and chronic hyperhomocysteinemia. *Circulation*, *109*(19), 2331-2336. doi: 10.1161/01.CIR.0000129138.08493.4D
- Doring, Y., Noels, H., Mandl, M., Kramp, B., Neideck, C., Lievens, D., . . . Weber, C. (2014). Deficiency of the Sialyltransferase St3Gal4 Reduces Ccl5-Mediated Myeloid Cell Recruitment and Arrest: Short Communication. *Circ Res*, *114*(6), 976-981. doi: 10.1161/CIRCRESAHA.114.302426
- Drechsler, M., Megens, R. T., van Zandvoort, M., Weber, C., & Soehnlein, O. (2010). Hyperlipidemia-triggered neutrophilia promotes early atherosclerosis. *Circulation*, *122*(18), 1837-1845. doi: 10.1161/CIRCULATIONAHA.110.961714
- Durand, P., Lussier-Cacan, S., & Blache, D. (1997). Acute methionine load-induced hyperhomocysteinemia enhances platelet aggregation, thromboxane biosynthesis, and macrophage-derived tissue factor activity in rats. *FASEB J*, *11*(13), 1157-1168.
- Eberhardt, R. T., Forgione, M. A., Cap, A., Leopold, J. A., Rudd, M. A., Trolliet, M., . . . Loscalzo, J. (2000). Endothelial dysfunction in a murine model of mild hyperhomocyst(e)inemia. *J Clin Invest*, *106*(4), 483-491. doi: 10.1172/JCI8342
- Ferrara, N., Gerber, H. P., & LeCouter, J. (2003). The biology of VEGF and its receptors. *Nat Med*, *9*(6), 669-676. doi: 10.1038/nm0603-669
- Folkman, J. (2007). Angiogenesis: an organizing principle for drug discovery? *Nat Rev Drug Discov*, *6*(4), 273-286. doi: 10.1038/nrd2115
- Folsom, A. R., Nieto, F. J., McGovern, P. G., Tsai, M. Y., Malinow, M. R., Eckfeldt, J. H., . . . Davis, C. E. (1998). Prospective study of coronary heart disease incidence in relation to fasting total homocysteine, related genetic polymorphisms, and B vitamins: the Atherosclerosis Risk in Communities (ARIC) study. *Circulation*, *98*(3), 204-210.

- Frost, A., Unger, V. M., & De Camilli, P. (2009). The BAR domain superfamily: membrane-molding macromolecules. *Cell*, *137*(2), 191-196. doi: 10.1016/j.cell.2009.04.010
- Geisel, J., Jodden, V., Obeid, R., Knapp, J. P., Bodis, M., & Herrmann, W. (2003). Stimulatory effect of homocysteine on interleukin-8 expression in human endothelial cells. *Clin Chem Lab Med*, *41*(8), 1045-1048. doi: 10.1515/CCLM.2003.161
- Giroux, S., Tremblay, M., Bernard, D., Cardin-Girard, J. F., Aubry, S., Larouche, L., . . . Charron, J. (1999). Embryonic death of Mek1-deficient mice reveals a role for this kinase in angiogenesis in the labyrinthine region of the placenta. *Curr Biol*, *9*(7), 369-372.
- Guba, S. C., Fonseca, V., & Fink, L. M. (1999). Hyperhomocysteinemia and thrombosis. *Semin Thromb Hemost*, *25*(3), 291-309. doi: 10.1055/s-2007-994932
- Guerrier, S., Coutinho-Budd, J., Sassa, T., Gresset, A., Jordan, N. V., Chen, K., . . . Polleux, F. (2009). The F-BAR domain of srGAP2 induces membrane protrusions required for neuronal migration and morphogenesis. *Cell*, *138*(5), 990-1004. doi: 10.1016/j.cell.2009.06.047
- Han, Y., Cui, J., Lu, Y., Sue, S., Arpaia, E., Mak, T. W., & Minden, M. D. (2012). FCHSD2 predicts response to chemotherapy in acute myeloid leukemia patients. *Leuk Res*, *36*(11), 1339-1346. doi: 10.1016/j.leukres.2012.06.011
- Harker, L. A., Harlan, J. M., & Ross, R. (1983). Effect of sulfinpyrazone on homocysteine-induced endothelial injury and arteriosclerosis in baboons. *Circ Res*, *53*(6), 731-739.
- Heil, S. G., De Vriese, A. S., Kluijtmans, L. A., Mortier, S., Den Heijer, M., & Blom, H. J. (2004). The role of hyperhomocysteinemia in nitric oxide (NO) and endothelium-derived hyperpolarizing factor (EDHF)-mediated vasodilatation. *Cell Mol Biol (Noisy-le-grand)*, *50*(8), 911-916.
- Hellman, A., & Chess, A. (2007). Gene body-specific methylation on the active X chromosome. *Science*, *315*(5815), 1141-1143. doi: 10.1126/science.1136352
- Henne, W. M., Boucrot, E., Meinecke, M., Evergren, E., Vallis, Y., Mittal, R., & McMahon, H. T. (2010). FCHO proteins are nucleators of clathrin-mediated endocytosis. *Science*, *328*(5983), 1281-1284. doi: 10.1126/science.1188462
- Hu, J., Mukhopadhyay, A., Truesdell, P., Chander, H., Mukhopadhyay, U. K., Mak, A. S., & Craig, A. W. (2011). Cdc42-interacting protein 4 is a Src substrate that regulates invadopodia and invasiveness of breast tumors by promoting MT1-MMP endocytosis. *J Cell Sci*, *124*(Pt 10), 1739-1751. doi: 10.1242/jcs.078014
- Hu, J., Troglio, F., Mukhopadhyay, A., Everingham, S., Kwok, E., Scita, G., & Craig, A. W. (2009). F-BAR-containing adaptor CIP4 localizes to early endosomes and regulates Epidermal Growth Factor Receptor trafficking and downregulation. *Cell Signal*, *21*(11), 1686-1697. doi: 10.1016/j.cellsig.2009.07.007

- Huang, X., Gong, R., Li, X., Virtue, A., Yang, F., Yang, I. H., . . . Wang, H. (2013). Identification of novel pretranslational regulatory mechanisms for NF-kappaB activation. *J Biol Chem*, 288(22), 15628-15640. doi: 10.1074/jbc.M113.460626
- Ingrosso, D., Cimmino, A., Perna, A. F., Masella, L., De Santo, N. G., De Bonis, M. L., . . . Zappia, V. (2003). Folate treatment and unbalanced methylation and changes of allelic expression induced by hyperhomocysteinaemia in patients with uraemia. *Lancet*, 361(9370), 1693-1699. doi: 10.1016/S0140-6736(03)13372-7
- Itoh, T., Erdmann, K. S., Roux, A., Habermann, B., Werner, H., & De Camilli, P. (2005). Dynamin and the actin cytoskeleton cooperatively regulate plasma membrane invagination by BAR and F-BAR proteins. *Dev Cell*, 9(6), 791-804. doi: 10.1016/j.devcel.2005.11.005
- Jacovina, A. T., Deora, A. B., Ling, Q., Broekman, M. J., Almeida, D., Greenberg, C. B., . . . Hajjar, K. A. (2009). Homocysteine inhibits neoangiogenesis in mice through blockade of annexin A2-dependent fibrinolysis. *J Clin Invest*, 119(11), 3384-3394. doi: 10.1172/JCI39591
- Jain, R. K. (2003). Molecular regulation of vessel maturation. *Nat Med*, 9(6), 685-693. doi: 10.1038/nm0603-685
- Jakubowski, H. (2006). Pathophysiological consequences of homocysteine excess. *J Nutr*, 136(6 Suppl), 1741S-1749S.
- Jakubowski, H., Zhang, L., Bardeguet, A., & Aviv, A. (2000). Homocysteine thiolactone and protein homocysteinylation in human endothelial cells: implications for atherosclerosis. *Circ Res*, 87(1), 45-51.
- Jamaluddin, M. D., Chen, I., Yang, F., Jiang, X., Jan, M., Liu, X., . . . Wang, H. (2007). Homocysteine inhibits endothelial cell growth via DNA hypomethylation of the cyclin A gene. *Blood*, 110(10), 3648-3655. doi: 10.1182/blood-2007-06-096701
- Jamaluddin, M. S., Yang, X., & Wang, H. (2007). Hyperhomocysteinemia, DNA methylation and vascular disease. *Clin Chem Lab Med*, 45(12), 1660-1666. doi: 10.1515/CCLM.2007.350
- Jiang, X., Yang, F., Tan, H., Liao, D., Bryan, R. M., Jr., Randhawa, J. K., . . . Wang, H. (2005). Hyperhomocysteinemia impairs endothelial function and eNOS activity via PKC activation. *Arterioscler Thromb Vasc Biol*, 25(12), 2515-2521. doi: 10.1161/01.ATV.0000189559.87328.e4
- Kamat, B. R., Galli, S. J., Barger, A. C., Lainey, L. L., & Silverman, K. J. (1987). Neovascularization and coronary atherosclerotic plaque: cinematographic localization and quantitative histologic analysis. *Hum Pathol*, 18(10), 1036-1042.
- Kamioka, Y., Fukuhara, S., Sawa, H., Nagashima, K., Masuda, M., Matsuda, M., & Mochizuki, N. (2004). A novel dynamin-associating molecule, formin-binding protein 17, induces tubular membrane invaginations and participates in endocytosis. *J Biol Chem*, 279(38), 40091-40099. doi: 10.1074/jbc.M404899200

- Katoh, M., & Katoh, M. (2004). Identification and characterization of human FCHSD1 and FCHSD2 genes in silico. *Int J Mol Med*, *13*(5), 749-754.
- Kim, C. S., Kim, Y. R., Naqvi, A., Kumar, S., Hoffman, T. A., Jung, S. B., . . . Irani, K. (2011). Homocysteine promotes human endothelial cell dysfunction via site-specific epigenetic regulation of p66shc. *Cardiovasc Res*, *92*(3), 466-475. doi: 10.1093/cvr/cvr250
- Kim, J. M., Hong, K., Lee, J. H., Lee, S., & Chang, N. (2009). Effect of folate deficiency on placental DNA methylation in hyperhomocysteinemic rats. *J Nutr Biochem*, *20*(3), 172-176. doi: 10.1016/j.jnutbio.2008.01.010
- Klemke, R. L., Cai, S., Giannini, A. L., Gallagher, P. J., de Lanerolle, P., & Cheresh, D. A. (1997). Regulation of cell motility by mitogen-activated protein kinase. *J Cell Biol*, *137*(2), 481-492.
- Koenen, R. R., von Hundelshausen, P., Nesmelova, I. V., Zerneck, A., Liehn, E. A., Sarabi, A., . . . Weber, C. (2009). Disrupting functional interactions between platelet chemokines inhibits atherosclerosis in hyperlipidemic mice. *Nat Med*, *15*(1), 97-103. doi: 10.1038/nm.1898
- Kofler, S., Nickel, T., & Weis, M. (2005). Role of cytokines in cardiovascular diseases: a focus on endothelial responses to inflammation. *Clin Sci (Lond)*, *108*(3), 205-213. doi: 10.1042/CS20040174
- Kokame, K., Kato, H., & Miyata, T. (1998). Nonradioactive differential display cloning of genes induced by homocysteine in vascular endothelial cells. *Methods*, *16*(4), 434-443. doi: 10.1006/meth.1998.0698
- Kovacevic, I., Hu, J., Siehoff-Icking, A., Opitz, N., Griffin, A., Perkins, A. C., . . . Oess, S. (2012). The F-BAR protein NOSTRIN participates in FGF signal transduction and vascular development. *EMBO J*, *31*(15), 3309-3322. doi: 10.1038/emboj.2012.176
- Kraus, J. P., Janosik, M., Kozich, V., Mandell, R., Shih, V., Sperandio, M. P., . . . Gaustadnes, M. (1999). Cystathionine beta-synthase mutations in homocystinuria. *Hum Mutat*, *13*(5), 362-375.
- Krishnaswamy, G., Kelley, J., Yerra, L., Smith, J. K., & Chi, D. S. (1999). Human endothelium as a source of multifunctional cytokines: molecular regulation and possible role in human disease. *J Interferon Cytokine Res*, *19*(2), 91-104.
- Lamallice, L., Le Boeuf, F., & Huot, J. (2007). Endothelial cell migration during angiogenesis. *Circ Res*, *100*(6), 782-794. doi: 10.1161/01.RES.0000259593.07661.1e
- Lee, K., Gallop, J. L., Rambani, K., & Kirschner, M. W. (2010). Self-assembly of filopodia-like structures on supported lipid bilayers. *Science*, *329*(5997), 1341-1345. doi: 10.1126/science.1191710

- Lee, M. E., & Wang, H. (1999). Homocysteine and hypomethylation. A novel link to vascular disease. *Trends Cardiovasc Med*, *9*(1-2), 49-54.
- Leloup, L., Shao, H., Bae, Y. H., Deasy, B., Stolz, D., Roy, P., & Wells, A. (2010). m-Calpain activation is regulated by its membrane localization and by its binding to phosphatidylinositol 4,5-bisphosphate. *J Biol Chem*, *285*(43), 33549-33566. doi: 10.1074/jbc.M110.123604
- Lentz, S. R. (1997). Homocysteine and vascular dysfunction. *Life Sci*, *61*(13), 1205-1215.
- Lentz, S. R., Sobey, C. G., Piegors, D. J., Bhopatkar, M. Y., Faraci, F. M., Malinow, M. R., & Heistad, D. D. (1996). Vascular dysfunction in monkeys with diet-induced hyperhomocyst(e)inemia. *J Clin Invest*, *98*(1), 24-29. doi: 10.1172/JCI118771
- Leonhardt, H., Page, A. W., Weier, H. U., & Bestor, T. H. (1992). A targeting sequence directs DNA methyltransferase to sites of DNA replication in mammalian nuclei. *Cell*, *71*(5), 865-873.
- Li, E., Bestor, T. H., & Jaenisch, R. (1992). Targeted mutation of the DNA methyltransferase gene results in embryonic lethality. *Cell*, *69*(6), 915-926.
- Li, S., Huang, N. F., & Hsu, S. (2005). Mechanotransduction in endothelial cell migration. *J Cell Biochem*, *96*(6), 1110-1126. doi: 10.1002/jcb.20614
- Liang, P., & Pardee, A. B. (1992). Differential display of eukaryotic messenger RNA by means of the polymerase chain reaction. *Science*, *257*(5072), 967-971.
- Liao, D., Tan, H., Hui, R., Li, Z., Jiang, X., Gaubatz, J., . . . Wang, H. (2006). Hyperhomocysteinemia decreases circulating high-density lipoprotein by inhibiting apolipoprotein A-I Protein synthesis and enhancing HDL cholesterol clearance. *Circ Res*, *99*(6), 598-606. doi: 10.1161/01.RES.0000242559.42077.22
- Liu, G., Nellaiappan, K., & Kagan, H. M. (1997). Irreversible inhibition of lysyl oxidase by homocysteine thiolactone and its selenium and oxygen analogues. Implications for homocystinuria. *J Biol Chem*, *272*(51), 32370-32377.
- Lonn, E., Yusuf, S., Arnold, M. J., Sheridan, P., Pogue, J., Micks, M., . . . Heart Outcomes Prevention Evaluation, Investigators. (2006). Homocysteine lowering with folic acid and B vitamins in vascular disease. *N Engl J Med*, *354*(15), 1567-1577. doi: 10.1056/NEJMoa060900
- Loscalzo, J. (1996). The oxidant stress of hyperhomocyst(e)inemia. *J Clin Invest*, *98*(1), 5-7. doi: 10.1172/JCI118776
- Majors, A., Ehrhart, L. A., & Pezacka, E. H. (1997). Homocysteine as a risk factor for vascular disease. Enhanced collagen production and accumulation by smooth muscle cells. *Arterioscler Thromb Vasc Biol*, *17*(10), 2074-2081.

- Maron, B. A., & Loscalzo, J. (2009). The treatment of hyperhomocysteinemia. *Annu Rev Med*, *60*, 39-54. doi: 10.1146/annurev.med.60.041807.123308
- Marquez-Rosado, L., Singh, D., Rincon-Arano, H., Solan, J. L., & Lampe, P. D. (2012). CASK (LIN2) interacts with Cx43 in wounded skin and their coexpression affects cell migration. *J Cell Sci*, *125*(Pt 3), 695-702. doi: 10.1242/jcs.084400
- Mayer, E. L., Jacobsen, D. W., & Robinson, K. (1996). Homocysteine and coronary atherosclerosis. *J Am Coll Cardiol*, *27*(3), 517-527.
- McCully, K. S. (1969). Vascular pathology of homocysteinemia: implications for the pathogenesis of arteriosclerosis. *Am J Pathol*, *56*(1), 111-128.
- Mehrad, B., Keane, M. P., & Strieter, R. M. (2007). Chemokines as mediators of angiogenesis. *Thromb Haemost*, *97*(5), 755-762.
- Mudd, S. H., & Poole, J. R. (1975). Labile methyl balances for normal humans on various dietary regimens. *Metabolism*, *24*(6), 721-735.
- O'Connor-Giles, K. M., Ho, L. L., & Ganetzky, B. (2008). Nervous wreck interacts with thickveins and the endocytic machinery to attenuate retrograde BMP signaling during synaptic growth. *Neuron*, *58*(4), 507-518. doi: 10.1016/j.neuron.2008.03.007
- Ohno, H., Hirabayashi, S., Kansaku, A., Yao, I., Tajima, M., Nishimura, W., . . . Hata, Y. (2003). Carom: a novel membrane-associated guanylate kinase-interacting protein with two SH3 domains. *Oncogene*, *22*(52), 8422-8431. doi: 10.1038/sj.onc.1206996
- Ojeh, N., Pekovic, V., Jahoda, C., & Maatta, A. (2008). The MAGUK-family protein CASK is targeted to nuclei of the basal epidermis and controls keratinocyte proliferation. *J Cell Sci*, *121*(Pt 16), 2705-2717. doi: 10.1242/jcs.025643
- Okano, M., Bell, D. W., Haber, D. A., & Li, E. (1999). DNA methyltransferases Dnmt3a and Dnmt3b are essential for de novo methylation and mammalian development. *Cell*, *99*(3), 247-257.
- Olek, A., Oswald, J., & Walter, J. (1996). A modified and improved method for bisulphite based cytosine methylation analysis. *Nucleic Acids Res*, *24*(24), 5064-5066.
- Omenn, G. S., Beresford, S. A., & Motulsky, A. G. (1998). Preventing coronary heart disease: B vitamins and homocysteine. *Circulation*, *97*(5), 421-424.
- Outinen, P. A., Sood, S. K., Pfeifer, S. I., Pamidi, S., Podor, T. J., Li, J., . . . Austin, R. C. (1999). Homocysteine-induced endoplasmic reticulum stress and growth arrest leads to specific changes in gene expression in human vascular endothelial cells. *Blood*, *94*(3), 959-967.
- Perna, A. F., Ingrosso, D., Zappia, V., Galletti, P., Capasso, G., & De Santo, N. G. (1993). Enzymatic methyl esterification of erythrocyte membrane proteins is impaired in chronic renal

- failure. Evidence for high levels of the natural inhibitor S-adenosylhomocysteine. *J Clin Invest*, *91*(6), 2497-2503. doi: 10.1172/JCI116485
- Perutelli, P., Amato, S., Minniti, G., Bottini, F., Calevo, M. G., Cerone, R., & Molinari, A. C. (2005). von Willebrand factor multimer composition is modified following oral methionine load in women with thrombosis, but not in healthy women. *Blood Coagul Fibrinolysis*, *16*(4), 267-273.
- Pichot, C. S., Arvanitis, C., Hartig, S. M., Jensen, S. A., Bechill, J., Marzouk, S., . . . Corey, S. J. (2010). Cdc42-interacting protein 4 promotes breast cancer cell invasion and formation of invadopodia through activation of N-WASp. *Cancer Res*, *70*(21), 8347-8356. doi: 10.1158/0008-5472.CAN-09-4149
- Poddar, R., Sivasubramanian, N., DiBello, P. M., Robinson, K., & Jacobsen, D. W. (2001). Homocysteine induces expression and secretion of monocyte chemoattractant protein-1 and interleukin-8 in human aortic endothelial cells: implications for vascular disease. *Circulation*, *103*(22), 2717-2723.
- Pogribny, I. P., & Beland, F. A. (2009). DNA hypomethylation in the origin and pathogenesis of human diseases. *Cell Mol Life Sci*, *66*(14), 2249-2261. doi: 10.1007/s00018-009-0015-5
- Postea, O., Koenen, R. R., Hristov, M., Weber, C., & Ludwig, A. (2008). Homocysteine up-regulates vascular transmembrane chemokine CXCL16 and induces CXCR6+ lymphocyte recruitment in vitro and in vivo. *J Cell Mol Med*, *12*(5A), 1700-1709. doi: 10.1111/j.1582-4934.2008.00223.x
- Potente, M., Gerhardt, H., & Carmeliet, P. (2011). Basic and therapeutic aspects of angiogenesis. *Cell*, *146*(6), 873-887. doi: 10.1016/j.cell.2011.08.039
- Qualmann, B., & Kelly, R. B. (2000). Syndapin isoforms participate in receptor-mediated endocytosis and actin organization. *J Cell Biol*, *148*(5), 1047-1062.
- Riba, R., Nicolaou, A., Troxler, M., Homer-Vaniasinkam, S., & Naseem, K. M. (2004). Altered platelet reactivity in peripheral vascular disease complicated with elevated plasma homocysteine levels. *Atherosclerosis*, *175*(1), 69-75. doi: 10.1016/j.atherosclerosis.2004.02.008
- Rodal, A. A., Blunk, A. D., Akbergenova, Y., Jorquera, R. A., Buhl, L. K., & Littleton, J. T. (2011). A presynaptic endosomal trafficking pathway controls synaptic growth signaling. *J Cell Biol*, *193*(1), 201-217. doi: 10.1083/jcb.201009052
- Rodal, A. A., Motola-Barnes, R. N., & Littleton, J. T. (2008). Nervous wreck and Cdc42 cooperate to regulate endocytic actin assembly during synaptic growth. *J Neurosci*, *28*(33), 8316-8325. doi: 10.1523/JNEUROSCI.2304-08.2008
- Roybal, C. N., Yang, S., Sun, C. W., Hurtado, D., Vander Jagt, D. L., Townes, T. M., & Abcouwer, S. F. (2004). Homocysteine increases the expression of vascular endothelial growth factor

by a mechanism involving endoplasmic reticulum stress and transcription factor ATF4. *J Biol Chem*, 279(15), 14844-14852. doi: 10.1074/jbc.M312948200

Sakurai, A., Fukuhara, S., Yamagishi, A., Sako, K., Kamioka, Y., Masuda, M., . . . Mochizuki, N. (2006). MAGI-1 is required for Rap1 activation upon cell-cell contact and for enhancement of vascular endothelial cadherin-mediated cell adhesion. *Mol Biol Cell*, 17(2), 966-976. doi: 10.1091/mbc.E05-07-0647

Schnyder, G., Roffi, M., Flammer, Y., Pin, R., & Hess, O. M. (2002). Effect of homocysteine-lowering therapy with folic acid, vitamin B12, and vitamin B6 on clinical outcome after percutaneous coronary intervention: the Swiss Heart study: a randomized controlled trial. *JAMA*, 288(8), 973-979.

Selhub, J., Jacques, P. F., Bostom, A. G., D'Agostino, R. B., Wilson, P. W., Belanger, A. J., . . . Rosenberg, I. H. (1995). Association between plasma homocysteine concentrations and extracranial carotid-artery stenosis. *N Engl J Med*, 332(5), 286-291. doi: 10.1056/NEJM199502023320502

Shastry, S., Tyagi, N., Hayden, M. R., & Tyagi, S. C. (2004). Proteomic analysis of homocysteine inhibition of microvascular endothelial cell angiogenesis. *Cell Mol Biol (Noisy-le-grand)*, 50(8), 931-937.

Shimada, A., Niwa, H., Tsujita, K., Suetsugu, S., Nitta, K., Hanawa-Suetsugu, K., . . . Yokoyama, S. (2007). Curved EFC/F-BAR-domain dimers are joined end to end into a filament for membrane invagination in endocytosis. *Cell*, 129(4), 761-772. doi: 10.1016/j.cell.2007.03.040

Silverman, M. D., Tumuluri, R. J., Davis, M., Lopez, G., Rosenbaum, J. T., & Lelkes, P. I. (2002). Homocysteine upregulates vascular cell adhesion molecule-1 expression in cultured human aortic endothelial cells and enhances monocyte adhesion. *Arterioscler Thromb Vasc Biol*, 22(4), 587-592.

Simons, M., & Ware, J. A. (2003). Therapeutic angiogenesis in cardiovascular disease. *Nat Rev Drug Discov*, 2(11), 863-871. doi: 10.1038/nrd1226

Small, J. V., Stradal, T., Vignal, E., & Rottner, K. (2002). The lamellipodium: where motility begins. *Trends Cell Biol*, 12(3), 112-120.

Spence, J. D. (2006). Homocysteine: call off the funeral. *Stroke*, 37(2), 282-283. doi: 10.1161/01.STR.0000199621.28234.e2

Stampfer, M. J., Malinow, M. R., Willett, W. C., Newcomer, L. M., Upson, B., Ullmann, D., . . . Hennekens, C. H. (1992). A prospective study of plasma homocyst(e)ine and risk of myocardial infarction in US physicians. *JAMA*, 268(7), 877-881.

Starkebaum, G., & Harlan, J. M. (1986). Endothelial cell injury due to copper-catalyzed hydrogen peroxide generation from homocysteine. *J Clin Invest*, 77(4), 1370-1376. doi: 10.1172/JCI112442

- Su, X., Sorenson, C. M., & Sheibani, N. (2003). Isolation and characterization of murine retinal endothelial cells. *Mol Vis*, *9*, 171-178.
- Sueishi, K., Yonemitsu, Y., Nakagawa, K., Kaneda, Y., Kumamoto, M., & Nakashima, Y. (1997). Atherosclerosis and angiogenesis. Its pathophysiological significance in humans as well as in an animal model induced by the gene transfer of vascular endothelial growth factor. *Ann N Y Acad Sci*, *811*, 311-322; 322-314.
- Sun, R., Su, Y., Zhao, X., Qi, J., Luo, X., Yang, Z., . . . Xia, Z. (2009). Human calcium/calmodulin-dependent serine protein kinase regulates the expression of p21 via the E2A transcription factor. *Biochem J*, *419*(2), 457-466. doi: 10.1042/BJ20080515
- Sung, F. L., Slow, Y. L., Wang, G., Lynn, E. G., & O, K. (2001). Homocysteine stimulates the expression of monocyte chemoattractant protein-1 in endothelial cells leading to enhanced monocyte chemotaxis. *Mol Cell Biochem*, *216*(1-2), 121-128.
- Sung, M. L., Wu, C. C., Chang, H. I., Yen, C. K., Chen, H. J., Cheng, J. C., . . . Chen, C. N. (2009). Shear stress inhibits homocysteine-induced stromal cell-derived factor-1 expression in endothelial cells. *Circ Res*, *105*(8), 755-763. doi: 10.1161/CIRCRESAHA.109.206524
- Swanson, D. A., Liu, M. L., Baker, P. J., Garrett, L., Stitzel, M., Wu, J., . . . Brody, L. C. (2001). Targeted disruption of the methionine synthase gene in mice. *Mol Cell Biol*, *21*(4), 1058-1065.
- Swift, M. R., & Weinstein, B. M. (2009). Arterial-venous specification during development. *Circ Res*, *104*(5), 576-588. doi: 10.1161/CIRCRESAHA.108.188805
- Tacheny, A., dos Santos, S., Huet, A. C., van Steenbrugge, M., Michiels, C., Holvoet, P., & Raes, M. (2002). Effects of homocysteine on the cellular responses of murine endothelial cells cultured in vitro. *Ann N Y Acad Sci*, *973*, 550-554.
- Takano, K., Toyooka, K., & Suetsugu, S. (2008). EFC/F-BAR proteins and the N-WASP-WIP complex induce membrane curvature-dependent actin polymerization. *EMBO J*, *27*(21), 2817-2828. doi: 10.1038/emboj.2008.216
- Takenawa, T., & Suetsugu, S. (2007). The WASP-WAVE protein network: connecting the membrane to the cytoskeleton. *Nat Rev Mol Cell Biol*, *8*(1), 37-48. doi: 10.1038/nrm2069
- Tan, H., Jiang, X., Yang, F., Li, Z., Liao, D., Trial, J., . . . Wang, H. (2006). Hyperhomocysteinemia inhibits post-injury reendothelialization in mice. *Cardiovasc Res*, *69*(1), 253-262. doi: 10.1016/j.cardiores.2005.08.016
- Teng, Y. W., Mehedint, M. G., Garrow, T. A., & Zeisel, S. H. Deletion of betaine-homocysteine s-methyltransferase in mice perturbs choline and 1-carbon metabolism, resulting in Fatty liver and hepatocellular carcinomas. *J Biol Chem*, *286*(42), 36258-36267.

- Teng, Y. W., Mehedint, M. G., Garrow, T. A., & Zeisel, S. H. (2011). Deletion of betaine-homocysteine S-methyltransferase in mice perturbs choline and 1-carbon metabolism, resulting in fatty liver and hepatocellular carcinomas. *J Biol Chem*, *286*(42), 36258-36267. doi: 10.1074/jbc.M111.265348
- Title, L. M., Cummings, P. M., Giddens, K., Genest, J. J., Jr., & Nassar, B. A. (2000). Effect of folic acid and antioxidant vitamins on endothelial dysfunction in patients with coronary artery disease. *J Am Coll Cardiol*, *36*(3), 758-765.
- Toguchi, M., Richnau, N., Ruusala, A., & Aspenstrom, P. (2010). Members of the CIP4 family of proteins participate in the regulation of platelet-derived growth factor receptor-beta-dependent actin reorganization and migration. *Biol Cell*, *102*(4), 215-230. doi: 10.1042/BC20090033
- Toole, J. F., Malinow, M. R., Chambless, L. E., Spence, J. D., Pettigrew, L. C., Howard, V. J., . . . Stampfer, M. (2004). Lowering homocysteine in patients with ischemic stroke to prevent recurrent stroke, myocardial infarction, and death: the Vitamin Intervention for Stroke Prevention (VISP) randomized controlled trial. *JAMA*, *291*(5), 565-575. doi: 10.1001/jama.291.5.565
- Tsai, J. C., Perrella, M. A., Yoshizumi, M., Hsieh, C. M., Haber, E., Schlegel, R., & Lee, M. E. (1994). Promotion of vascular smooth muscle cell growth by homocysteine: a link to atherosclerosis. *Proc Natl Acad Sci U S A*, *91*(14), 6369-6373.
- Tsai, J. C., Wang, H., Perrella, M. A., Yoshizumi, M., Sibinga, N. E., Tan, L. C., . . . Lee, M. E. (1996). Induction of cyclin A gene expression by homocysteine in vascular smooth muscle cells. *J Clin Invest*, *97*(1), 146-153. doi: 10.1172/JCI118383
- Tsuboi, S., Takada, H., Hara, T., Mochizuki, N., Funyu, T., Saitoh, H., . . . Ochs, H. D. (2009). FBP17 Mediates a Common Molecular Step in the Formation of Podosomes and Phagocytic Cups in Macrophages. *J Biol Chem*, *284*(13), 8548-8556. doi: 10.1074/jbc.M805638200
- Tsujita, K., Suetsugu, S., Sasaki, N., Furutani, M., Oikawa, T., & Takenawa, T. (2006). Coordination between the actin cytoskeleton and membrane deformation by a novel membrane tubulation domain of PCH proteins is involved in endocytosis. *J Cell Biol*, *172*(2), 269-279. doi: 10.1083/jcb.200508091
- Ulrey, C. L., Liu, L., Andrews, L. G., & Tollefsbol, T. O. (2005). The impact of metabolism on DNA methylation. *Hum Mol Genet*, *14 Spec No 1*, R139-147. doi: 10.1093/hmg/ddi100
- Wang, H., Jiang, X., Yang, F., Chapman, G. B., Durante, W., Sibinga, N. E., & Schafer, A. I. (2002). Cyclin A transcriptional suppression is the major mechanism mediating homocysteine-induced endothelial cell growth inhibition. *Blood*, *99*(3), 939-945.
- Wang, H., Yoshizumi, M., Lai, K., Tsai, J. C., Perrella, M. A., Haber, E., & Lee, M. E. (1997). Inhibition of growth and p21ras methylation in vascular endothelial cells by homocysteine but not cysteine. *J Biol Chem*, *272*(40), 25380-25385.

- Wang, L., Chen, X., Tang, B., Hua, X., Klein-Szanto, A., & Kruger, W. D. (2005). Expression of mutant human cystathionine beta-synthase rescues neonatal lethality but not homocystinuria in a mouse model. *Hum Mol Genet*, *14*(15), 2201-2208. doi: 10.1093/hmg/ddi224
- Watanabe, M., Osada, J., Aratani, Y., Kluckman, K., Reddick, R., Malinow, M. R., & Maeda, N. (1995). Mice deficient in cystathionine beta-synthase: animal models for mild and severe homocyst(e)inemia. *Proc Natl Acad Sci U S A*, *92*(5), 1585-1589.
- Weiss, N., Keller, C., Hoffmann, U., & Loscalzo, J. (2002). Endothelial dysfunction and atherothrombosis in mild hyperhomocysteinemia. *Vasc Med*, *7*(3), 227-239.
- Wilcken, D. E., & Wilcken, B. (1976). The pathogenesis of coronary artery disease. A possible role for methionine metabolism. *J Clin Invest*, *57*(4), 1079-1082. doi: 10.1172/JCI108350
- Williams, J. K., Armstrong, M. L., & Heistad, D. D. (1988). Vasa vasorum in atherosclerotic coronary arteries: responses to vasoactive stimuli and regression of atherosclerosis. *Circ Res*, *62*(3), 515-523.
- Wu, M., Huang, B., Graham, M., Raimondi, A., Heuser, J. E., Zhuang, X., & De Camilli, P. (2010). Coupling between clathrin-dependent endocytic budding and F-BAR-dependent tubulation in a cell-free system. *Nat Cell Biol*, *12*(9), 902-908. doi: 10.1038/ncb2094
- Yang, G., Wu, L., Jiang, B., Yang, W., Qi, J., Cao, K., . . . Wang, R. (2008). H₂S as a physiologic vasorelaxant: hypertension in mice with deletion of cystathionine gamma-lyase. *Science*, *322*(5901), 587-590.
- Yang, Q., Botto, L. D., Erickson, J. D., Berry, R. J., Sambell, C., Johansen, H., & Friedman, J. M. (2006). Improvement in stroke mortality in Canada and the United States, 1990 to 2002. *Circulation*, *113*(10), 1335-1343. doi: 10.1161/CIRCULATIONAHA.105.570846
- Yates-Binder, C. C., Rodgers, M., Jaynes, J., Wells, A., Bodnar, R. J., & Turner, T. (2012). An IP-10 (CXCL10)-derived peptide inhibits angiogenesis. *PLoS One*, *7*(7), e40812. doi: 10.1371/journal.pone.0040812
- Yi, P., Melnyk, S., Pogribna, M., Pogribny, I. P., Hine, R. J., & James, S. J. (2000). Increase in plasma homocysteine associated with parallel increases in plasma S-adenosylhomocysteine and lymphocyte DNA hypomethylation. *J Biol Chem*, *275*(38), 29318-29323. doi: 10.1074/jbc.M002725200
- Yu, B. D., Hanson, R. D., Hess, J. L., Horning, S. E., & Korsmeyer, S. J. (1998). MLL, a mammalian trithorax-group gene, functions as a transcriptional maintenance factor in morphogenesis. *Proc Natl Acad Sci U S A*, *95*(18), 10632-10636.
- Zamir, M., & Silver, M. D. (1985). Vasculature in the walls of human coronary arteries. *Arch Pathol Lab Med*, *109*(7), 659-662.

- Zeng, X., Dai, J., Remick, D. G., & Wang, X. (2003). Homocysteine mediated expression and secretion of monocyte chemoattractant protein-1 and interleukin-8 in human monocytes. *Circ Res*, *93*(4), 311-320. doi: 10.1161/01.RES.0000087642.01082.E4
- Zhang, C., Cai, Y., Adachi, M. T., Oshiro, S., Aso, T., Kaufman, R. J., & Kitajima, S. (2001). Homocysteine induces programmed cell death in human vascular endothelial cells through activation of the unfolded protein response. *J Biol Chem*, *276*(38), 35867-35874. doi: 10.1074/jbc.M100747200
- Zhang, D., Chen, Y., Xie, X., Liu, J., Wang, Q., Kong, W., & Zhu, Y. (2012). Homocysteine activates vascular smooth muscle cells by DNA demethylation of platelet-derived growth factor in endothelial cells. *J Mol Cell Cardiol*, *53*(4), 487-496. doi: 10.1016/j.yjmcc.2012.07.010
- Zhang, D., Fang, P., Jiang, X., Nelson, J., Moore, J. K., Kruger, W. D., . . . Wang, H. (2012). Severe hyperhomocysteinemia promotes bone marrow-derived and resident inflammatory monocyte differentiation and atherosclerosis in LDLr/CBS-deficient mice. *Circ Res*, *111*(1), 37-49. doi: 10.1161/CIRCRESAHA.112.269472
- Zhang, D., Jiang, X., Fang, P., Yan, Y., Song, J., Gupta, S., . . . Wang, H. (2009). Hyperhomocysteinemia promotes inflammatory monocyte generation and accelerates atherosclerosis in transgenic cystathionine beta-synthase-deficient mice. *Circulation*, *120*(19), 1893-1902. doi: 10.1161/CIRCULATIONAHA.109.866889
- Zhang, D., Xie, X., Chen, Y., Hammock, B. D., Kong, W., & Zhu, Y. (2012). Homocysteine upregulates soluble epoxide hydrolase in vascular endothelium in vitro and in vivo. *Circ Res*, *110*(6), 808-817. doi: 10.1161/CIRCRESAHA.111.259325
- Zhang, G., & Wang, Z. (2011). MAGI1 inhibits cancer cell migration and invasion of hepatocellular carcinoma via regulating PTEN. *Zhong Nan Da Xue Xue Bao Yi Xue Ban*, *36*(5), 381-385. doi: 10.3969/j.issn.1672-7347.2011.05.002
- Zhang, H. S., Cao, E. H., & Qin, J. F. (2003). Intracellular redox status modulates monocyte chemoattractant protein-1 expression stimulated by homocysteine in endothelial cells. *J Cardiovasc Pharmacol*, *42*(2), 258-265.
- Zhang, Y., Cliff, W. J., Schoefl, G. I., & Higgins, G. (1993). Immunohistochemical study of intimal microvessels in coronary atherosclerosis. *Am J Pathol*, *143*(1), 164-172.
- Zhu, X., Song, J., Mar, M. H., Edwards, L. J., & Zeisel, S. H. (2003). Phosphatidylethanolamine N-methyltransferase (PEMT) knockout mice have hepatic steatosis and abnormal hepatic choline metabolite concentrations despite ingesting a recommended dietary intake of choline. *Biochem J*, *370*(Pt 3), 987-993.